A SCOPING STUDY OF ADVANCED THORIUM FUEL CYCLES FOR CANDU REACTORS

A SCOPING STUDY OF ADVANCED THORIUM FUEL CYCLES FOR CANDU REACTORS

By

YONATAN FRIEDLANDER, B.A.Sc.

A Thesis Submitted to the School of Graduate Studies in Partial Fulfilment of the Requirements for the Degree Master of Applied Science in Engineering Physics

McMaster University

MASTER OF APPLIED SCIENCE (2011) MCMASTER UNIVERSITY
(Engineering Physics) Hamilton, Ontario, Canada

TITLE: A Scoping Study of Advanced Thorium Fuel Cycles for CANDU Reactors

AUTHOR: Yonatan Friedlander, B. A.Sc. (Queen's University)

SUPERVISOR: Dr. J. Luxat

NUMBER OF PAGERS: xvi, 120

Abstract

A study was conducted to scope the relative merits of various thorium fuel cycles in CANDU reactors. It was determined that, due to the very large reprocessing demands of the self-sustaining equilibrium thorium fuel cycle, an additional fissile driver fuel is required for a practical thorium fuel cycle. The driver fuels considered were PWR- and CANDU- derived plutonium, PWR-derived MOX fuel, and low-enriched uranium. The addition a RU-fuelled CANDU reactor with possible americium, curium, and lanthanides recycling was also considered. The fuel cycles were evaluated for natural uranium consumption and reprocessing demands as well as spent fuel characteristics such as: thermal and gamma power, radioactivity, and ingestion and inhalation hazards.

The two-dimensional multigroup code, WIMS-AECL, was used to calculate the burnup and some controllability properties of the CANDU reactors. ORIGEN, a depletion and decay module, was used to evaluate the spent fuel characteristics and the systems code, DESAE, was used to simulate the introduction of the thorium fuel cycle to a growing global reactor park.

It was determined that ^{233}U production in the thorium fuels is optimized at lower exit burnups. Therefore, less external fissile driver material is required for the operation of the thorium reactors and natural uranium savings of the overall fuel cycle are increased. Furthermore, it was determined that driving the thorium fuel cycle with low-enriched uranium is the most efficient way to minimize natural uranium consumption. Assuming that a 40 MWd/kg exit burnup was achieved in the CANDU reactors, the fuel cycle yielded an 82% savings of natural uranium, compared to a scenario in which all power came from PWRs, while a 20 MWd/kg exit burnup increased the savings to 94%. The savings ranged over those exit burnups from 55%-69% for the variant with PWR-derived plutonium, 60%-73% for PWR-derived MOX fuel, and 78%-87% for CANDU-derived plutonium. The thermal power, radioactivity, and health hazards of the spent

fuel were the highest for the case with MOX fuel driver but americium recycling proved effective for decreasing the long term dangers. In a global reactor park, the introduction of the thorium fuel cycle was hampered by the availability of fissile resources and, for a PWR-derived driver, natural uranium consumption was only reduced by 22% over 100 years relative to the PWR only scenario.

Acknowledgements

I would like to thank the advanced fuel cycles group at Chalk River, namely Bronwyn, Geoff, and Jeremy. Without their help, guidance, and *patience* I wouldn't have been able to come even close to completing my thesis. David Hummel's work at maintaining the computer cluster and providing technical support must also be mentioned. I'd also like to thank my supervisor, Dr. Luxat, for his support over the past two years. Lastly, I'd like to acknowledge the financial support from NSERC, UNENE and CNS..

Contents

List of Figures

List of Tables

List of Abbreviations and Symbols

ACR	Advanced CANDU reactor
AECL	Atomic energy of Canada Ltd.
ATBR	Advanced thorium breeder reactor
BU_i	Burnup of reactor i
CANDU	Canada deuterium-uranium
C_i	Consumption rate of resource i
CVR	Coolant void reactivity
CR	Conversion ratio
DESAE	Dynamics of energy system of atomic energy
DUPIC	Direct use of spent PWR fuel
GAINS	Global architecture of innovative nuclear energy systems
HEU	High enriched uranium
IAEA	International atomic energy agency
ITREC	Impianto trattamento elementi combustibile (Element Processing and Refabricating Plant)
L	Fraction of fissile resources lost during reprocessing
LEU	Low-enriched uranium
LWR	Light water reactor
M_i	Weight percentage of isotope i
MOX	Mixed-oxide
NU	Natural uranium
OECD	Organisation for economic co-operation and development

ORIGEN	Oak ridge isotope generation
P_i	Rate of production of driver fuel i
PHWR	Pressurized heavy water reactor
PWR	Pressurized water reactor
PWR-OT	Pressurized water reactor once-through
RTF	Radkowsky thorium fuel
R_i	Reprocessing rate of spent fuel i
RU	Reprocessed uranium
SCALE	Standardized computer analyses for licensing evaluations
$SR_{i:j}$	Support ratio of reactor i to j
SSET	Self-sustaining equilibrium thorium
THTR	Thorium high-temperature reactor
TRU	Transuranic
U_i	Net production or consumption of ^{233}U in n reactor i
v_d	β yield
WIMS	Winfrith Improved Multigroup Reactor code
η	Neutron yield
σ_a	Absorption cross-section
σ_γ	Capture cross-section

1 Background

Global industrialization, especially the growing urbanization in the Far East, has pushed humankind's ability to produce energy to the edge of the Earth's capacity. The most common source for energy, fossil fuels, has had an undeniable contribution to anthropogenic climate change leading engineers to look for new sources of energy. However, with the exception of nuclear energy, no technology has the ability to provide comparable amounts of energy to fossil fuels and emit no greenhouse gases. This makes nuclear energy the leading candidate to power the world's economy late into this century and beyond. Therefore, it is imperative to investigate the limits of our nuclear capacity and what means exist to extend it.

1.1 Nuclear Resources

At present, there is ample uranium ore to fuel the world's nuclear reactors. However, reports have suggested that conventional uranium resources will be depleted by mid- to late-century [1-3]. Although less conventional uranium reserves will still be available, the shortages will likely lead to a steep increase in the cost of uranium ore. The localization of uranium deposits further compounds this issue. Even before the global uranium reserves start to diminish, many countries will face national shortages. Figure 1.1 shows that some nuclear powers, such as India and China, lack substantial local uranium reserves [2]. Therefore, there is a need for the nuclear industry to embrace alternative reactor fuels.

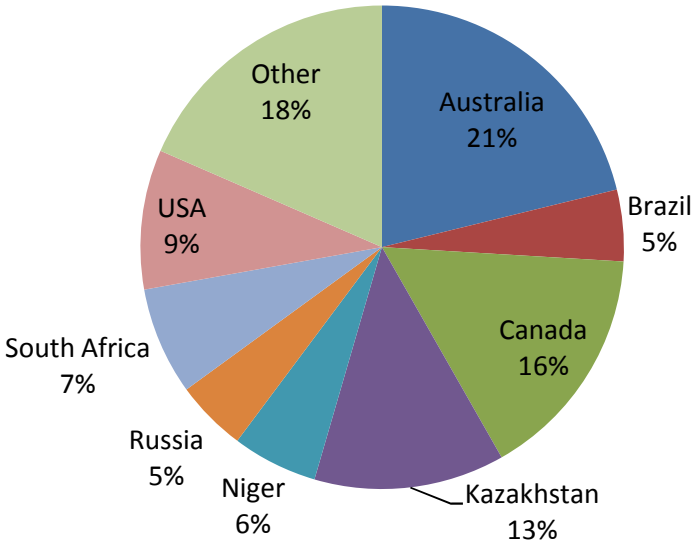

Figure 1.1 – Distribution of global uranium reserves

Thorium reserves are estimated to be 3 times more abundant globally, making it a promising alternative. This is especially true in India where it is 10 times more abundant than uranium reserves [4]. Furthermore, as is shown in the following chapters, the superior breeding attributes of thorium fuel give it an advantage beyond just its natural abundance.

1.2 Nuclear Fission

In a nuclear fission reaction, a fissile atom absorbs a neutron, splitting it into two smaller atoms and releasing a tremendous amount of energy as well as 2 or more neutrons. If another fissile atom absorbs one of the emitted neutrons, it can undergo the same reaction. When this happens repeatedly in a self sustaining manner, it is referred to as a chain reaction and is the fundamental concept behind a nuclear fission reactor. A nuclear reactor uses the energy released by the fission reactions to generate steam which turns a turbine. The rotating turbine generates power which can then be distributed to the population. An element that can sustain a chain reaction of fission is

referred to as fissile. Therefore, nuclear fuel must contain at least one of the 4 fissile isotopes: ^{233}U, ^{235}U, ^{239}Pu, or ^{241}Pu.

The simplest fuel for a nuclear reactor is ^{235}U which comprises 0.71% of natural uranium, (NU). The rest of the NU is almost entirely ^{238}U. Some heavy water moderated reactors, such as the CANDU reactor, can sustain a chain reaction with NU. However, most reactors require a larger fissile source so the amount of ^{235}U in the uranium is enriched using either centrifuges or gaseous diffusion. Although ^{238}U does not fission, it does absorb neutrons while in the reactor transmuting it to ^{239}Pu and, eventually, ^{241}Pu. Because ^{238}U produces fissile material, it is referred to as fertile.

The fissile plutonium isotopes are always present in discharged uranium fuel. Therefore, if spent fuel is reprocessed, it presents a new source for nuclear fuel. This is currently practiced in a few countries around the world such as Japan, the UK, and France but, as separated plutonium can be diverted to make nuclear weapons, it is disallowed through government policy decisions in several countries including Canada and The United States.

The least used fissile isotope, ^{233}U, does not occur naturally nor is it created during the uranium fuel cycle. Instead, it is created when thorium absorbs a neutron as shown in equation (1.1).

$$^{232}Th \xrightarrow{n,\gamma} {}^{233}Th \xrightarrow{\beta-} {}^{233}Pa \xrightarrow{\beta-} {}^{233}U \tag{1.1}$$

Thorium is a mononuclidic element which is found abundantly in nature. However, as thorium is fertile, not fissile, an external neutron source is required to drive the reaction. This source, referred to as the driver fuel, can be any one of the aforementioned fissile isotopes.

1.3 Thorium Fuel Cycle

Unlike uranium fuel, thorium fuel can be used as a thermal breeder. This means that, under certain conditions in a reactor, thorium fuel can produce more fissile material than it consumes. Thorium has several attributes that make it better suited for this than uranium. The thermal absorption cross section of ^{232}Th is roughly twice as large as that of ^{238}U. The capture cross section of ^{233}U is lower and the neutron yield is higher than ^{235}U or ^{239}Pu. Overall, this leads to a greater production of fissile material per neutron absorbed in the fuel. The neutronic characteristics of the isotopes are summarized in Table 1.1 [5].

	^{232}Th	^{238}U	^{233}U	^{235}U	^{239}Pu
σ_a	5.13	2.73			
σ_γ			47.7	98.6	268.8
η			2.287	2.068	2.108

Table 1.1 – Comparison of the cross-sections of the fertile and fissile nuclides in the NU and thorium fuel cycle. The cross-sections are for neutrons with an energy of 0.0253eV.

Even if the thorium reactor is not operated as a breeder, the rate of fissile fuel production in a thorium reactor is better than that of a uranium reactor, leading to a greater incentive for recycling the spent fuel. A special case of the thorium fuel cycle, in which a thorium-fuelled reactor is driven only by the ^{233}U that it has produced, is referred to as the Self-Sustaining Equilibrium Thorium (SSET) fuel cycle.

1.3.1 Self-Sustaining Equilibrium Thorium Fuel Cycle

If the breeding ratio of the thorium reactor is higher enough, then the amount of ^{233}U that is discharged from the reactor can be equal to the amount of ^{233}U that is required to drive the reactor. In this case, the fuel can be recycled by removing the fission products and transuranics and adding a small amount of natural thorium to compensate for those losses. This is the SSET cycle and is shown in Figure 1.2. What

differentiates this from other thorium fuel cycles is that the thorium can be used without the requirement of additional fissile resources.

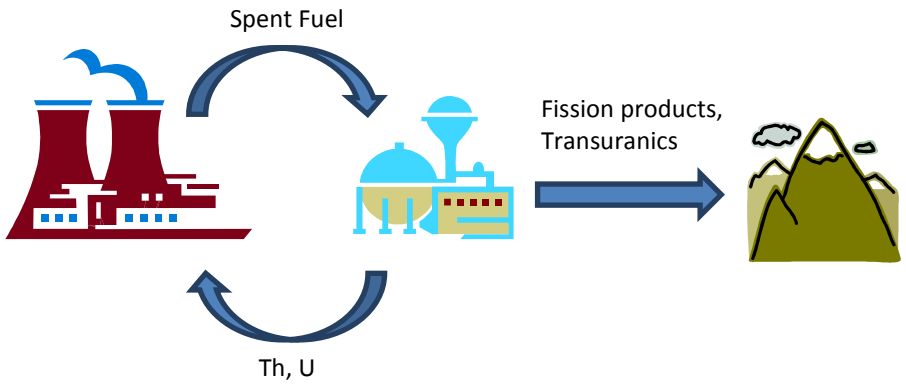

Figure 1.2 – Illustration of the self-sustaining equilibrium thorium fuel cycle

The benefit of the SSET fuel cycle is that, by repeatedly passing it through the reactor, the thorium ore is almost completely fissioned – releasing all of its potential energy. This leads to almost zero resource consumption. By comparison the uranium once-through cycle fissions less than 1% of the ore. Unfortunately, as will be shown later, the SSET fuel cycle requires very frequent reprocessing which may lead to prohibitively high costs. For that reason, a lot of the thorium fuel cycles consider using an external fissile fuel to drive the reaction. In this case, the thorium reactor will not be a net producer of fissile material (i.e. a thermal breeder) but may still produce as much or more ^{233}U than it consumes.

1.4 Experience with Thorium Fuels

Although limited in comparison to uranium fuels, there is experience with thorium fuel fabrication, irradiation, and reprocessing. The studies, in both CANDU and other reactors, have indicated that thorium is a viable reactor fuel. In fact, it has been suggested that thorium has some superior fuel characteristics in comparison to uranium fuel such as higher thermal conductivity and greater chemical inertness [6].

Atomic Energy of Canada Ltd., (AECL), has fabricated thorium fuel by both dry-blending and wet-powder blending and, in the 1970s, thorium fuel was also irradiated in the experimental reactor WR-1. Currently, AECL is developing a reprocessing method that co-precipitates thorium and uranium via the dry reprocessing method known as fluoride volatility [6]. The closest to full-scale commercial implementation of the thorium-fuelled CANDU reactors is in China where they have built 2 CANDU reactors as part of Qinshan Phase III for the explicit use of the thorium fuel cycle. Also being constructed is a large reprocessing plant to extract the uranium from the spent fuel. The reactor will first irradiate a few channels of thorium fuel before it reaches the final goal of a full core irradiation [7].

In 1977, the Shippingport pressurizer water reactor, (PWR), in the United States was loaded with uranium and thorium in a seed-blanket configuration. The experiment resulted in the first demonstration of ^{233}U breeding in a commercial light water reactor [8]. Other notable thorium experiments in the United States include the Indian Point Reactor 1 which was fully loaded with thorium fuel driven by high enriched uranium, (HEU), and the Elk River Reactor, where 20 thorium-uranium fuel assemblies were irradiated. These assemblies were then remotely reprocessed using a wet co-precipitating method at the Element Processing and Refabricating Plant, (ITREC), in Italy [9].

In Germany, the 300MW Thorium High-Temperature Reactor (THTR-300) was built as a prototype pebble-bed high-temperature reactor. Although it was shut down after only 6 years of operation, valuable information was collected about the behaviour of thorium fuels at high temperatures in a commercial reactor [10]. In India, the pressurized heavy water reactor, (PHWR), Kakrapar-1 uses thorium for flux shape flattening [11]. Experience gained from the behaviour of the thorium fuel will be used by India in the design of thorium-fuelled heavy water reactor.

2 Outline

In chapter 1 the background information on the nuclear industry and thorium fuel cycles was presented. Chapter 3 will present a literature review which outlines the current state of research on the topic. Chapter 4 will introduce the fuel cycles which will be examined in the thesis. The models with which the fuel cycles are simulated will be presented in chapter 5. Chapters 6 and 7 will present the properties of thorium-fuelled CANDU reactors. The mass flows from the steady-state scenario will be presented in chapter 8 and the mass flows from the changing reactor park will be presented in chapter 9. Chapter 10 will characterize the spent fuel from each variant and in chapter 11 conclusions will be drawn from the results and suggestion for future research will be presented.

3 Literature Review

The conclusion one makes about thorium fuel cycles is dependent on the nature of the study that's conducted. This section intends to show the different approaches that have been taken in studying thorium fuel cycles and, through those differences, show the merit of this study. As will be shown, there has been extensive research on different aspects of the thorium fuel cycle. However, there has only been limited research on the long term implications of equilibrium thorium fuel cycles in CANDU reactors. Recently, there has been some interest in this area from AECL and this study intends to build on that effort by characterizing and comparing different reactor parks that can be considered for the long term exploitation of thorium resources.

The fuel cycle studies have been broadly categorized by the following characteristics: stage of the reactor park, the metrics used to evaluate the fuel cycles, the fissile driver material, and the reactors employed.

3.1 Stage of Reactor Park

As shown in chapter 1.3, the fissile component of the thorium fuel cycle, ^{233}U, is not naturally occurring but must be produced in a reactor. Therefore, at the introduction of a thorium fuel cycle, the composition of the fissile driver changes with each reactor pass. After some time, the reactor park can reach equilibrium where it produces and consumes equal amounts of ^{233}U. In this stage, the fuel isotopics do not change between reactor passes. Lastly, one can consider a system where the size of the reactor park is changing. In this case, the isotopics of the fuel may remain constant for each reactor pass but an equilibrium ^{233}U production and consumption is never reached. Using this guideline, the systems studies of thorium fuel cycles can be categorized in one of three ways: approach to equilibrium, equilibrium, and changing reactor park.

In an approach to equilibrium study, it is assumed that no ^{233}U is present at the introduction of the reactor park. The ^{233}U is bred with each reactor pass until a sufficient amount is available so that the reactor's fissile output isotopics can match the input. The ^{233}U can be bred using a thorium once-through cycle or small, increasing amounts of ^{233}U can be recycled until equilibrium conditions are met. This approach may take several years or may extend over several reactor lifetimes as was shown by Veeder and Didsbury [12]. This stage is often the focus in studies on the near-term implementation of thorium fuel cycles. [13-15].

In an equilibrium fuel cycle, sufficient ^{233}U exists to drive the fuel cycle. However, with the exception of the SSET cycle, an external fissile source is also needed. In this stage, the characteristics of the reactors and fuels do not change over time so the complexity of analysis is reduced. This approach has been used to examining the rate of plutonium consumption in the thorium fuel cycle [16] as well as the benefits of a SSET cycle [14, 17-19].

In a realistic implementation of a thorium fuel cycle, one must consider that the cycle does not exist in the absence of a national or global reactor park. Varying demand for nuclear power, limited reprocessing capacities and fissile sources, and practical lead times will affect the characteristics of the fuel cycle. Therefore, the effectiveness of a thorium fuel cycle must be evaluated not only in an equilibrium case, but also in the context of an evolving reactor park. Obviously, predicting long term global trends introduces much more uncertainty into the study. For example, the study of the thorium fuel cycle conducted by Banerjee et al in 1977 quickly became irrelevant because they could not have predicted the decreased demand for nuclear power created by the Three Mile Island accident in 1979 and the Chernobyl disaster in 1986 [20]. In light of the increased uncertainty, the advantage of examining a fuel cycle in a global context is better demonstrated when it used as means of comparing different advanced fuel cycle options. A study in this vein was conducted by AECL as a part of GAINS, a global initiative to examine various advanced closed fuel cycles. In their report, the effectiveness of introducing a thorium fuel cycle to global reactor park was compared to a 'business as usual' case and the case where fast reactors are introduced [1]. Although this approach assumes an unprecedented amount of global cooperation and foresight and ignores the restrictions on international trade of fissile resources, it does give great insight into the relative merit of different fuel cycles. One way to reduce the uncertainty in the study is to scale down the scope to a national level. This is the approach that was used to analyze the introduction of thorium fuel cycles in Korea [21]. However, a national study on thorium fuel cycles may be less appropriate in the context of Canada's nuclear industry as there are immense native uranium reserves.

The motivation for choosing a specific fuel cycle for the approach to equilibrium may differ from that of an equilibrium fuel cycle. Furthermore, as their individual merits are largely independent, it is plausible to study one without the other. This study

chooses to focus on the longer term implication of the thorium fuel cycle so the approach to equilibrium case is not considered.

3.2 Metrics of Evaluation

Another choice for fuel cycles studies is the metric by which will they be evaluated. The common characteristics used for evaluating advanced fuel cycles include: economics, proliferation resistance, mass flows, and spent fuel characteristics.

3.2.1 Economics

In the early studies of thorium-fuelled CANDU reactors, economics were a major focus [12, 20, 22-24]. This is likely due to the fact that uranium shortages were a more distant concern and spent fuel accumulation was yet to be an issue. The predicted costs in these studies are long out-dated rendering them largely irrelevant. This highlights the time dependence of economic analyses and the need for parametric uncertainty analysis. Even at the present, the costs of unproved advanced fuel cycle technology are highly speculative so economics is not the focus of this study.

3.2.2 Proliferation Resistance

Proliferation resistance is an attribute that has been extensively studied in advanced fuel cycles. However, it is one of the more nebulous metrics. The risk of malicious diversion of fissile material is a relatively subjective and unquantifiable value. In the context of thorium fuel cycles, an attempt to quantify proliferation resistance is often done by evaluating the amount of plutonium consumed. However, even this has subjective value. The consumption of potentially dangerous fissile material, especially weapons grade plutonium, may be viewed as positive proliferation resistance [16, 25]. On the other hand, large mass flows of separated plutonium may be viewed as a proliferation risk. The merit of plutonium consumption is further complicated by the

potential economic value of separated fissile material. With the introduction of fast reactors and the thorium fuel cycle, plutonium may be better viewed as a valuable resource and commodity than dangerous waste. Because of the subjectivity of proliferation resistance, it is not used as a metric of comparison in this study.

3.2.3 Mass Flows

The three major components of a fuel cycle's mass flow are: resource consumption, spent fuel accumulation, and reprocessing throughput. The first two are often the foremost goal of advanced fuel cycles so they are included in many studies. Reprocessing can give broad generalizations about the economic feasibility of the fuel cycle without needing forecasts on costs. Therefore, it is also sometimes included. All three are considered in this study. An interesting metric not included in this study is the percent of energy derived from thorium in the fuel cycle. This has been adopted in recent studies by AECL [26, 27]. Although this metric implies results about uranium consumption, it is better suited for optimization of a reactor design than a fuel cycle as a whole.

3.2.4 Spent Fuel Characteristics

When evaluating the spent fuel from the fuel cycle, many misleading values are used. Radiotoxicity, inhalation hazard, and other quantities that define that danger of the fuel when exposed to humans do not give an accurate representation of the difficulty of long term disposal. In the proper circumstances, the fuel should remain out of contact of humans and, therefore, the correct values to quantify are those that pose a risk to disposal. Those values are the mobility and thermal power of the spent fuel [28]. Mobility is a difficult value to calculate and depends on the form of disposal so thermal power is the primary attribute used when characterizing the spent fuel in this and other

studies [1, 29]. Although other spent fuel characteristics will be discussed in this report, thermal power will be the main metric for evaluation.

3.2.5 Controllability

Some studies, rather than focussing on comparing the thorium fuel cycle to other advanced fuel cycles, opt to determine the controllability of thorium-fuelled reactors. The most commonly optimized trait is the coolant void reactivity, (CVR) [18, 30-32]. However, other optimized parameters include the linear element rating and temperature coefficients [19, 26, 33]. Although it is not the raison d'être of this study, it is an important design feature so some aspects of reactor controllability are examined.

3.3 Driver Fuel

As described in the previous chapter, thorium fuel cycles can either be a SSET fuel cycle or can be driven in part by some added fissile material. Much research has been done to show the possibility of operating a SSET cycle in CANDU reactors, especially by Bergelson et al [14, 17-19]. All the research indicates that the SSET cycle is only achievable for exit burnups less than 10 MWd/kg. The exorbitant reprocessing demand from such a low exit burnup is generally ignored in their conclusions. However, in his discussion thorium recycling options, W.B. Lewis does comment that the reprocessing demands for SSET are likely to be prohibitively high [34].

When an added fissile material is used, the type of driver differs between studies. The fissile driver for the thorium fuel cycle is commonly uranium (ranging from NU to HEU) or plutonium (from spent fuel or weapon stockpiles). However, using a more exotic driver, such as DUPIC, (direct use of spent PWR fuel), has also been suggested [21, 35].

During reprocessing of the spent thorium fuel, it is generally assumed that the uranium and thorium and are removed uncontaminated. However, several studies have

suggested only a limited removal of the fission products during reprocessing and Veeder and Didsbury suggested including a limited amount of plutonium recycling [15, 35]. Many of these options are considered in this study. Another variant that has been suggested is to periodically remove the fuel from the reactor. This allows the ^{233}Pa to decay without being irradiated and would maximize the amount of ^{233}U production [12, 33, 36]. However, this demands complicated fuelling schemes which are better suited for a full core simulation so it is not considered in this study.

3.4 Reactors

Although this study focuses on the use of CANDU reactors, other reactors have been considered for the thorium fuel cycle. Radkowsky Thorium Fuel, (RTF), is a seed-blanket concept for pressurized water reactors. The design, which was adopted at the Shippingport reactor, proposes to use a subcritical thorium blanket that is driven by a seed comprised of either zirconium and plutonium or enriched uranium [37]. The objective of this configuration is to maximize the ^{233}U breeding while still using pre-existing PWR technology. However, due to a superior neutron economy, heavy water reactors have been proven to be better suited for breeding [38]. Rather than using existing reactor technology, India has proposed a reactor designed specifically for thorium fuels called the Advanced Thorium Breeder Reactor, (ATBR) [30]. The ATBR is a vertical heavy-water moderated reactor with boiling light water coolant. The reactor is designed to maximize the advantages of thorium fuel while maintaining near-zero reactivity coefficients. In Canada, the focus is on the CANDU reactor, however, the use of thorium in the advanced CANDU reactor, (ACR), has also been considered [29].

Modifications to the existing CANDU reactor are also considered in some studies. The use of advanced bundle designs containing 42, 43, or 52 fuel elements [21, 27, 29] has been suggested. Another design aspect that can be examined is the heterogeneity of the reactor. As a lattice code is used in this study, only heterogeneity at the fuel bundle

level is considered. Other reactor design aspects that have been investigated in studies include: the lattice pitch, moderator ratio, specific power, fuel density, and refuelling rate [13-15, 20, 32, 39, 40]. Several of these are investigated in this study.

4 Fuel Cycles

This chapter presents the fuel cycles and their variants that are considered in this study. All of the fuel cycles considered incorporate two CANDU reactors and some source of added fissile driver. The first CANDU reactor, hereafter referred to as Reactor A, is loaded with thorium, ^{233}U, and the driver fuel. As will be shown later, Reactor A produces more ^{233}U than it consumes. The excess ^{233}U is loaded in a second CANDU reactor, Reactor B, which is loaded with only ^{233}U and thorium and consumes more ^{233}U than it produces. The fuel loadings of Reactor A and Reactor B are chosen so that the fuel cycle produces and consumes equal amounts of ^{233}U. The driver fuels considered include CANDU- and light water reactor- , (LWR), derived plutonium, LWR-derived MOX fuel, and enriched uranium. Other variants include adding a CANDU reactor fuelled by LWR-derived reprocessed uranium, (RU), and a CANDU reactor that burns americium and curium. The fuel cycles will be compared to the base case of a LWR once-through cycle. The fuel cycles are summarized in Table 4.1.

Variant	Fuel Cycle
Base case	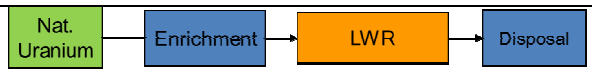
1a	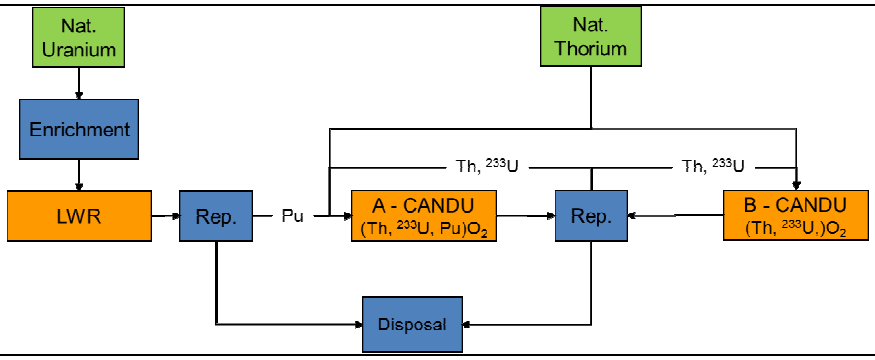

1b

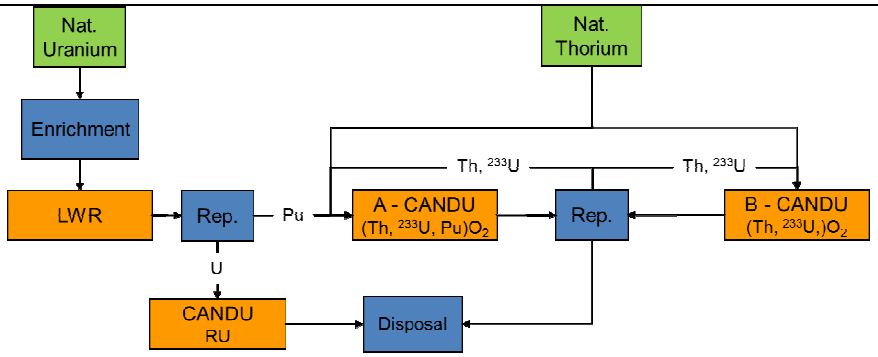
Nat. Uranium
Enrichment
LWR
Rep.
Pu
U
CANDU RU
Nat. Thorium
Th, 233U
Th, 233U
A - CANDU (Th, 233U, Pu)O2
Rep.
B - CANDU (Th, 233U,)O2
Disposal

1c

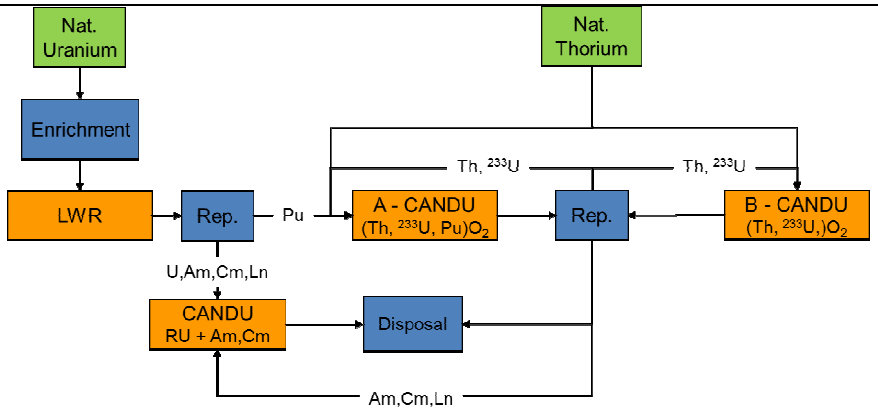
Nat. Uranium
Enrichment
LWR
Rep.
Pu
U,Am,Cm,Ln
CANDU RU + Am,Cm
Nat. Thorium
Th, 233U
Th, 233U
A - CANDU (Th, 233U, Pu)O2
Rep.
B - CANDU (Th, 233U,)O2
Disposal
Am,Cm,Ln

2a

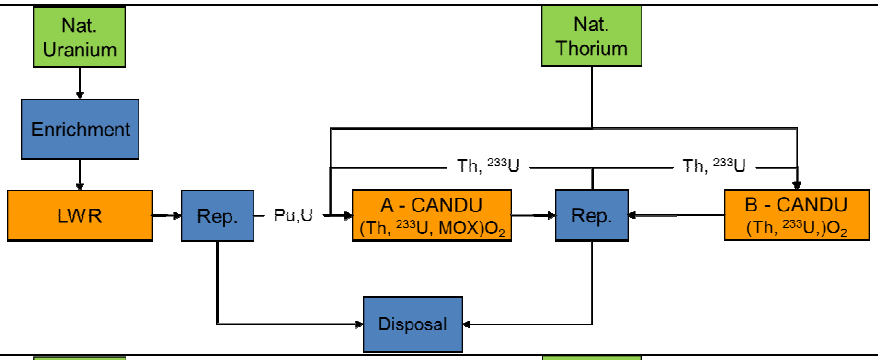
Nat. Uranium
Enrichment
LWR
Rep.
Pu,U
Nat. Thorium
Th, 233U
Th, 233U
A - CANDU (Th, 233U, MOX)O2
Rep.
B - CANDU (Th, 233U,)O2
Disposal

2b

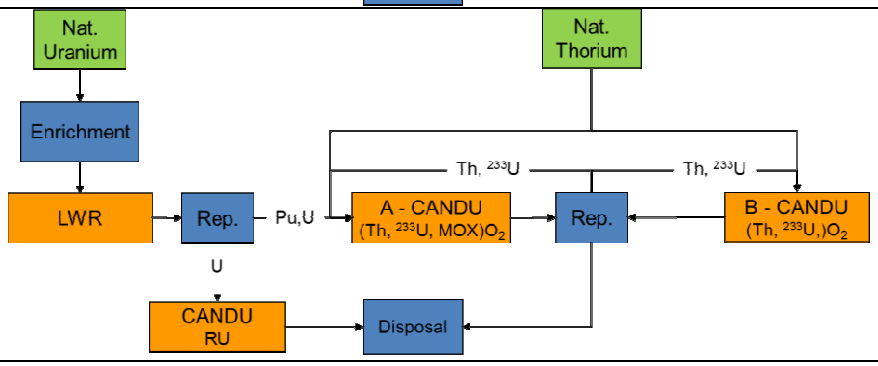
Nat. Uranium
Enrichment
LWR
Rep.
Pu,U
U
CANDU RU
Nat. Thorium
Th, 233U
Th, 233U
A - CANDU (Th, 233U, MOX)O2
Rep.
B - CANDU (Th, 233U,)O2
Disposal

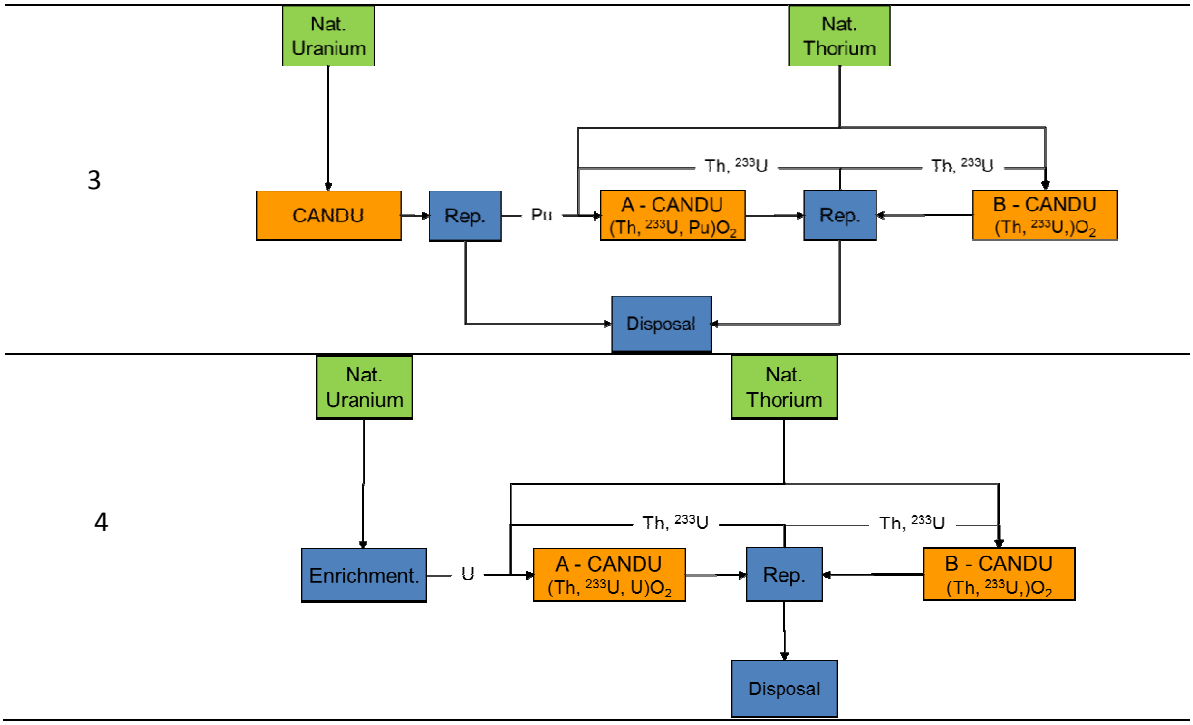

Table 4.1 – The fuel cycles considered in this study

5 Models

To simulate the reactors and fuel cycles, three codes are used: WIMS, DESAE, and ORIGEN. This chapter discusses how these codes are employed and how the reactors are modelled.

5.1 CANDU

CANada Deuterium Uranium, (CANDU), reactors are Canadian designed reactors that are fuelled with natural uranium. The typical 900MW reactor has 480 horizontal fuel channels. Each fuel channel contains 13 fuel bundles which each bundle containing 37 elements. A typical layout of a CANDU reactor assembly is shown in Figure 5.1 [41].

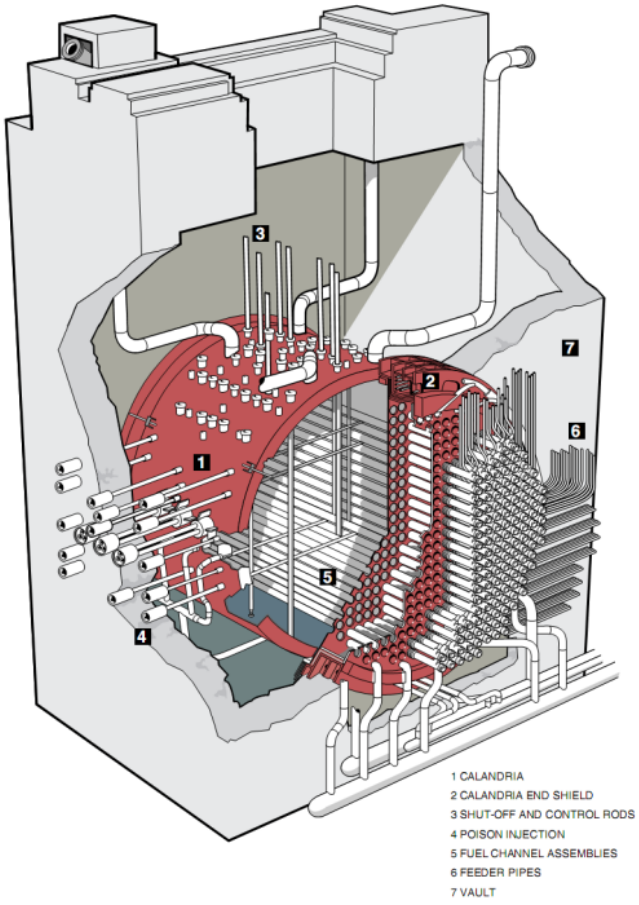

Figure 5.1 – A model of the CANDU-6 reactor assembly

To compensate for the lack of reactivity in natural uranium, CANDU reactors have two unique characteristics: heavy water coolant and moderation, and on-line refuelling. Heavy water has a significantly lower absorption cross section than light water, leading to an improved neutron economy. This means that fewer neutrons are captured in the moderator and more neutrons are available to interact with the fuel. Online refuelling maintains the criticality of the reactor by replacing spent fuel with fresh fuel on a regular basis. This allows the fuel to be irradiated longer than it would have been if the reactor were batch refuelled. The measure of criticality in a reactor is 'k-effective'. When the k-effective is 1 or greater, the reactor is critical. As k-effective is dependent on the contents of the fuel, it changes over burnup. In batch refuelling, the fuel is removed

once the k-effective reaches 1. However, with online refuelling, the core contains fuel from all stages of burnup. Therefore, the criticality of the core must be calculated using a k-effective that is integrated over the entire burnup. In a CANDU reactor, the fuel is removed from the core once the integrated k-effective reaches 1. In some simulations, the reactor core is modelled as an infinite array of cells. In this case, components such as the guide tubes, absorbed rods, and flux detectors are explicitly ignored and a measure of the core's reactivity is referred to as the k-infinity. The difference between k-effective and k-infinity is referred to as the parasitic absorption. In a typical CANDU reactor, the parasitic absorption is assumed to be 35 mk. These concepts are shown in Figure 5.2.

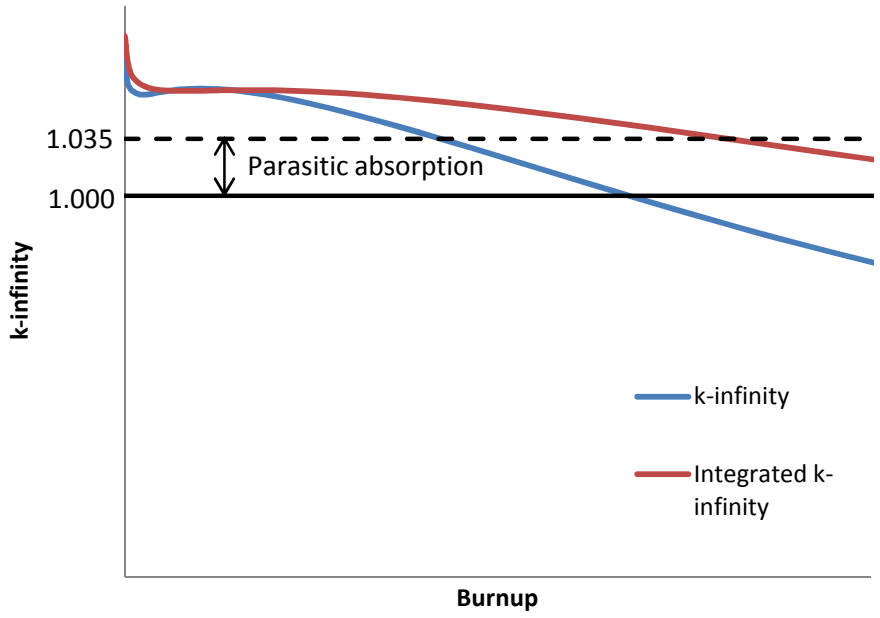

Figure 5.2 – A comparison of k-infinity and integrated k-infinity for a NU CANDU reactor. The dashed line represents when the fuel reaches exit burnup.

To simplify the simulation of a CANDU reactor, the core is often represented by a single two-dimensional lattice cell. The lattice cell contains one fuel bundle and is infinitely repeated in all directions with a reflective boundary condition. This is an adequate model for a fuel channel that is not near the boundary of the reactor. The fuel

bundle is shown in Figure 5.3. It consists of 37 fuel elements arranged in four concentric rings. In order, they are referred to as the centre, inner, intermediate, and outer elements. The elements are surrounded by the coolant which is inside a zirconium alloy (Zr-2.5%Nb) pressure tube. Surrounding the pressure tube is a gap filled with CO_2 and then a zirconium alloy (Zr-2) calandria tube. The entire calandria tube is surrounded by the moderator. The lattice pitch, being the distance between the centre of each fuel channel, is defined by the size of the reflective boundary. During the simulation, the cell is irradiated at a constant power over discreet time steps. The properties of the lattice cell are summarized in Table 5.1.

Component	Material	Outer radius (cm)
Fuel	*Variable*	0.652183
Coolant	D_2O	5.41155
Pressure Tube	Zirconium	6.4478
Calandria Tube	Zirconium	8.6
Moderator	D_2O	*Variable (determined by the lattice pitch)*

Table 5.1 – Properties of CANDU lattice cell

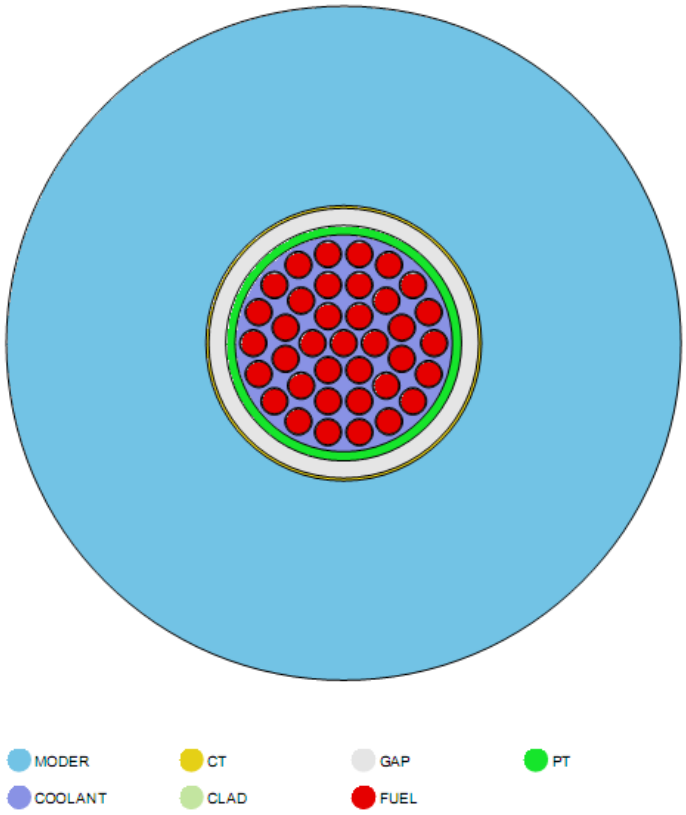

Figure 5.3 – CANDU lattice cell used in WIMS calculations

The simulation is conducted using WIMS-AECL. WIMS is a two-dimensional multigroup code that uses the collision probability method to solve the integral neutron transport equation. As it is much less computationally intensive than full-core models, it is often used to perform burnup calculations and generate average cross-sections and diffusion coefficients that are used in the full-core simulations [42].

5.2 Light Water Reactor

In this study, the LWR is not modelled. Instead it is represented using data from existing reactors. The isotopics of the spent plutonium was chosen to match that of the plutonium used in various studies at AECL [26]. For all other properties, the LWR is represented by data from Takahama-3. Takahama-3 is a 2653 MW(th) PWR that was

built in Japan in 1985. Spent fuel from the reactor underwent a post irradiation examination and the results are readily available through Nuclear Energy Agency website [43]. The fuel rod, whose isotopic data is used in this study, was loaded with 4.11% enriched uranium fuel and was irradiated to an exit burnup of 42.16 MWd/kg. The composition of the spent fuel is summarized in Table 5.2.

Element	Mass Number	Weight Fraction	Element	Mass Number	Weight Fraction
Uranium	234	2.01E-04	**Plutonium**	238	2.59E-04
	235	1.03E-02		239	6.22E-03
	236	5.31E-03		240	2.47E-03
	238	9.28E-01		241	1.69E-03
Neptunium	237	5.84E-04		242	6.53E-04
Curium	243	6.95E-07	**Americium**	241	4.93E-05
	244	5.73E-05		242m	1.18E-06
	245	3.74E-06		243	1.41E-04
	246	3.66E-07	**Strontium**	90	2.70E-04
	247	4.96E-09	**Caesium**	131	1.50E-05
			Samarium	151	1.58E-03

Table 5.2 – The composition of spent LWR fuel used in this study

5.3 Fuel Cycle

To characterize the spent fuel from the fuel cycle, ORIGEN, (Oak Ridge Isotope GENereation), is used. ORIGEN is the depletion and decay module of the transport code SCALE, (Standardized Computer Analyses for Licensing Evaluations), and can model all of the important actinides and fission products in the fuel cycle. The input to ORIGEN includes the contents of the spent fuel and decay and irradiation times. For this study, ORIGEN is only being used to evaluate spent fuel so the irradiation time is held at zero. The outputs from ORIGEN include: nuclide concentrations, thermal and gamma power, inhalation and ingestion hazards, and radioactivity.

To simulate a global reactor park, the systems code DESAE, (Dynamics of Energy System of Atomic Energy), was used [44]. The code, developed at Russian Research

Centre Kurchatov Institute, simulates a reactor park containing up to 7 different reactors far into the future. The program does not contain a burnup code so input and output isotopics of the reactors must be supplied by the user. Also, the code does not account for the reprocessing losses [45]. For this study it is assumed that there is unlimited reprocessing capacity. The global nuclear energy demand is based on the moderate demand case predicted by the IAEA, (International Atomic Energy Agency), and is shown in Figure 5.4. Other key assumptions are summarized in Table 5.3.

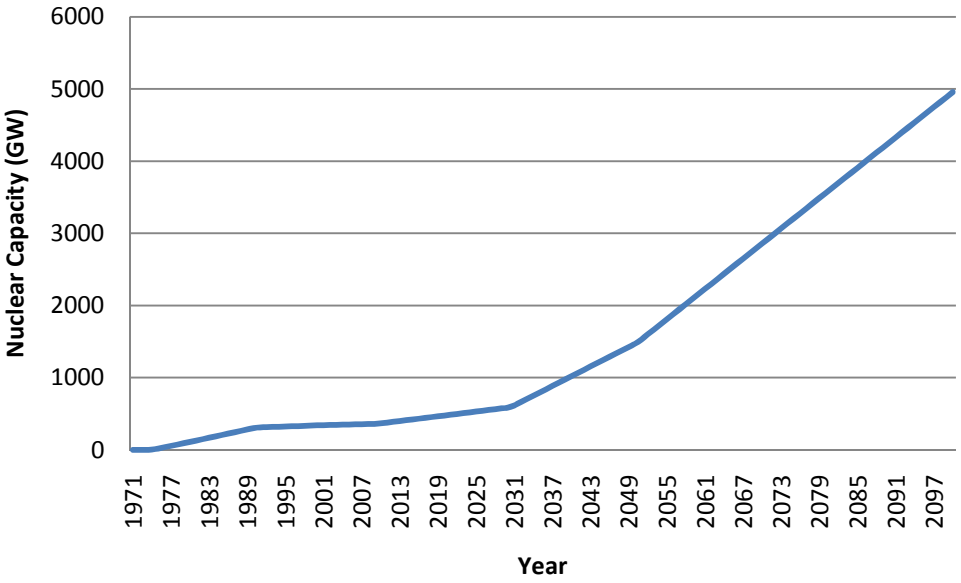

Figure 5.4 – Global nuclear energy demands to 2100

Reactor Lifetime (y)	Spent fuel cooling time (y)	CANDU thermal efficiency	LWR thermal efficiency	Tails enrichment	Capacity factor
50	6	32.26%	33%	0.20%	0.8

Table 5.3 – Fuel cycle characteristics

DESAE outputs information regarding resource consumption, actinide and fission product accumulation, reprocessing demands, and economics. The major drawback of the code is that it does not optimize a recycling scheme based on the available fissile resources. For example, the program allows a plutonium consuming reactor to be

introduced before a sufficient supply of plutonium has been generated. Therefore, if it desired that new reactors are introduced as soon as a sufficient fissile supply is available, then a crude guess-and-check optimization must be performed by the user.

6 Reactor B

Reactor B is a thorium- and ^{233}U-fuelled CANDU reactor with the dimensions that are outlined in Table 5.1. The base case assumes the same lattice pitch as a standard CANDU reactor, 28.575 cm, and a parasitic absorption of 30 mk. It has been shown that a thorium-fuelled CANDU reactor can operate with removed adjustor rods and therefore will have a lower parasitic absorption than that of a NU-fuelled CANDU reactor, 35 mk [29].

The specific power density of the base case is 20 W/g which is significantly lower than the power density of a standard full power CANDU reactor, 32 W/g. A low specific power density has been suggested as a means of retarding the neutron capture in ^{233}Pa and promoting ^{233}U production. ^{233}Pa has a half-life of 27 days and, as a result of this, an appreciable amount of ^{233}Pa can capture neutrons before decaying to ^{233}U. If it captures a neutron, ^{233}Pa transmutes to ^{234}Pa which then decays to ^{234}U with a half-life of 6.75 h. Upon capturing another neutron, ^{234}U transmutes to the fissile isotope, ^{235}U. This process, outlined in equation (6.1), requires an extra neutron capture to create fissile material in comparison the production of ^{233}U shown in equation (1.1). Therefore, increased irradiation of ^{233}Pa leads to an inferior neutron economy and fissile production rate. The amount of irradiation is proportional to the flux in the reactor. In WIMS, the lattice cell is simulated with a constant specific power density which is used to determine the flux. Therefore, decreasing the specific power density decreases the amount of irradiation.

$$^{233}Pa \xrightarrow{n,\gamma} {}^{234}Pa \xrightarrow{\beta-} {}^{234}U \xrightarrow{n,\gamma} {}^{235}U \tag{6.1}$$

6.1 Fissile Inventories

The conversion ratio, (CR), is a measure of the net production or consumption of ^{233}U in a reactor and is given by equation (6.2)

$$CR \equiv \frac{(M_{U233} + M_{Pa233})_{exit}}{M_{U233_{initial}}} \tag{6.2}$$

where M_i is the weight percentage of isotope i. A CR greater than 1 implies a net production of ^{233}U and a CR less than 1 implies a net consumption.

In the SSET fuel cycle outlined in chapter 1.3.1, the reactor must have a CR greater than or equal to 1. For a CANDU reactor, this is only achievable at exit burnups less than 10 MWd/kg which, as will be discussed later, may require prohibitively frequent reprocessing. Figure 6.1 shows the CR for a CANDU reactor loaded with thorium and varying concentrations of ^{233}U. Increasing the initial ^{233}U concentration increases the exit burnup but decreases the CR.

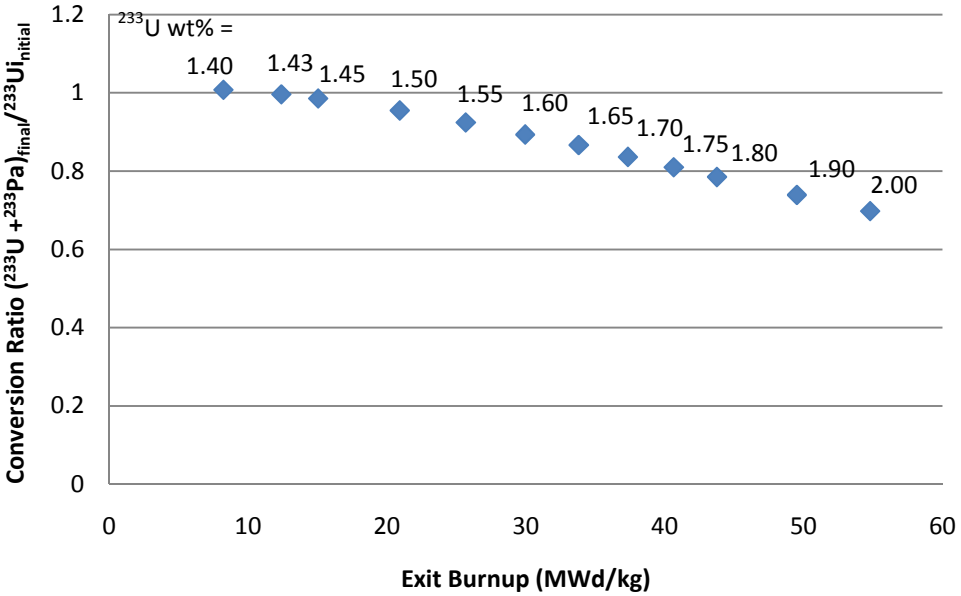

Figure 6.1 – Conversion ratio of reactor B with varying initial ^{233}U concentration

During reprocessing, it is not possible to completely separate spent fuel into its individual constituents. In the thorium fuel cycle, the amount of ^{233}U that is not separated from the rest of the fuel presents a loss in fissile production rate. Taking this into account, the ^{233}U production or consumption in a reactor is given by equation (6.3).

$$U_i \equiv \left[\frac{CR(1-L)-1}{BU_i}\right] M_{U233_{initial}} \tag{6.3}$$

where U_i is the net production or consumption of ^{233}U in kg/MWd in reactor i, BU is the exit burnup in MWd/kg, and L is the fraction of ^{233}U lost during reprocessing. The base case assumes a reprocessing loss of 0.5%. U_i will be negative when ^{233}U is consumed in the reactor and positive when it is produced. The ^{233}U consumption, (i.e. $-U_B$), in reactor B is shown in Figure 6.2.

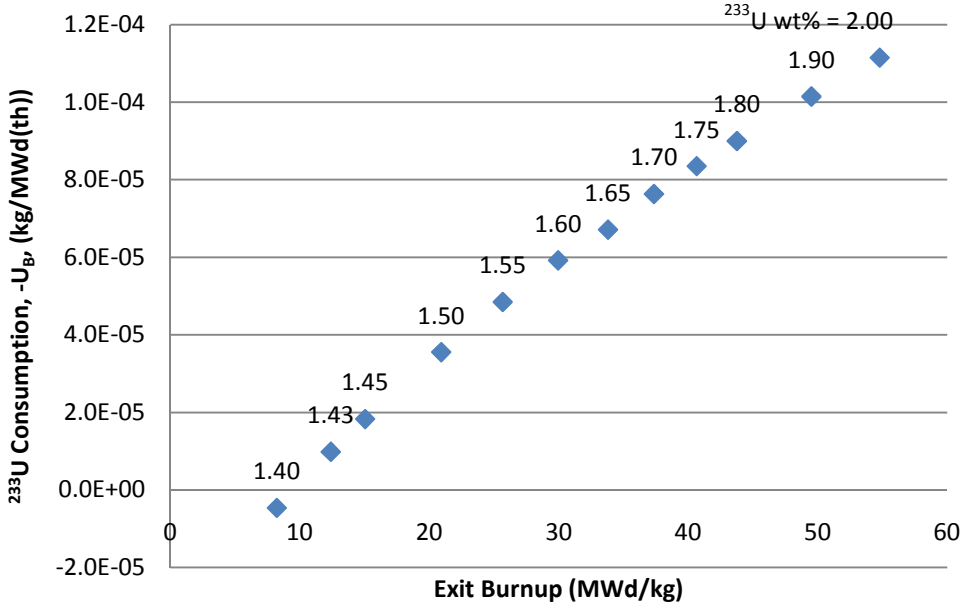

Figure 6.2 – ^{233}U consumption in reactor B for varying initial ^{233}U concentration

6.2 Sensitivity

The ^{233}U consumption in reactor B was tested for sensitivity to the following changes:

- Parasitic absorption increased to 35 mk from 30 mk
- Reprocessing losses doubled to 1%
- Reactor specific power density at 18, 22, and 32 W/g
- Lattice pitch changed to 26 cm and 30 cm
- Fuel bundle heterogeneity

Figure 6.3 shows the sensitivity of ^{233}U consumption to increased reprocessing losses and parasitic absorption.

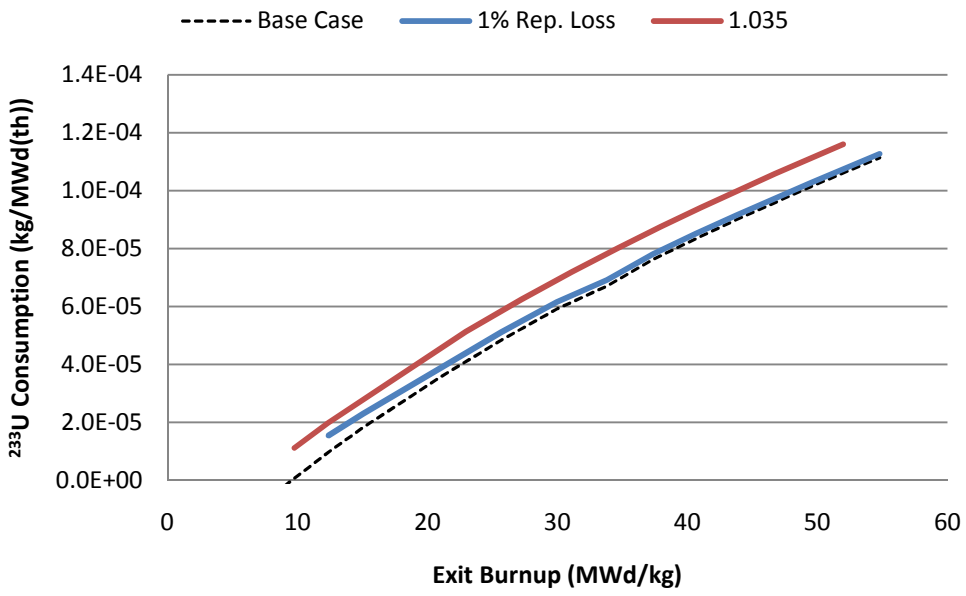

Figure 6.3 – Sensitivity of ^{233}U consumption in reactor B to increased reprocessing losses and parasitic absorption

Reprocessing losses are speculative as commercial scale thorium reprocessing plants are yet to be developed. Current uranium reprocessing plants have reprocessing

losses between 0.5% and 1%. At low exit burnups, when the fuel is more frequently reprocessed, increasing the reprocessing losses has a larger effect. Increasing the parasitic absorption decreases the amount fuel that can be fissioned in a reactor pass, increasing the rate of ^{233}U consumption.

As previously mentioned, a typical full-power CANDU reactor has a specific power density of 32 W/g. The base case assumes a lower power density of 20 W/g in order to decrease the amount of neutron capture in ^{233}Pa and promote the production of ^{233}U. The effect of varying the power density is shown in Figure 6.4. As can be seen, there is a significant increase in ^{233}U consumption for full-power conditions.

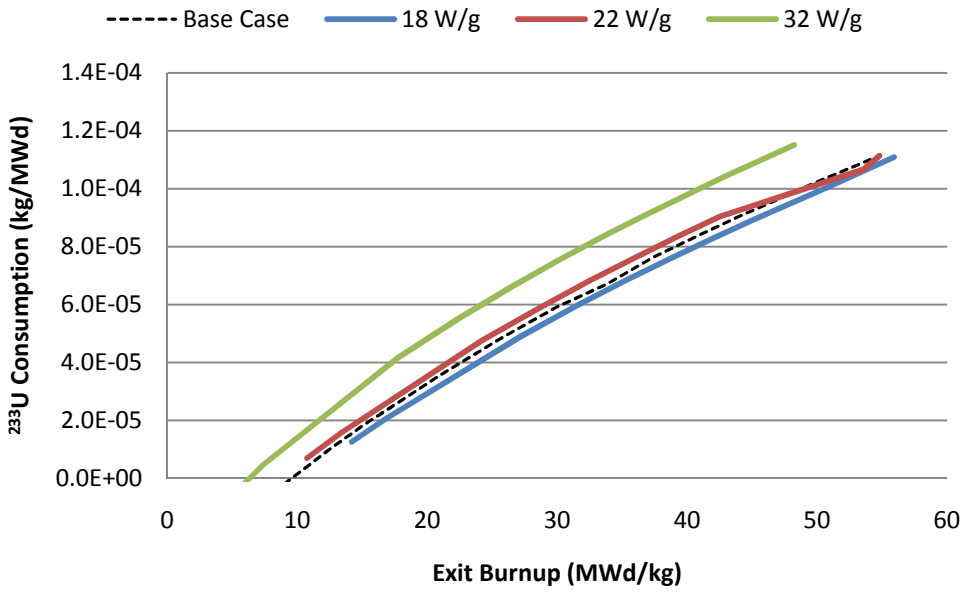

Figure 6.4 – Sensitivity of ^{233}U consumption in reactor B to changes in specific power density

Decreasing the lattice pitch is a common means of suppressing the CVR. However, as shown in Figure 6.5, decreasing the lattice pitch increases the ^{233}U consumption. The merit of decreasing the lattice pitch at the cost of increased resource

consumption depends on how effectively it suppresses the CVR. This will be examined in section 6.4.1.

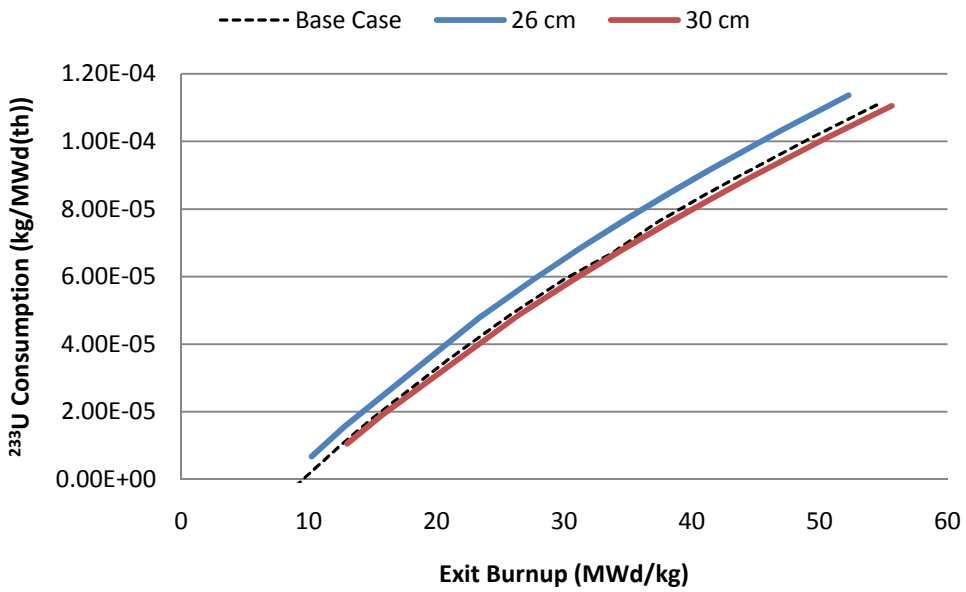

Figure 6.5 – Sensitivity of ^{233}U consumption in reactor B to changes in the lattice pitch

The results of the sensitivity analysis are summarized in Table 6.1. It can be seen that, especially at lower exit burnups, the ^{233}U consumption is very sensitive to the reactor design.

Parameter changed	Change in ^{233}U Consumption at Exit Burnup	
	20 MWd/kg	40 MWd/kg
Increase in parasitic absorption to 35 mk	32.42%	12.42%
Reprocessing losses doubled to 1%	12.91%	1.78%
Reactor power decreased to 18 W/g	-8.35%	-4.04%
Reactor power increased to 22 W/g	11.66%	3.48%
Reactor power increased to 32 W/g	47.26%	20.26%
Lattice pitch decreased to 26 cm	17.46%	8.52%
Lattice pitch increased to 30 cm	-3.49%	-2.53%

Table 6.1 – Summary of sensitivity of ^{233}U consumption in reactor B

6.3 Spent Fuel

The majority of the spent fuel from Reactor B is, of course, thorium. However, the the composition of the rest of the spent fuel changes with exit burnup. The transuranic, actinides, (TRUs), (i.e. plutonium, americium, and curium) are produced from successive neutron captures in the fuel. Therefore, fuels with a higher exit burnup will produce more TRUs. Also, fuels with lower mass numbers require more neutron captures to produce the higher actinides. Because thorium has a lower mass number than uranium (232 vs. 238), spent thorium fuels tend to have fewer TRUs than conventional fuels. The spent fuel production rate for reactor B is summarized in

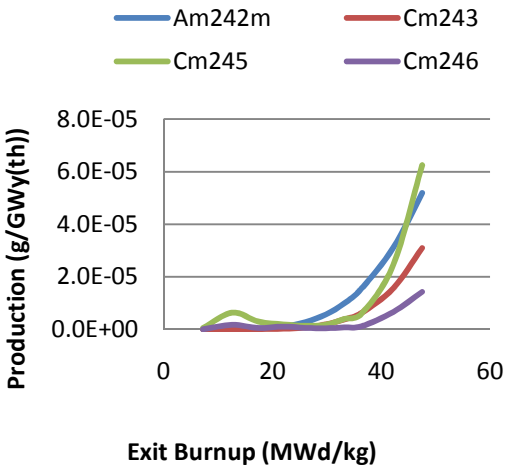

Figure 6.6. The important minor actinides and fission products are shown. The characteristics of the spent fuel are further discussed in chapter 10.

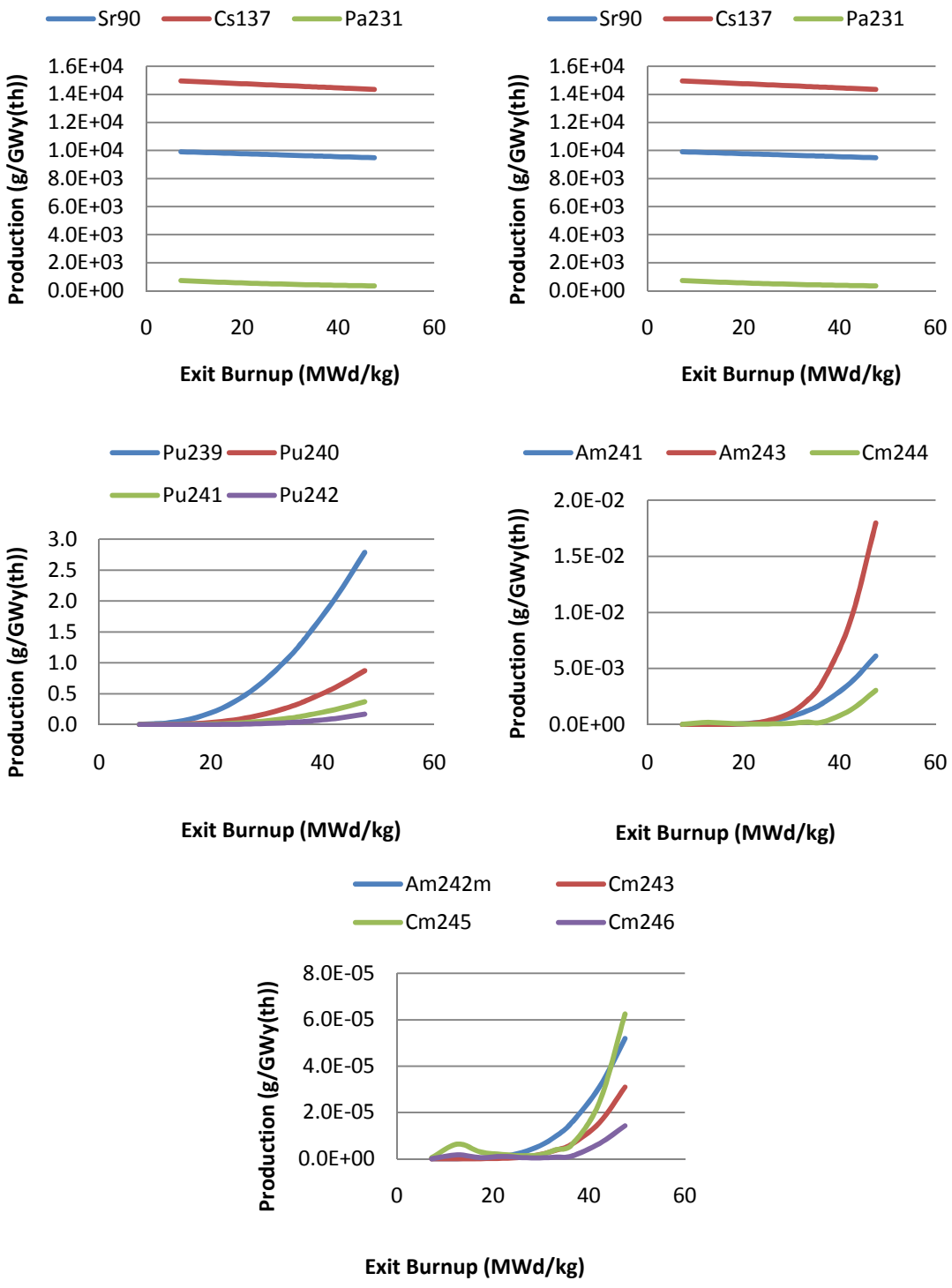

Figure 6.6 – Rate of production of transuranics and medium lived fission products in reactor B

6.4 Controllability

To conclusively determine the controllability of a reactor, a greater depth of modelling is required than is within the scope of this study. However, two metrics – the CVR and delayed β fraction – are presented in this chapter. From them, general trends and characteristics of the reactor's controllability can be ascertained.

6.4.1 Coolant Void Reactivity

Coolant void reactivity, (CVR), is a measure of the reactivity feedback due to the coolant changing from liquid phase to vapour phase. It is important because it strongly governs a reactor's response to a sudden loss of coolant. It is calculated by subtracting the reactivity of a normal-condition core from the reactivity of a core with 100% voided coolant. As the CVR is burnup dependent and a reactor with online refuelling contains fuel of varying burnup, the reactor's CVR is calculated as the average over the entire burnup. A typical NU-fuelled CANDU reactor has a CVR of approximately 10 mk averaged over all burnups. It is desirable for a new reactor design to have negative or near-zero CVR. As a minimum, the design basis should be a void reactivity equal or less than that of current CANDU reactors.

The instantaneous CVR of reactor B decreases as burnup increases, as shown in Figure 6.7. Therefore, increasing the exit burnup will decrease the average CVR. The average CVR as a function of exit burnup is shown in Figure 6.8. Although the following CVR calculations assume a reactor power 20 W/g, it can be seen that the CVR is largely independent of reactor power.

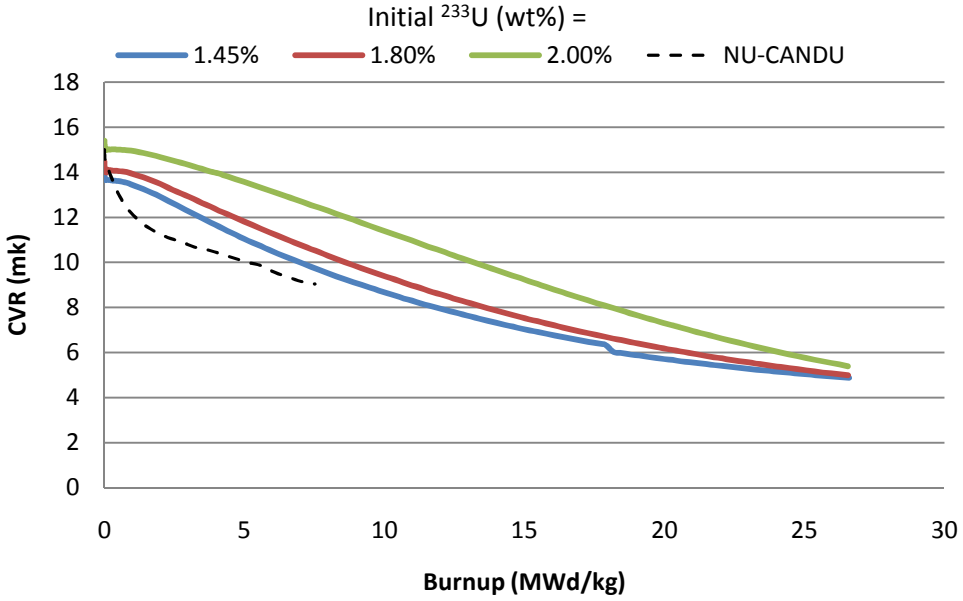

Figure 6.7 – The instantaneous CVR of reactor B with varying initial ^{233}U concentration

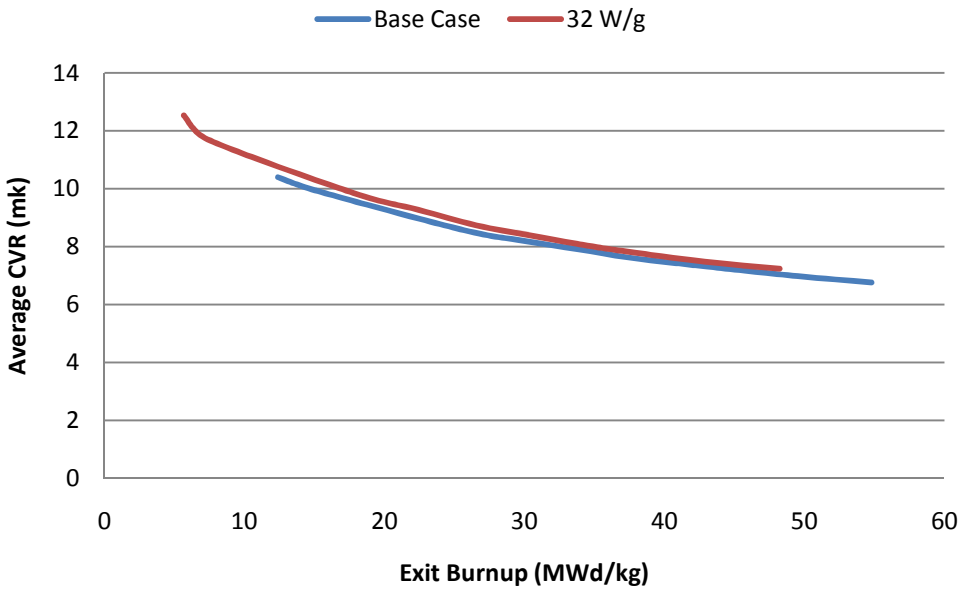

Figure 6.8 – The average CVR of reactor B for the base case and 32 W/g specific power density

For exit burnups greater than approximately 15 MWd/kg, the CVR for reactor B is lower than that of a NU-fuelled CANDU reactor. However, the values are still large and

positive. To decrease the CVR, the lattice pitch can be decreased. This is shown in Figure 6.9.

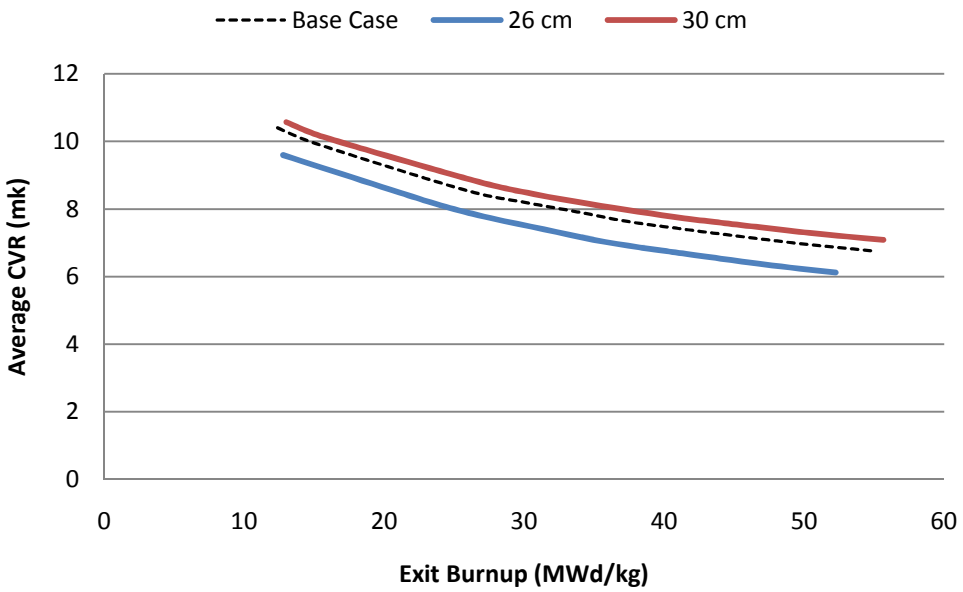

Figure 6.9 – The average CVR of reactor B with varying lattice pitch

Another means of suppressing the CVR is to introduce a poison into the centre pin of the lattice. One possible poison being considered is hafnium in zirconia. Using the natural abundances of the isotopes of these elements the overall composition would be:

Isotope	^{174}Hf	^{176}Hf	^{177}Hf	^{178}Hf	^{179}Hf	^{180}Hf
wt%	0.18	5.1	18.13	26.66	13.52	34.4

Isotope	^{90}Zr	^{91}Zr	^{92}Zr	^{94}Zr	^{96}Zr
wt%	1.03	0.23	0.34	0.35	0.06

Table 6.2 – Composition of centre pin poison

The poison displaces some of the fuel in the centre pin as shown in Figure 6.10.

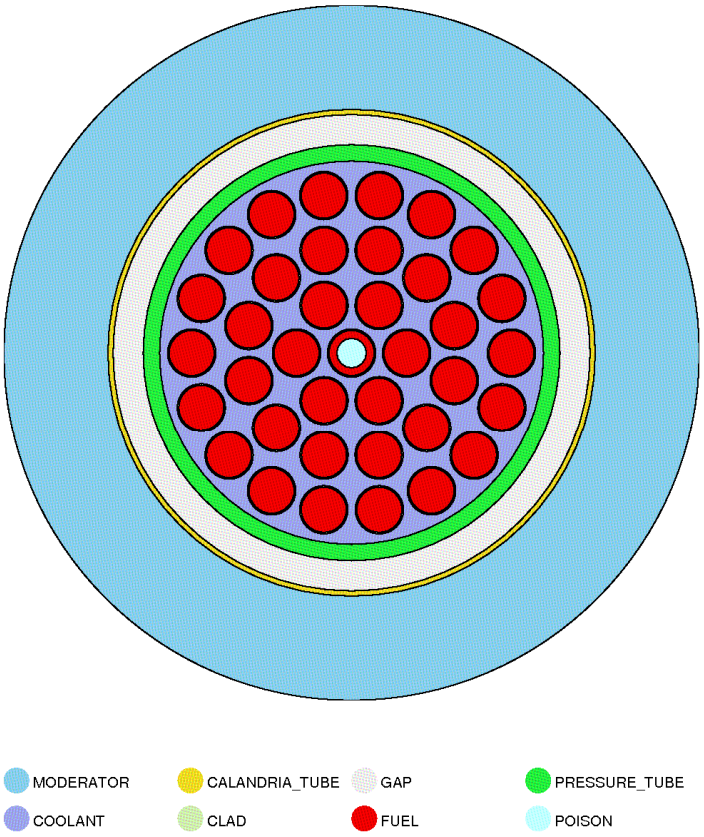

Figure 6.10 – Lattice cell with a centre pin poison

The more poison that is introduced, the greater the CVR is suppressed. This effect is shown in Figure 6.11.

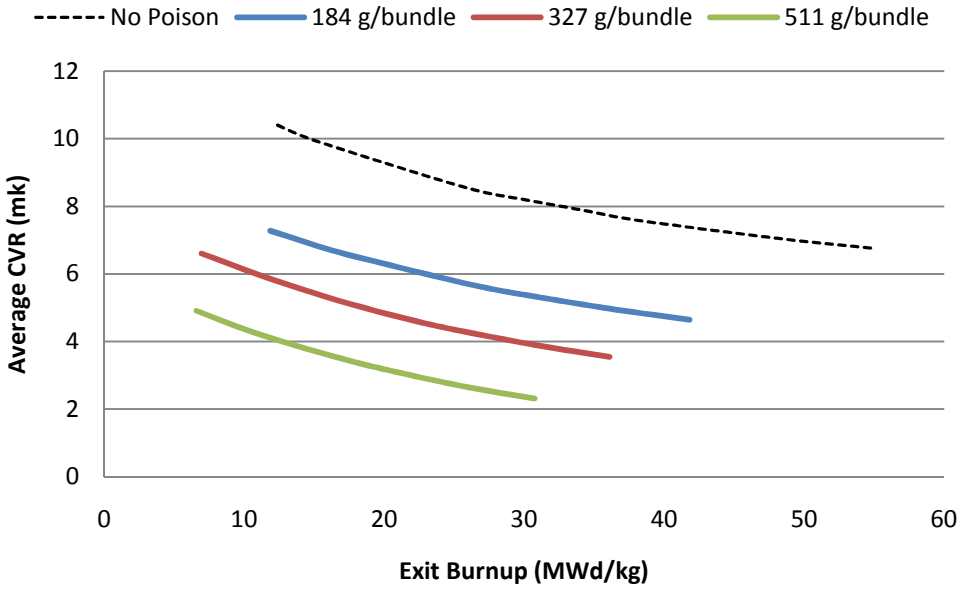

Figure 6.11 – The average CVR of reactor B with varying amounts of centre pin poison

The last considered means for suppressing CVR is to grade the enrichment by loading only the outer ring with ^{233}U. Interestingly, graded enrichment causes the CVR to increase with increasing burnup. This effect can be explained by considering that, as the burnup progresses, ^{233}U is bred in the inner rings and is consumed in the outer ring. This causes the bundle to approach the uniform fuel enrichment case which has a higher CVR. The consequences of graded enrichment are shown in Figure 6.12 and Figure 6.13.

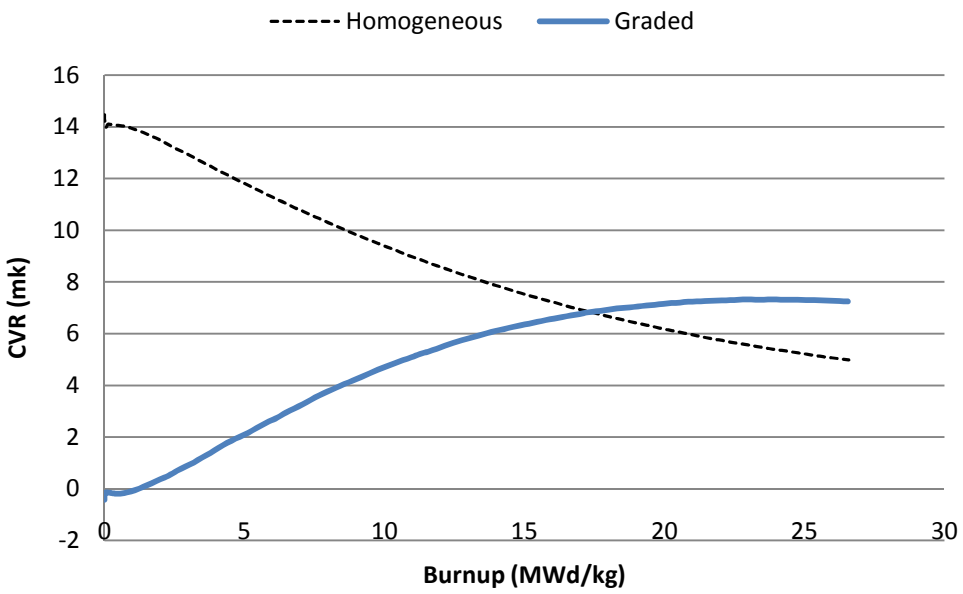

Figure 6.12 – The instantaneous CVR of reactor B with graded enrichment

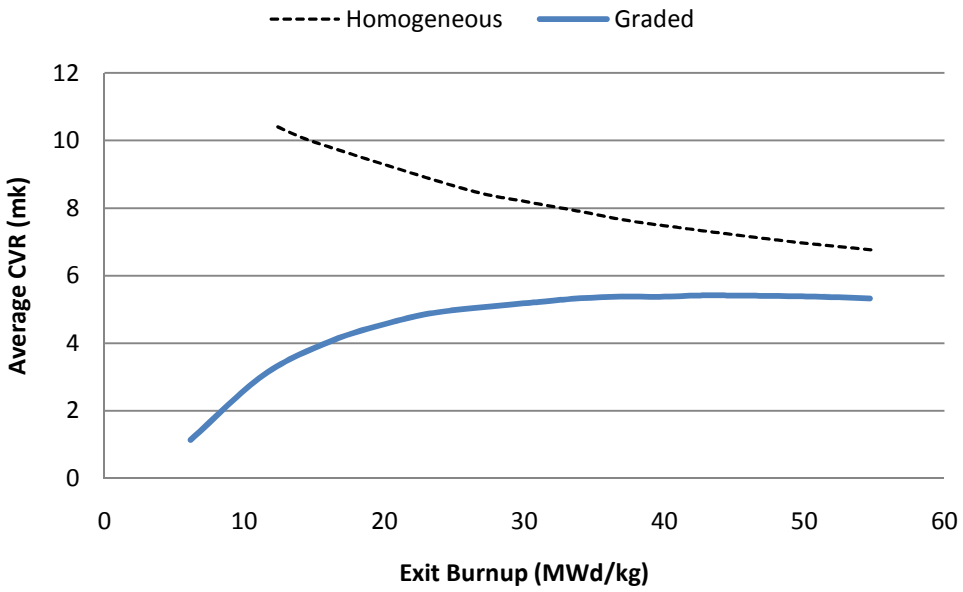

Figure 6.13 – The average CVR of reactor B with graded enrichment

Neither a centre pin poison nor graded enrichment decreases the CVR to zero. However, a negative CVR is achievable when both of these design modifications are combined as shown in Figure 6.14.

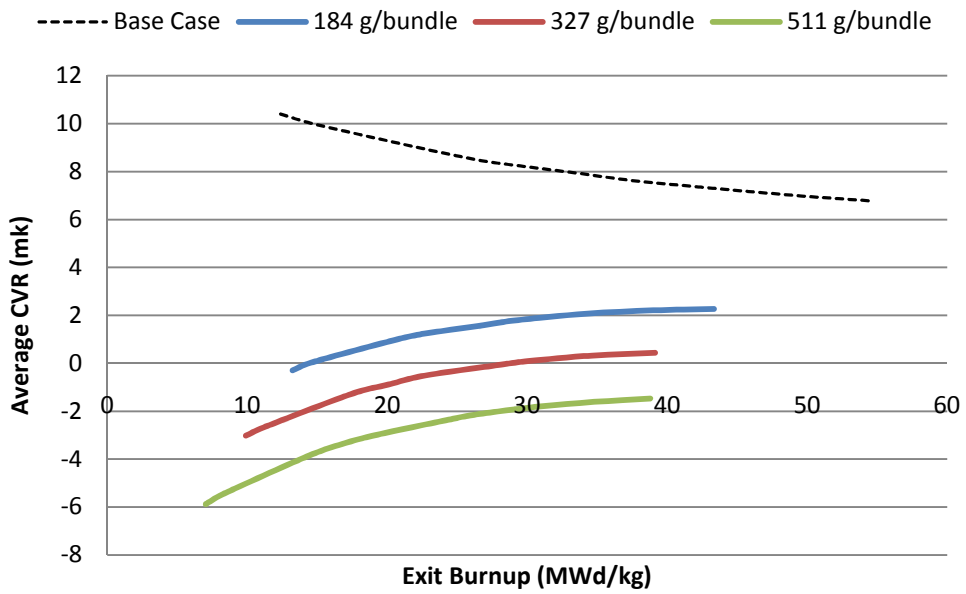

Figure 6.14 – Effect of graded enrichment and a centre poison on instantaneous CVR

Unfortunately, graded enrichment and a centre pin poison both increase the ^{233}U consumption of the reactor. This is shown in Figure 6.15 and Figure 6.16

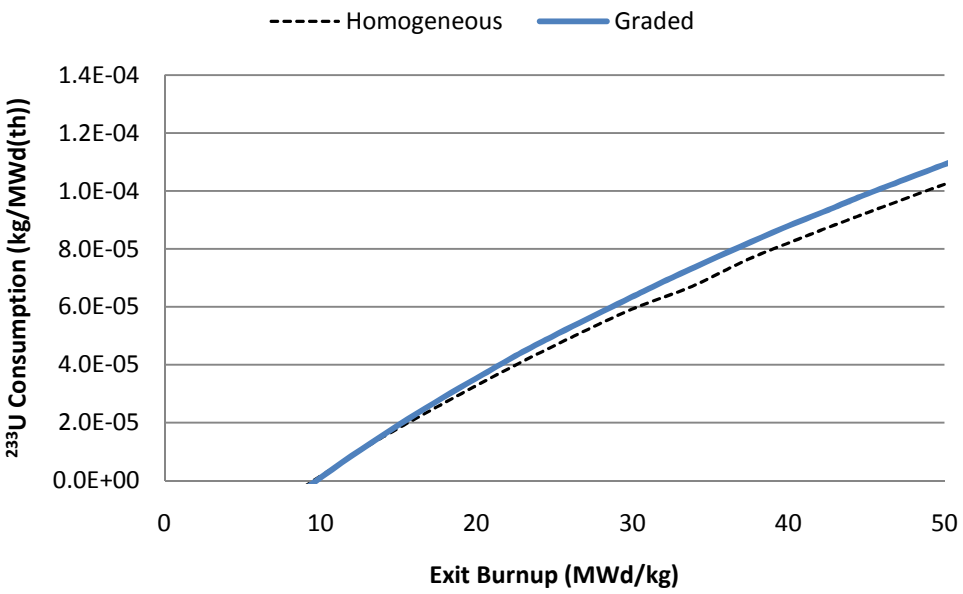

Figure 6.15 – ^{233}U consumption of reactor B with graded enrichment

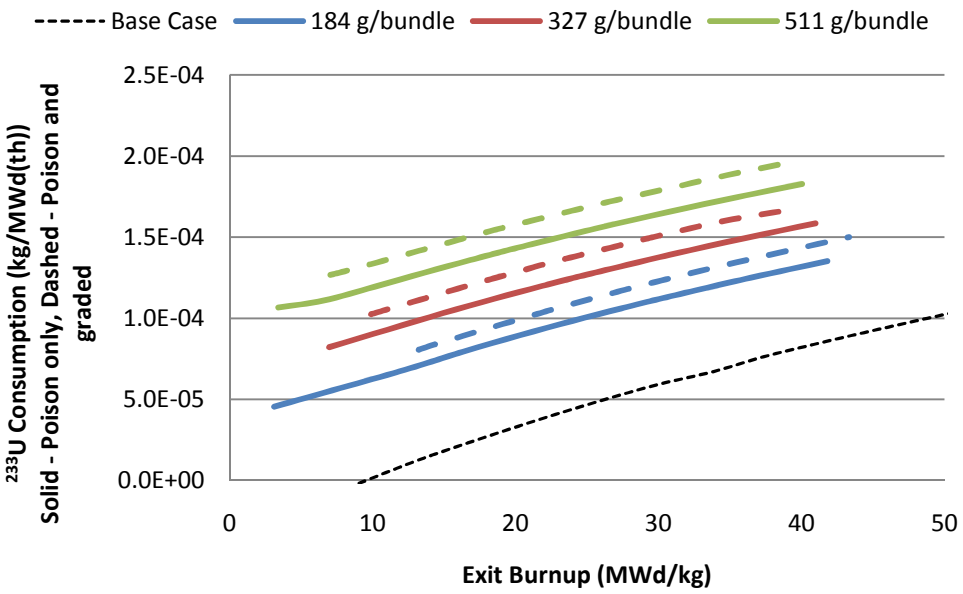

Figure 6.16 – ^{233}U consumption of reactor B with a centre pin poison and graded enrichment

Table 6.3 summarizes the changes in CVR and ^{233}U consumption relative to the base case for each design modification. It can be seen that for the base case graded

enrichment is capable of greatly suppressing the CVR while requiring a comparatively small increase in resource consumption.

Design Modification		Exit burnup (MWd/kg)	Δ CVR	Δ Consumption
Homogenous	Lattice pitch 26 cm	20	-0.66	18%
		40	-0.71	9%
	Poison 184 g/bundle	20	-3.00	176%
		40	-2.73	61%
	Poison 327 g/bundle	20	-4.46	260%
		40	-4.15	91%
	Poison 511 g/bundle	20	-6.23	344%
		40	-5.75	127%
Graded	Base	20	-4.74	8%
		40	-2.09	8%
	Poison 184 g/bundle	20	-8.42	208%
		40	-5.26	75%
	Poison 327 g/bundle	20	-10.20	301%
		40	-7.01	106%
	Poison 327 g/bundle	20	-12.19	392%
		40	-8.91	141%

Table 6.3 – Summary of the effects of reactor and bundle design on CVR and ^{233}U consumption relative to the base case

6.4.2 Delayed β fraction

Neutrons that are born from fission events are referred to as prompt neutrons while neutrons that are emitted from the fission products are referred to as delayed neutrons. If a nuclear reactor core was critical from prompt neutrons only, then even the slightest increase in reactivity would make the reactor supercritical and the reaction rate would increase exponentially at a very high rate. In practice, nuclear reactors are subcritical from prompt neutrons but achieve criticality from delayed neutrons. In this state, the rate of neutron population growth is governed by the fraction of delayed neutrons, called the delayed β fraction. The larger the delayed β fraction is, the slower the growth. This allows more time for the reactor's reactivity control mechanisms to act.

Therefore, the delayed β fraction is an inherent measure of reactor safety. The β yield, v_d, of the various isotopes is shown in Table 6.4 [5]. As can be seen, the β yield of ^{233}U is less than that of ^{235}U and ^{241}Pu and only slightly larger than ^{239}Pu. This leads to smaller delayed β fractions in thorium fuels than NU fuel.

Isotope	**^{232}Th**	**^{233}U**	**^{235}U**	**^{238}U**	**^{239}Pu**	**^{240}Pu**	**^{241}Pu**
v_d	0.0527	0.0074	0.01668	0.046	0.00645	0.009	0.0157

Table 6.4 – Delayed β yield of various isotopes

In Figure 6.17, it is shown that the delayed β fraction is largely independent of initial ^{233}U content and is less than that of a NU-fuelled CANDU reactor over the entire burnup. This emphasizes the need for suppressed reactivity coefficients.

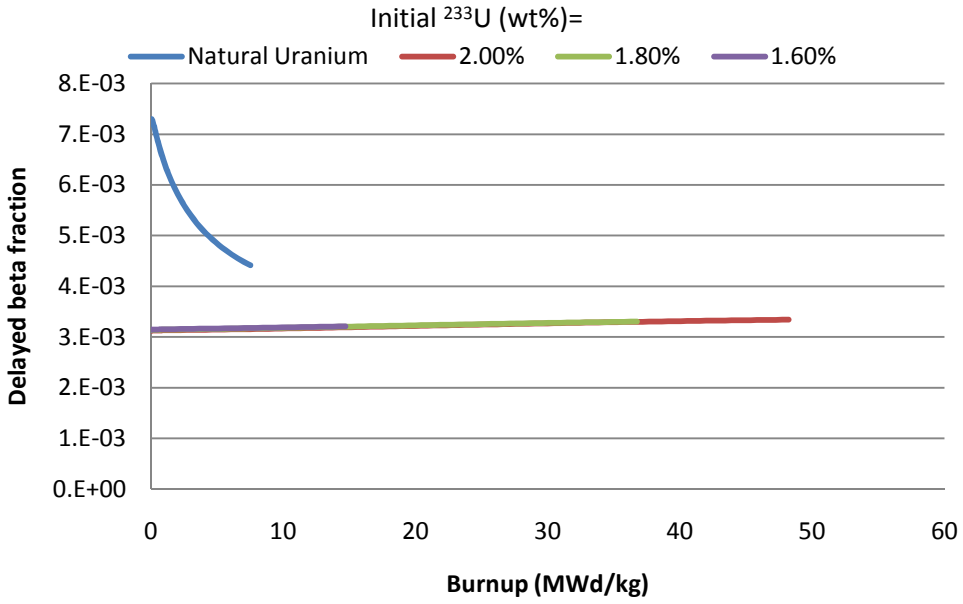

Figure 6.17 – Delayed β fraction in reactor B for varying initial ^{233}U concentration

7 Reactor A

The fuel cycles outlined in chapter 4 have a net even production and consumption of ^{233}U. As was shown in the previous chapter, reactor B is a net consumer

of ^{233}U. Therefore, a reactor that produces ^{233}U is also required. In this chapter, it will be demonstrated that, by adding another fissile driver, reactor A can produce more ^{233}U than it consumes. Three driver fuels are considered: plutonium, MOX (mixed-oxide), and LEU (low-enriched uranium). Other than the composition of the fuel, the design of reactor A is consistent with that of reactor B.

7.1 Plutonium Driver

This chapter examines variant 1 in which reactor A is a thorium-, plutonium-, and ^{233}U-fuelled CANDU reactor. The plutonium is derived from the spent fuel of the LWR outlined in chapter 5.2 and is assumed to be separated with no contamination. Later in this chapter, variant 3 will also be examined where the plutonium is derived from spent CANDU fuel.

7.1.1 Fissile Inventories

Adding plutonium allows the reactor to achieve higher exit burnups than reactor B while maintaining a CR > 1 as shown in Figure 7.1.

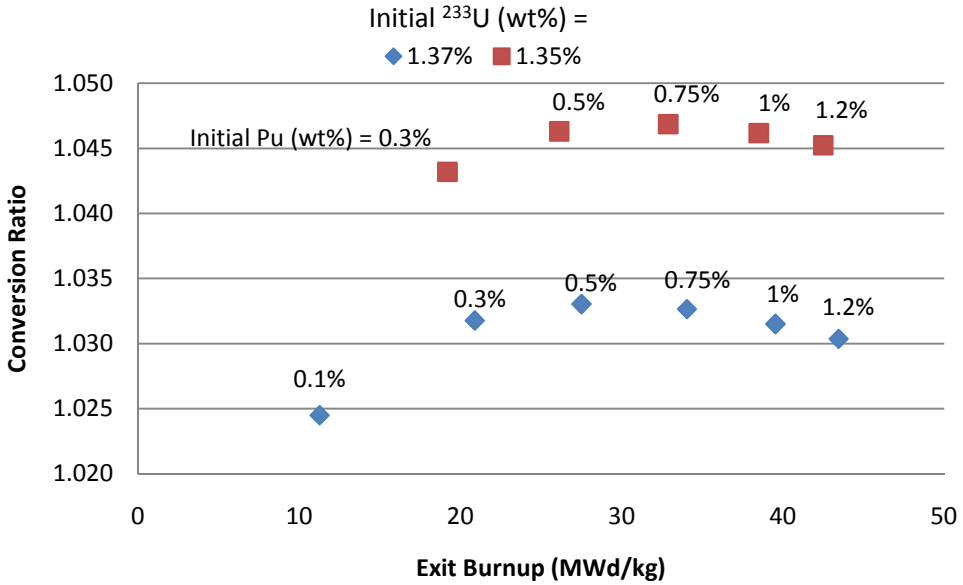

Figure 7.1 – Conversion ratio of a (Th,^{233}U,Pu)-fuelled CANDU reactor

Figure 7.2 gives an explanation as to why a maximum CR can be seen in the above figure. Although increased plutonium loading increases the CR for a given burnup, it does not necessarily lead to a higher CR at the exit burnup.

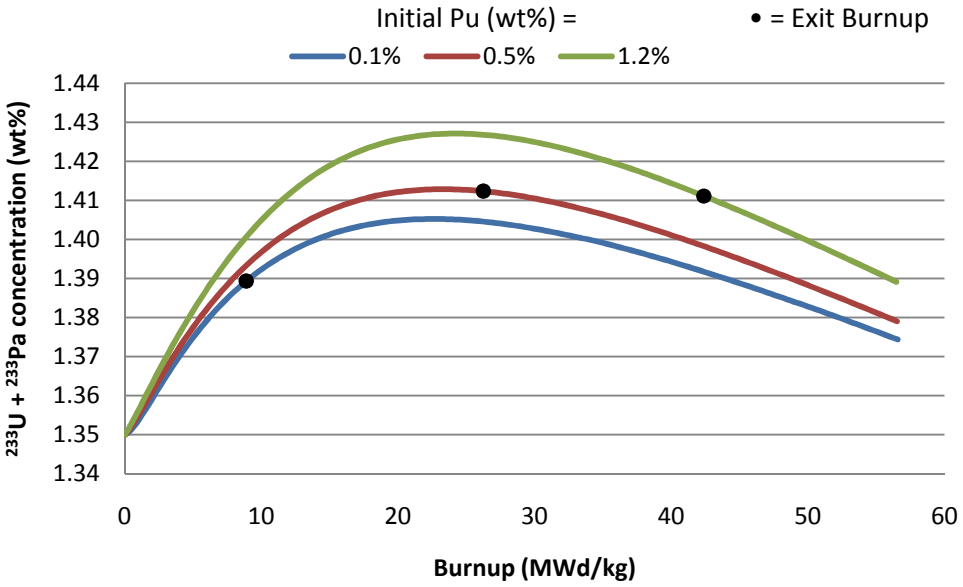

Figure 7.2 – ^{233}U and ^{233}Pa concentration of a (Th,^{233}U,Pu)-fuelled CANDU reactor

The rate of driver fuel consumption in reactor A is inversely proportional the exit burnup and directly proportional to the amount of driver fuel loaded in the reactor. This relationship is given by equation (7.1).

$$C_i = \frac{M_i}{BU} \tag{7.1}$$

where C_i is the consumption rate of driver fuel i in kg/MWd(th), M_i is the mass fraction of the driver fuel and BU is the exit burnup MWd/kg.

For the same exit burnup, a reactor loaded with less ^{233}U must be loaded with more plutonium. This translates into a greater rate of ^{233}U production but also a greater rate of plutonium consumption. This is shown in Figure 7.3.

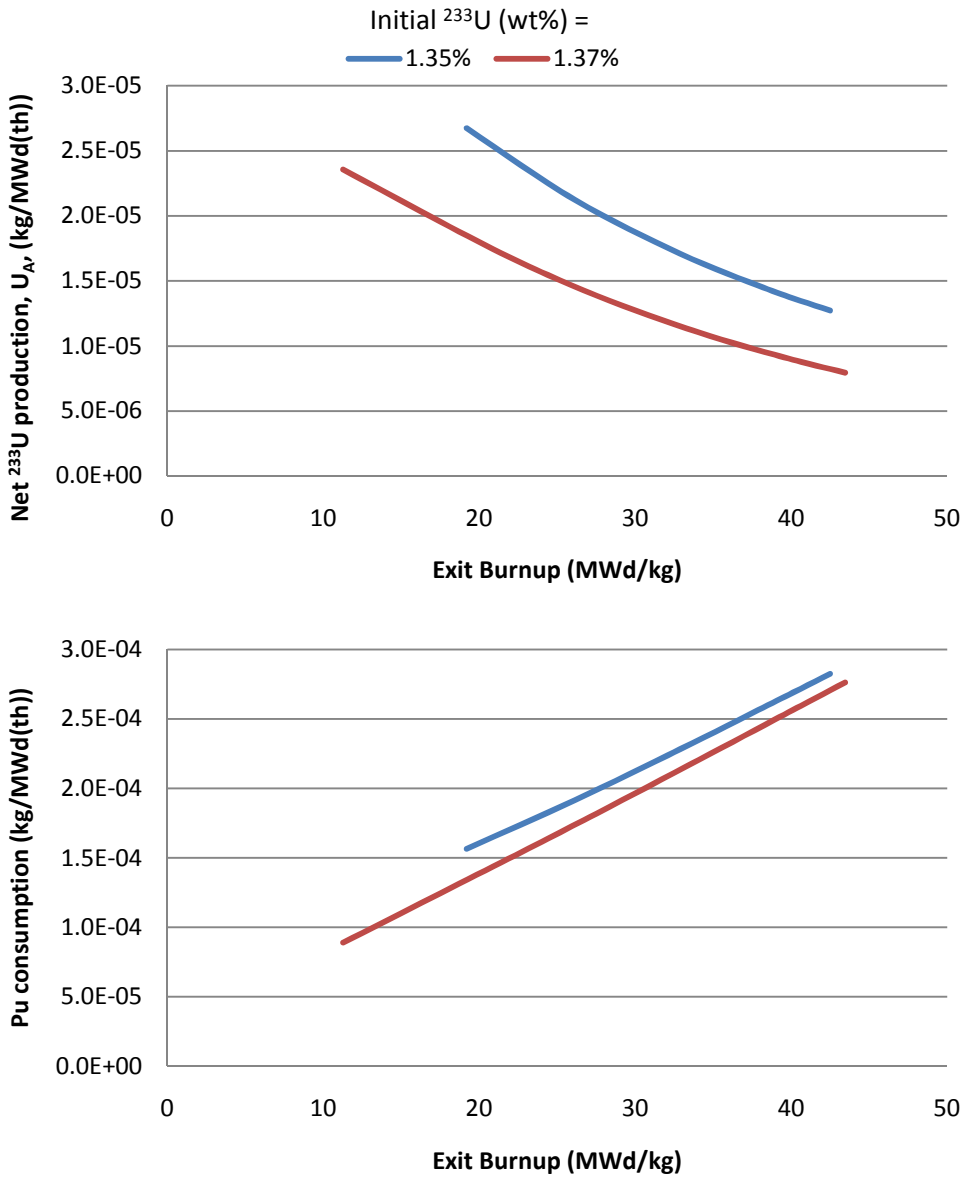

Figure 7.3 – ^{233}U production and plutonium consumption rates of a (Th,^{233}U,Pu)-fuelled CANDU reactor

7.1.2 Sensitivity

Reactor A was tested for sensitivity to the following design changes:

- Parasitic absorption increased to 35 mk from 30 mk
- Reprocessing losses doubled to 1%
- Reactor specific power density at 18, 22, and 32 W/g
- Lattice pitch changed to 26 cm and 30 cm
- Fuel bundle heterogeneity
- Fissile content of plutonium changed by ± 10%

Figure 7.4 shows the sensitivity of ^{233}U production and plutonium consumption in reactor A to increased parasitic absorption and reprocessing losses. In contrast to reactor B, ^{233}U production increases with increasing parasitic absorption. This can be explained by referring back to Figure 7.1. The CR tends to increase for small decreases in exit burnup and it would be expected for ^{233}U production to exhibit the same behaviour. However, increased parasitic absorption also increases the plutonium consumption. ^{233}U reprocessing losses have no effect on plutonium consumption.

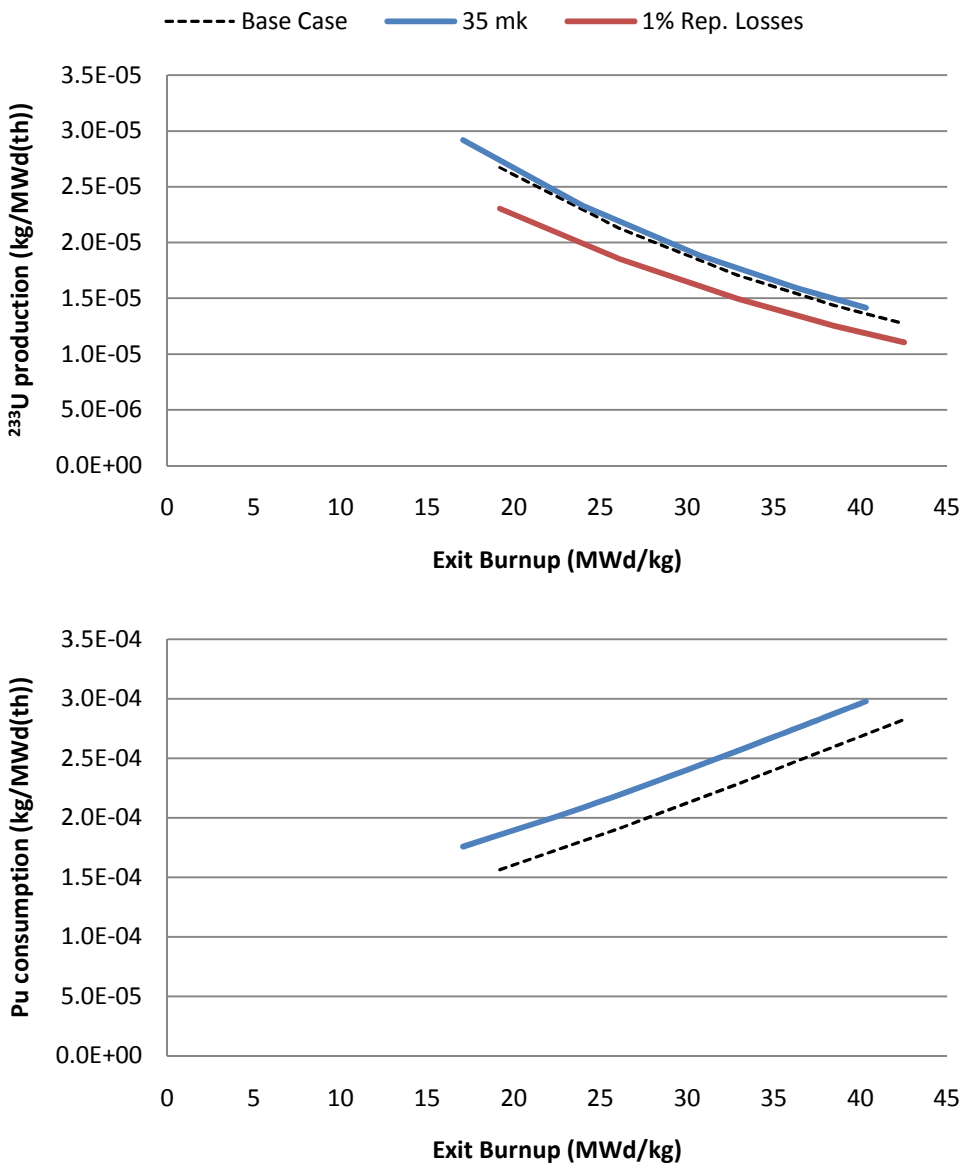

Figure 7.4 – Sensitivity of ^{233}U production and plutonium consumption in a (Th,^{233}U,Pu)-fuelled CANDU reactor to increased parasitic absorption and reprocessing losses

Figure 7.5 and Figure 7.6 show the effect of varying the specific power density and lattice pitch. As expected, reactor A exhibits similar behaviour to reactor B.

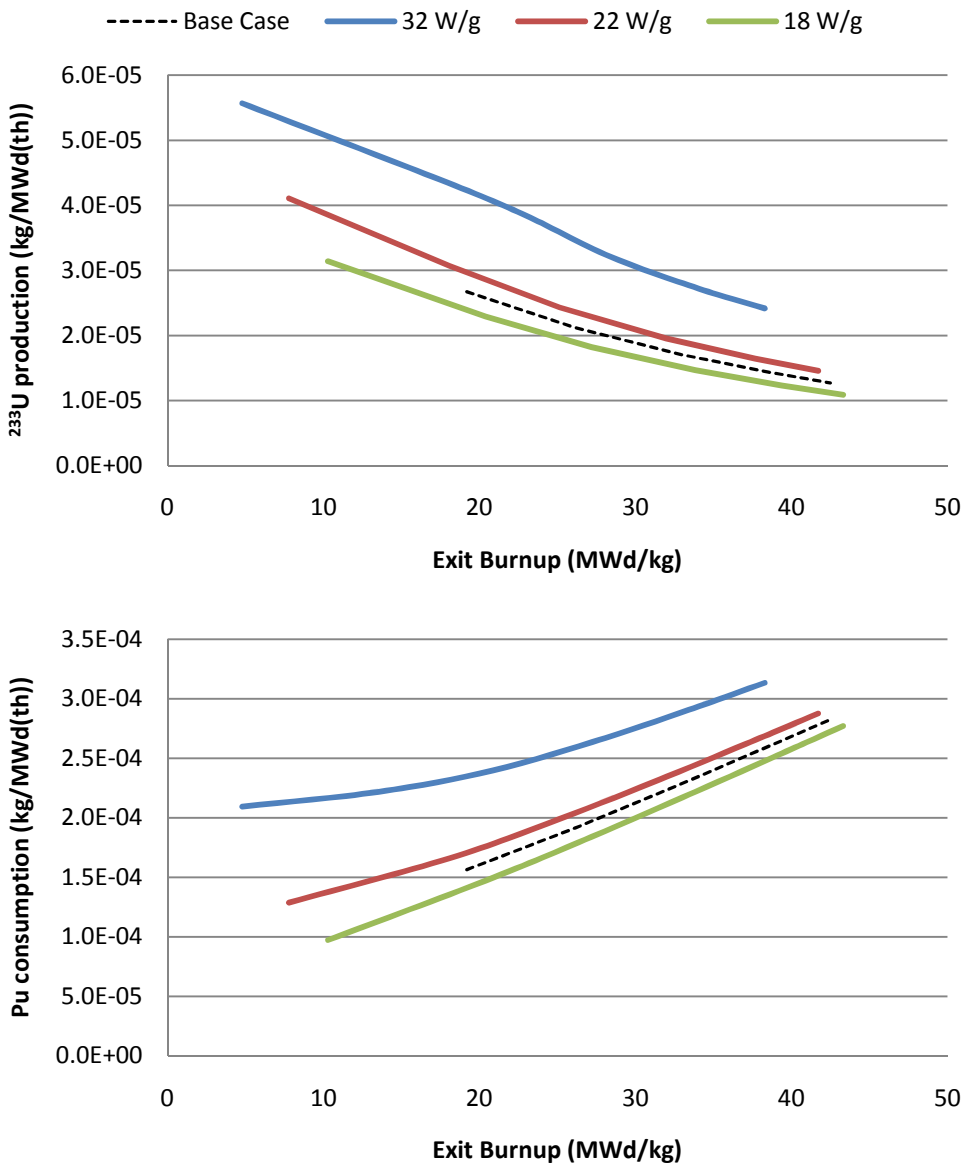

Figure 7.5 – Sensitivity of ^{233}U production and plutonium consumption in a (Th,^{233}U,Pu)-fuelled CANDU reactor to changes in specific power density

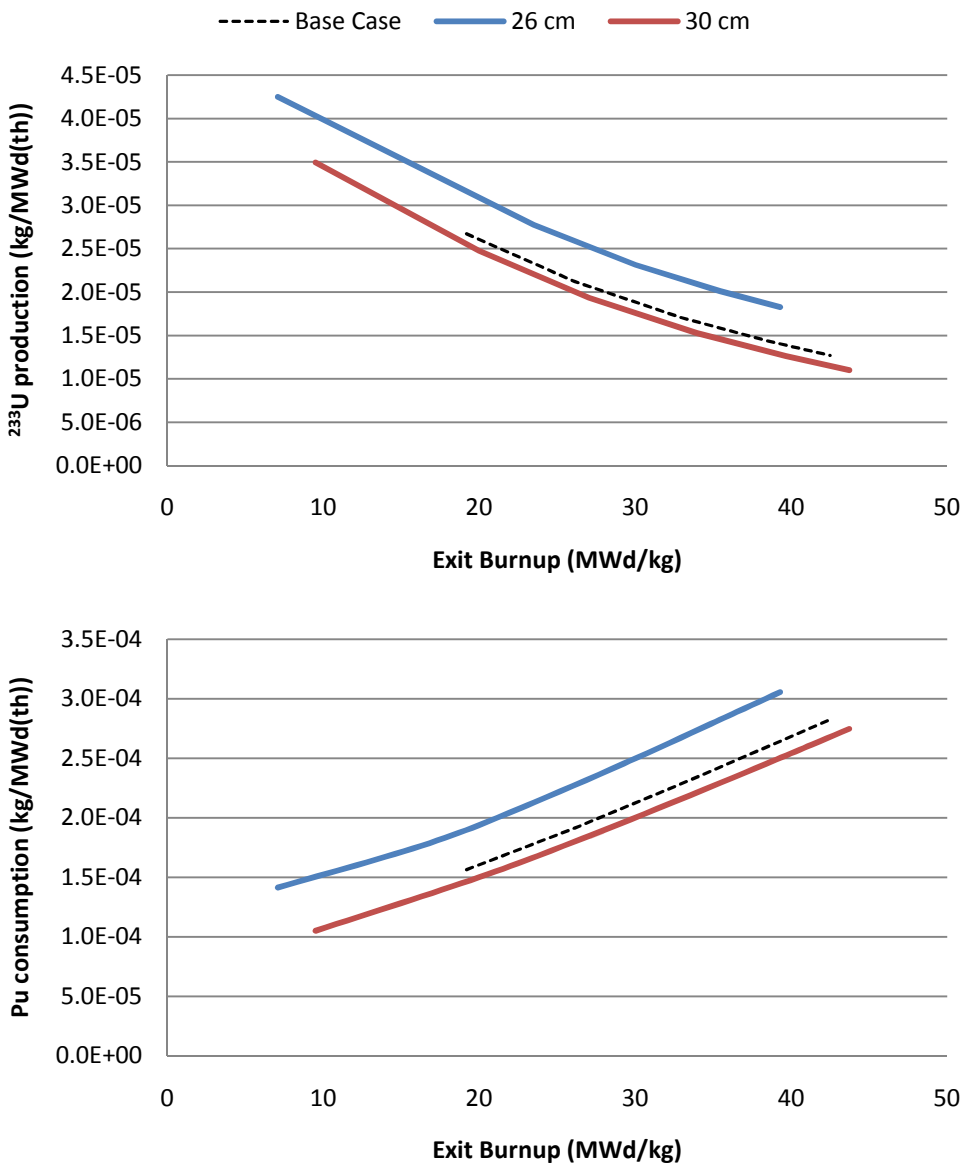

Figure 7.6 – Sensitivity of ^{233}U production and plutonium consumption in a (Th,^{233}U,Pu)-fuelled CANDU reactor to changes in lattice pitch

The isotopics of spent LWR fuel will vary between reactors and within the reactor itself. Therefore, it is important to test the thorium reactor's sensitivity to such changes. To do so, the fissile content of the plutonium was varied by ± 10%. Decreasing the fissile content of the plutonium in the spent LWR fuel decreases the exit burnup of reactor A

and, similarly to increased parasitic absorption, results in an increase in ^{233}U production. However, it also results in a large increase in plutonium consumption.

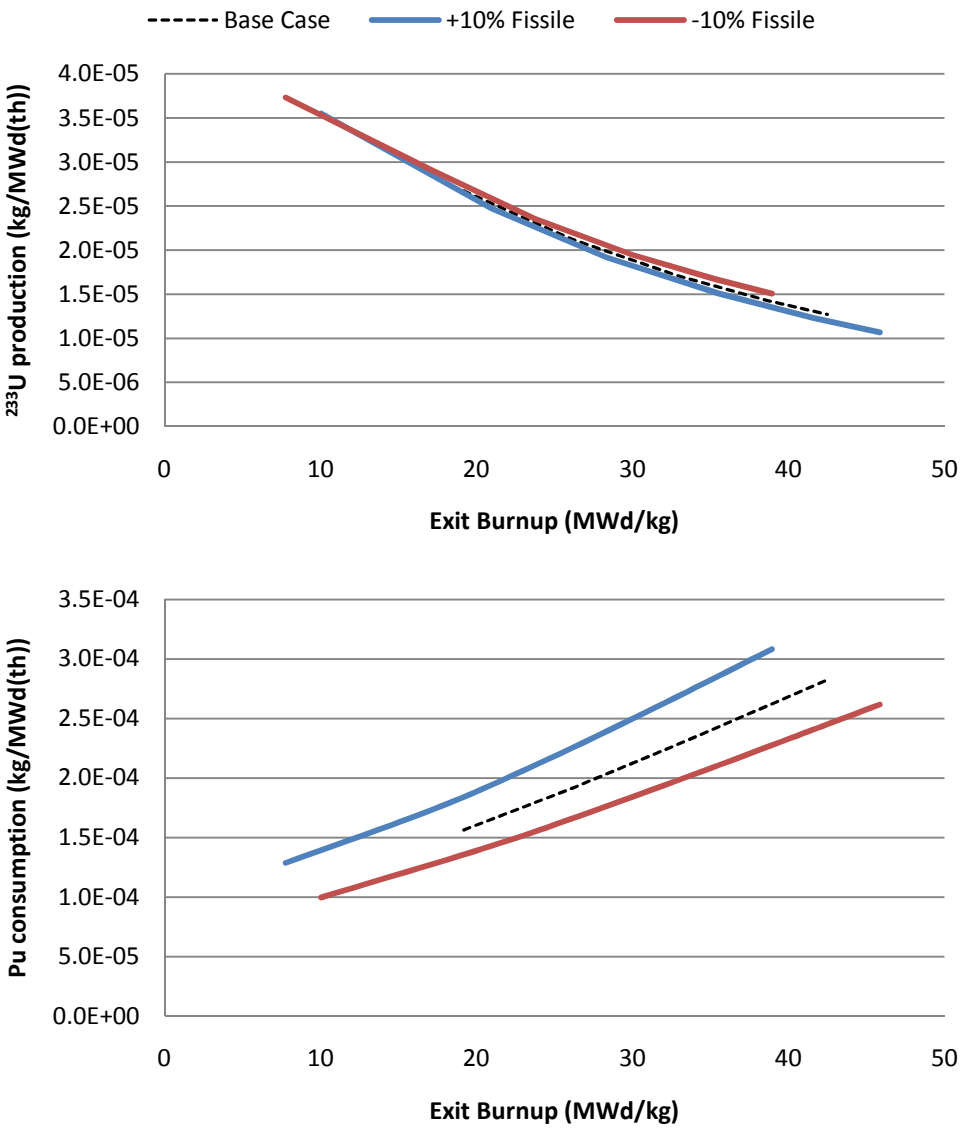

Figure 7.7 – Sensitivity of ^{233}U production and plutonium consumption in a (Th,^{233}U,Pu)-fuelled CANDU reactor to changes in isotopic composition of plutonium in spent LWR fuel

The sensitivity of ^{233}U production and plutonium consumption in reactor A is summarized in Table 7.1.

Parameter changed	Change in ^{233}U Production at Exit Burnup (MWd/kg)		Change in Pu Consumption at Exit Burnup (MWd/kg)	
	20	**40**	**20**	**40**
Increase in parasitic absorption to 35 mk	2.24%	4.59%	18.15%	10.41%
Reprocessing losses doubled to 1%	-13.24%	-11.94%	n/a	n/a
Reactor power decreased to 18 W/g	-10.46%	-10.61%	-9.08%	-3.89%
Reactor power increased to 22 W/g	10.89%	13.19%	9.62%	3.87%
Reactor power increased to 32 W/g	57.48%	64.83%	48.36%	20.60%
Lattice pitch decreased to 26 cm	18.13%	30.99%	22.15%	16.37%
Lattice pitch increased to 30 cm	-4.56%	-9.04%	-5.80%	-5.26%
Fissile content increased by 10%	-1.24%	-6.52%	-12.81%	-13.38%
Fissile content decreased by 10%	2.30%	8.03%	18.25%	17.96%

Table 7.1 – Summary of sensitivity of ^{233}U production in plutonium consumption in a (Th,^{233}U,Pu)-fuelled CANDU reactor

7.1.3 Spent Fuel

Adding plutonium leads to higher concentrations of TRUs in the spent fuel. However, adding ^{233}U allows the fuel to achieve the same exit burnup with less plutonium, leading to smaller concentrations of TRUs in the spent fuel. This is shown in

Figure 7.8. The consequences of this will be further discussed in chapter 10.

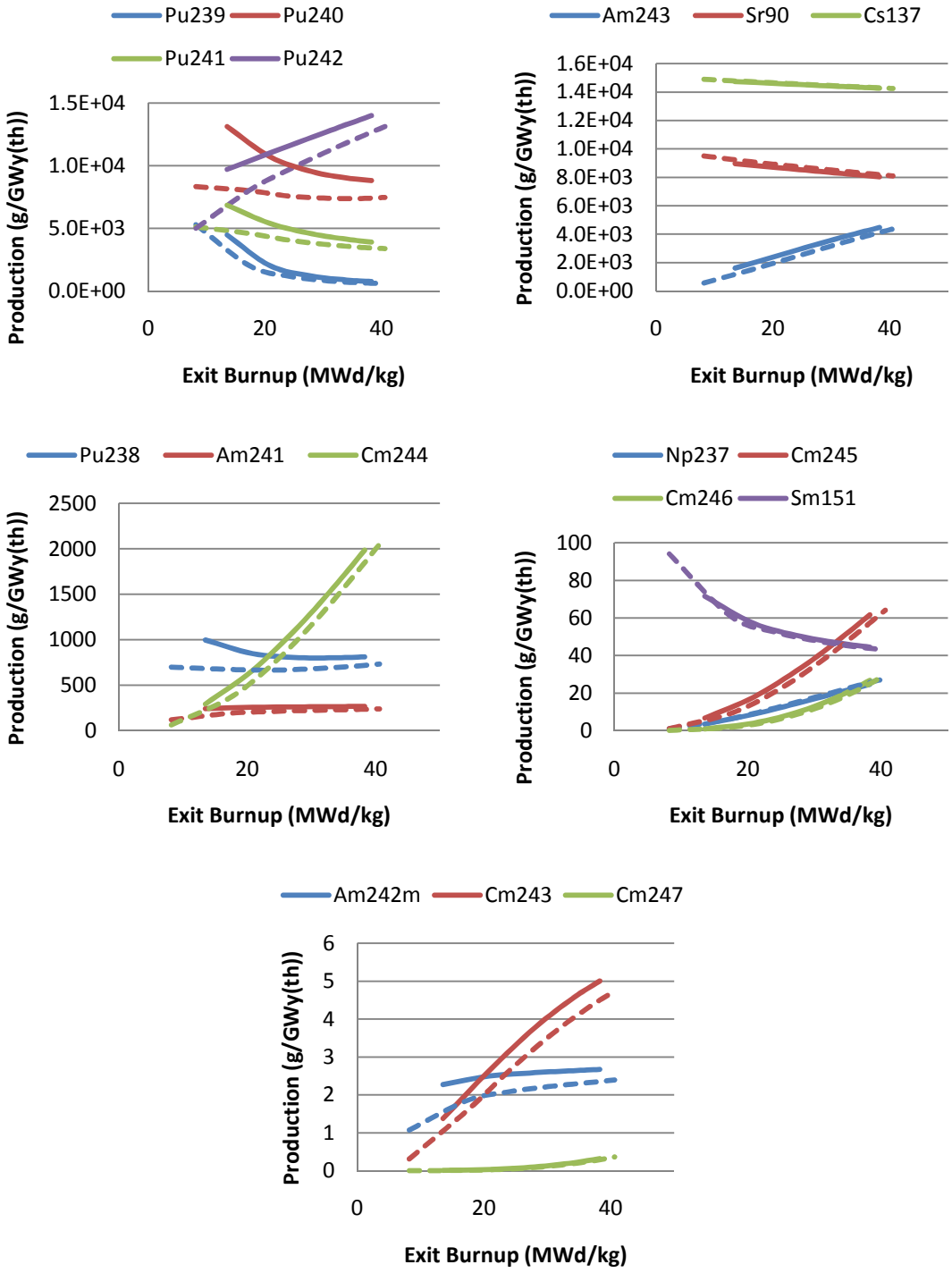

Figure 7.8 – Rate of production of minor actinides and medium lived fission products in a (Th,^{233}U,Pu)-fuelled CANDU reactor with 1.35% (solid) and 1.40% (dashed) initial ^{233}U concentration

7.1.4 Controllability

7.1.4.1 Coolant Void Reactivity

Figure 7.9 and Figure 7.10 show the CVR in reactor A. Adding plutonium increases the instantaneous CVR of the reactor but also increases the exit burnup, decreasing the average CVR.

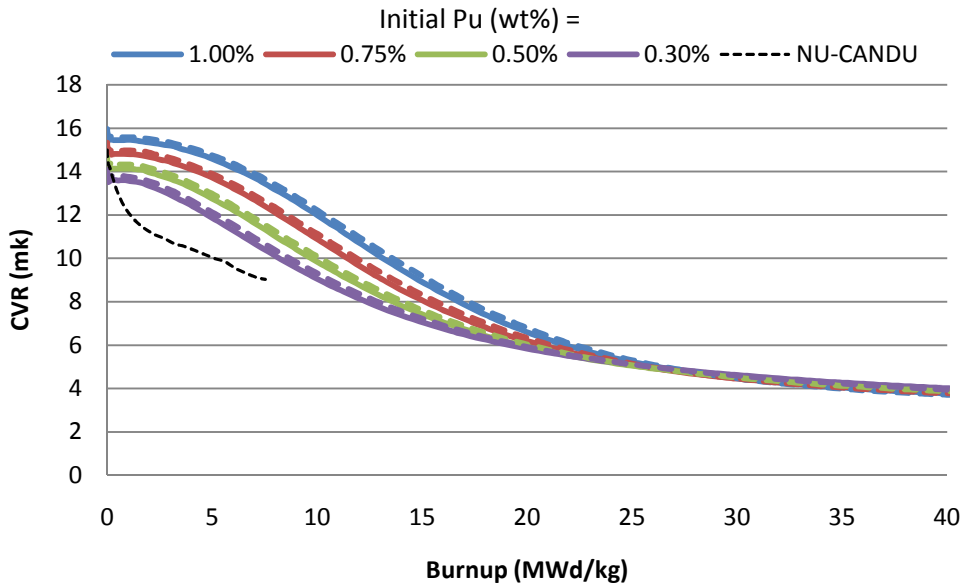

Figure 7.9 – Instantaneous CVR of a (Th,^{233}U,Pu)-fuelled CANDU reactor with 1.35% (solid) and 1.40% (dashed) initial ^{233}U concentration

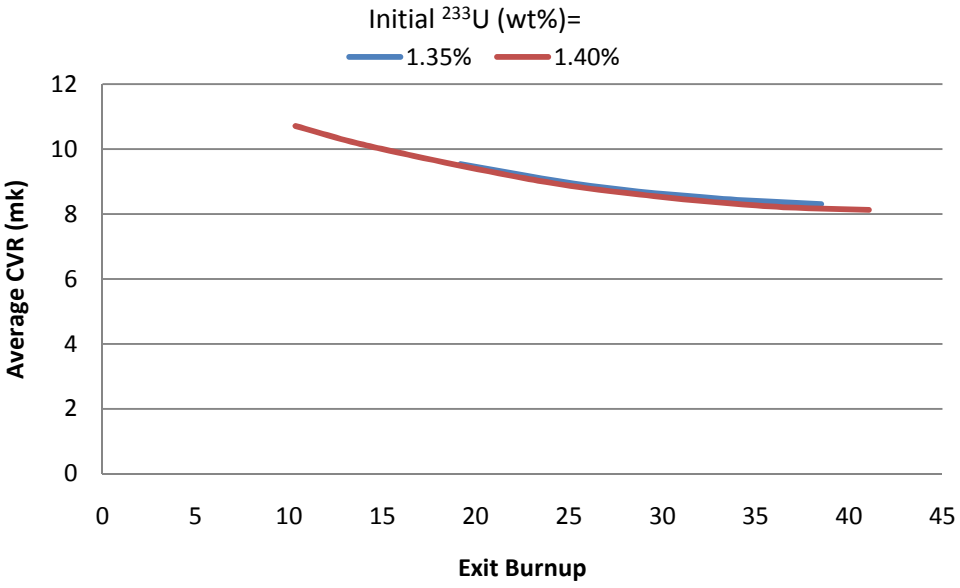

Figure 7.10 – Average CVR of a (Th,^{233}U,Pu)-fuelled CANDU reactor

The effect on CVR of plutonium and uranium heterogeneity was tested. Figure 7.11 shows the instantaneous CVR when the different fissile components are loaded only in the outer ring of the fuel bundle.

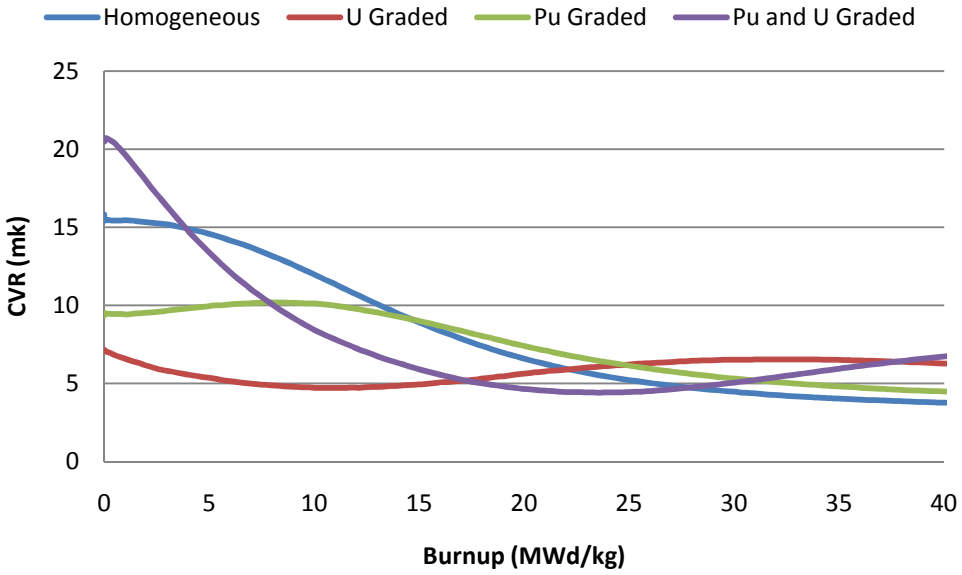

Figure 7.11 – Instantaneous CVR of a (Th,^{233}U,Pu)-fuelled CANDU reactor with graded enrichment

Figure 7.12 shows the effect of each design modification on the average CVR of reactor A. As can be seen, graded uranium enrichment exhibits a greater suppression of the CVR than graded plutonium enrichment. Near-zero and even negative CVRs are achievable when graded enrichment is combined with the centre pin poison described in Table 6.2.

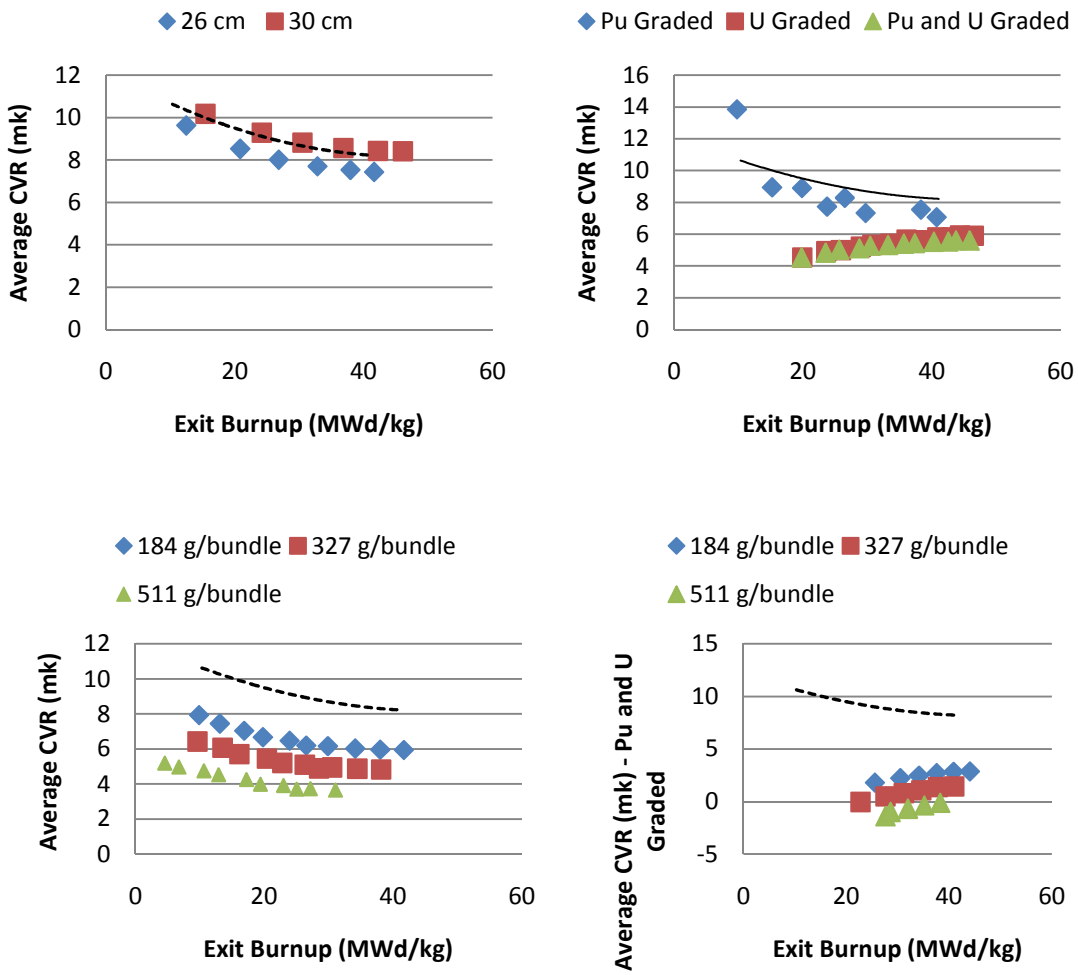

Figure 7.12 – Average CVR of a (Th,^{233}U,Pu)-fuelled CANDU reactor with graded enrichment, a centre poison, and changed lattice pitch. The dashed line shows the base case

Introducing a centre pin poison increases the ^{233}U production but also greatly increases the plutonium consumption as shown in Figure 7.13.

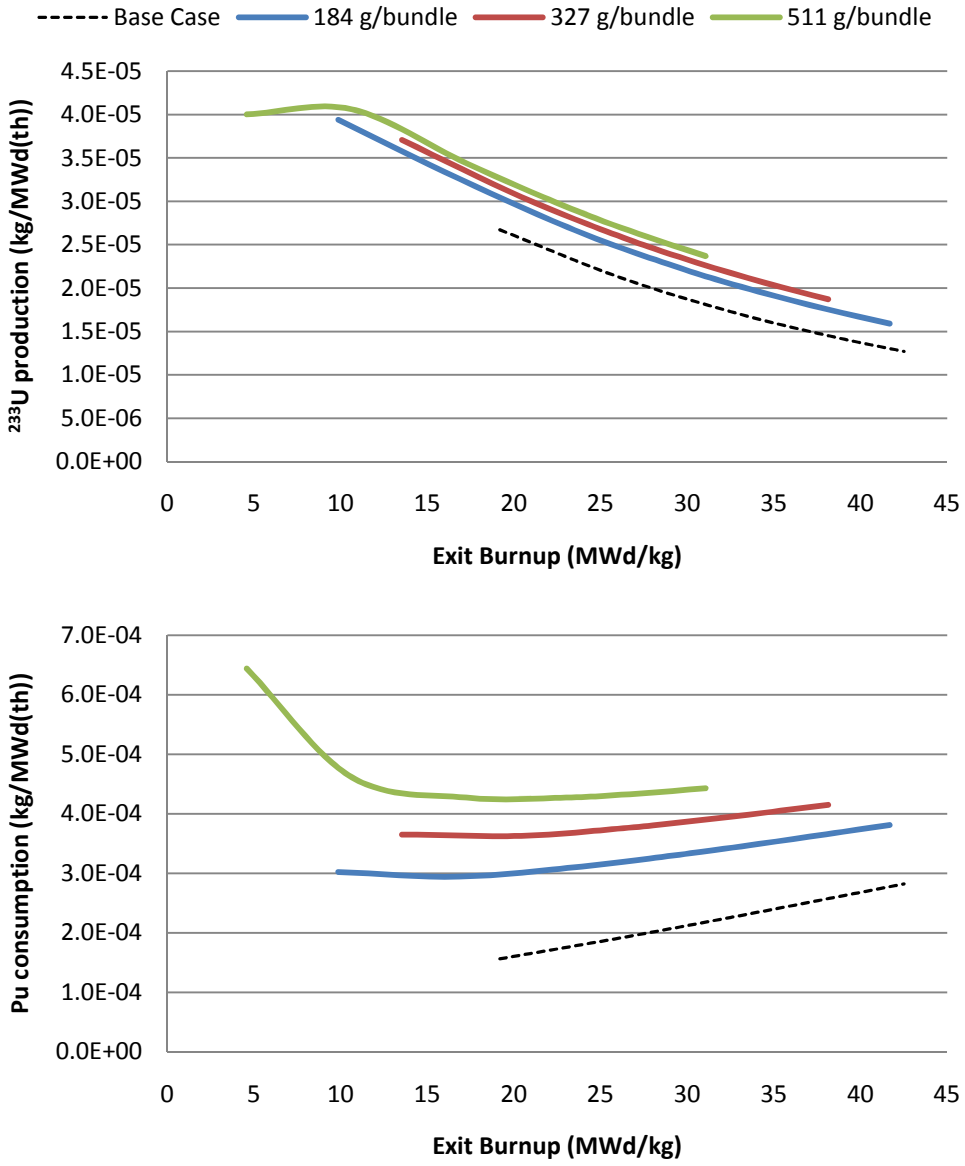

Figure 7.13 – ^{233}U production and plutonium consumption of a (Th,^{233}U,Pu)-fuelled CANDU reactor with a centre poison

Grading the plutonium enrichment has little effect on the mass flows but grading the uranium enrichment greatly decreases both the ^{233}U production and the plutonium consumption rates. This is shown in Figure 7.14.

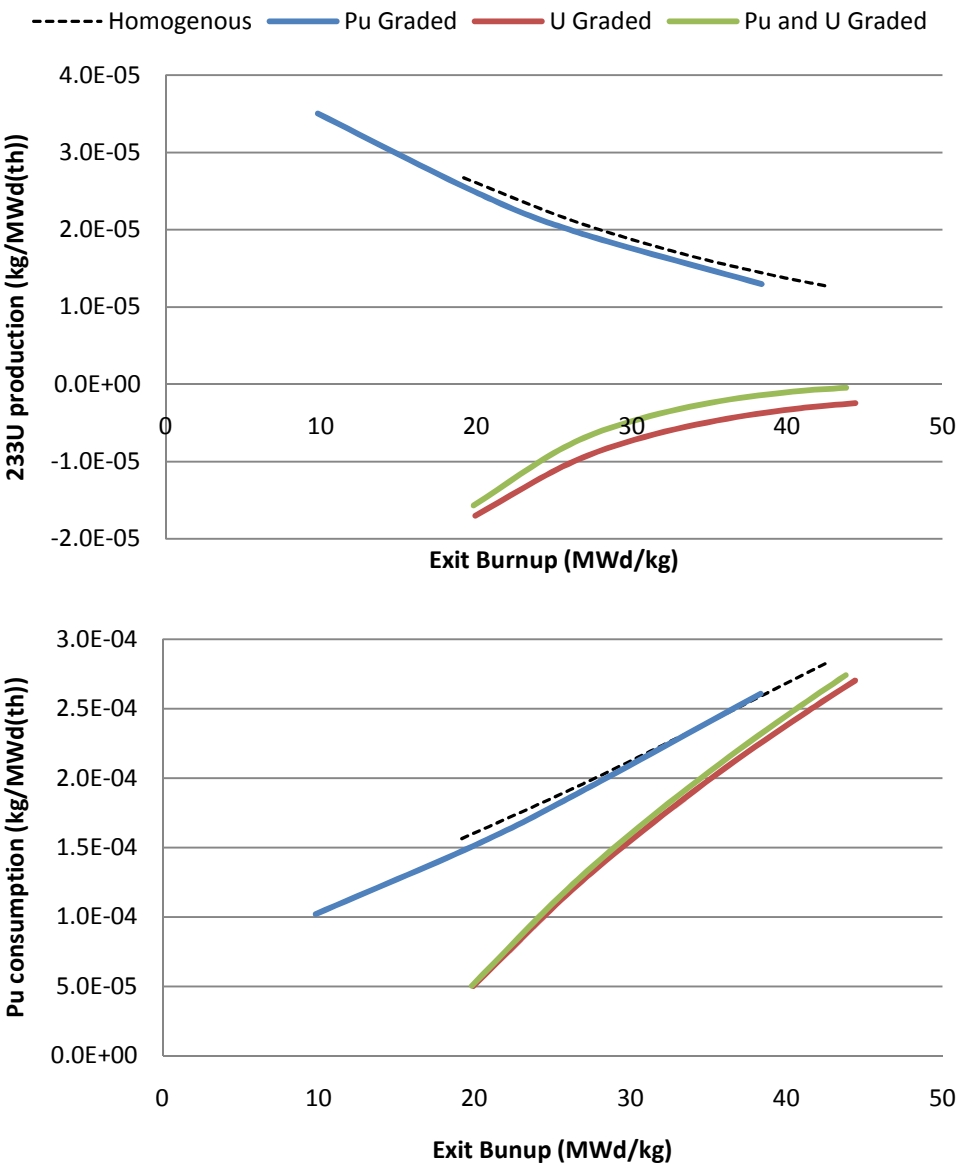

Figure 7.14 – ^{233}U production and plutonium consumption of a (Th,^{233}U,Pu)-fuelled CANDU reactor with graded enrichment

7.1.4.2 Delayed β Fraction

The reactor's delayed β fraction exhibits a small dependence on the plutonium concentration and, similarly to reactor A, is always lower than that of a NU-fuelled CANDU reactor. This is shown in Figure 7.15.

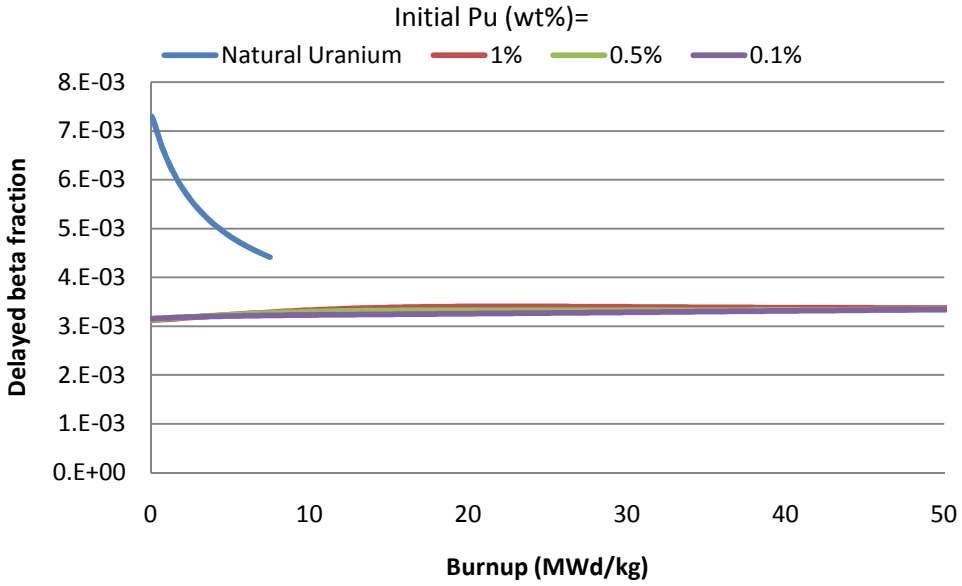

Figure 7.15 – Delayed β of a (Th,^{233}U,Pu)-fuelled CANDU reactor

7.1.5 CANDU-Derived Plutonium

For variant 3, reactor A is loaded with CANDU-derived plutonium. The plutonium vector in the spent fuel from a NU-fuelled CANDU reactor is given in Table 7.2.

Isotope	^{238}Pu	^{239}Pu	^{240}Pu	^{241}Pu	^{242}Pu
wt%	0.11	65.69	27.74	4.84	1.62

Table 7.2 – Plutonium vector in the spent fuel from a NU-fuelled CANDU reactor

The fissile content of CANDU-derived plutonium is very similar to that of LWR-derived plutonium (70.53% vs. 70.05%). However, the CANDU-derived plutonium has a higher ^{239}Pu concentration (65.69% vs. 55.08%) and a correspondingly lower ^{241}Pu concentration (4.84% vs. 14.97). Figure 7.16 shows that this results in in both higher ^{233}U production and plutonium consumption.

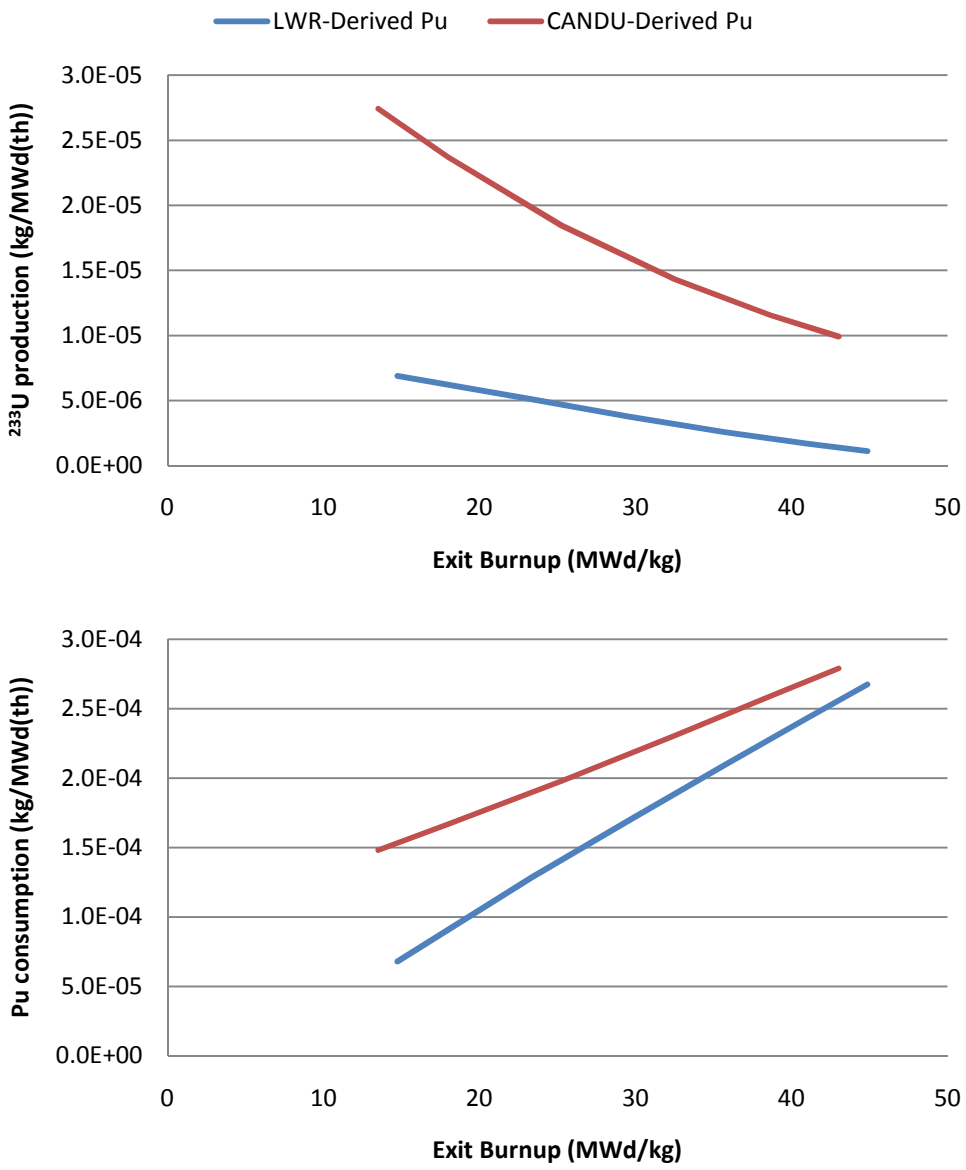

Figure 7.16 – ^{233}U production and plutonium consumption of a (Th,^{233}U,Pu)-fuelled CANDU reactor with CANDU-derived plutonium

7.2 Mixed-Oxide Driver

In variant 2 the thorium fuel cycle is driven by uranium and plutonium that is co-precipitated from spent LWR fuel. In general, MOX fuel can consist of any two oxides.

However, commonly, as well as in this thesis, it refers strictly to a mixture of plutonium and uranium oxides.

As it is difficult to separate spent fuel isotopically, the higher isotopes of uranium must be kept separate from the thorium and ^{233}U. To do this, four heterogeneous bundle designs are considered:

Centre	Inner	Intermediate	Outer	%MOX
MOX	MOX	Th,^{233}U	Th,^{233}U	18.92
Th,^{233}U	MOX	Th,^{233}U	Th,^{233}U	16.22
Th,^{233}U	Th,^{233}U	MOX	Th,^{233}U	32.42
Th,^{233}U	Th,^{233}U	Th,^{233}U	½ - Th,^{233}U ½ - MOX	24.32

Table 7.3 – Configuration of heterogeneous bundles for MOX-driven reactor

In the last case in Table 7.3, the pins in the outer ring alternate between thorium and MOX fuel. This is shown in Figure 7.17.

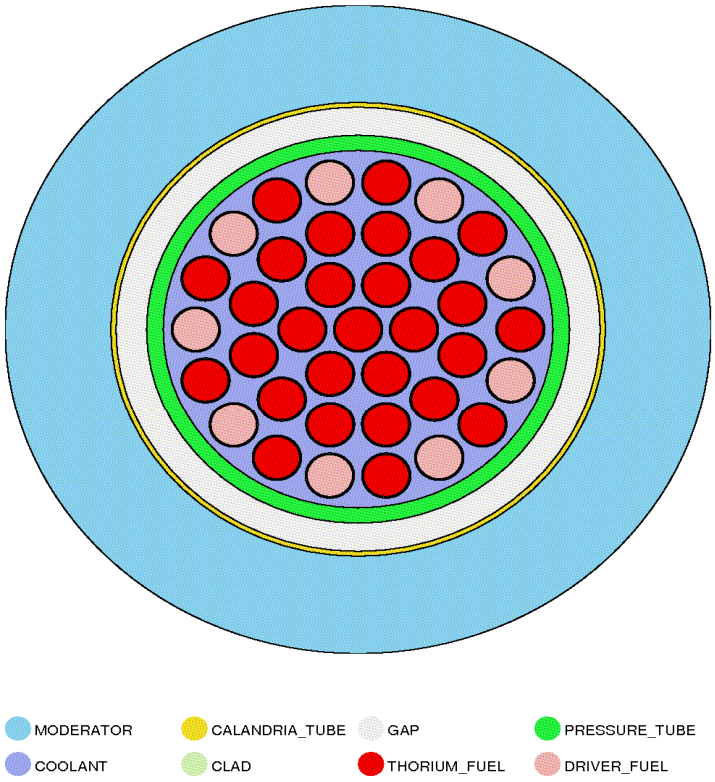

Figure 7.17 - Lattice cell with driver in alternating pins in the outer ring

To compare the effects of MOX loading, homogenous cases are also considered. As is standard in many MOX fuels, it is assumed that the plutonium is enriched to 9% of the fuel by weight during reprocessing [46]. Only the full power case (i.e. 32 W/g) is considered for this variant.

7.2.1 Fissile Inventories

Figure 7.18 shows the effect of MOX loading on uranium production and MOX consumption rates. Similarly as to what was seen in chapter 7.1, increased exit burnup results in lower ^{233}U production and driver-fuel consumption.

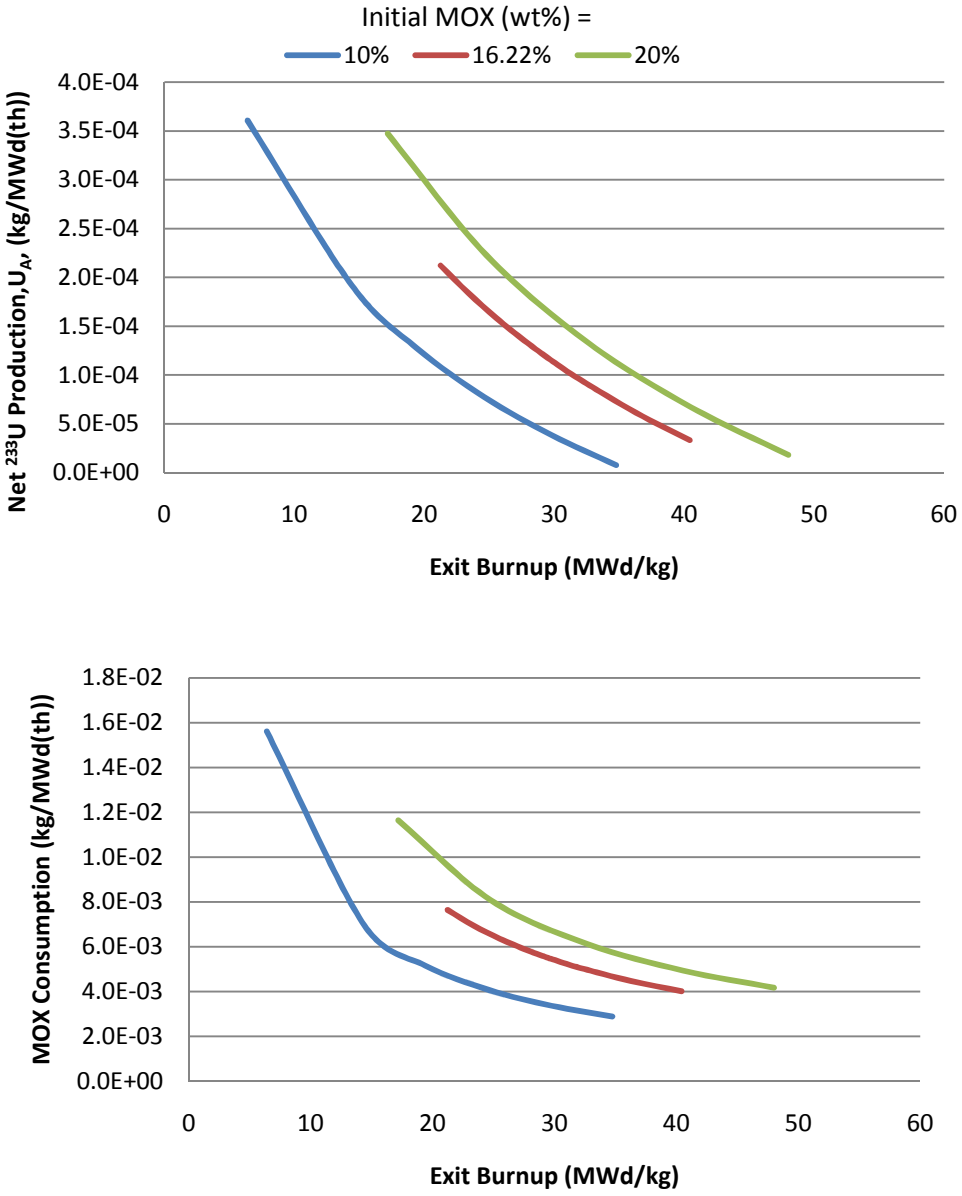

Figure 7.18 – ^{233}U production and MOX consumption rates of a (Th,^{233}U,MOX)-fuelled CANDU reactor with a homogenous lattice

This trend is consistent when the fuel is graded as shown in Figure 7.19.

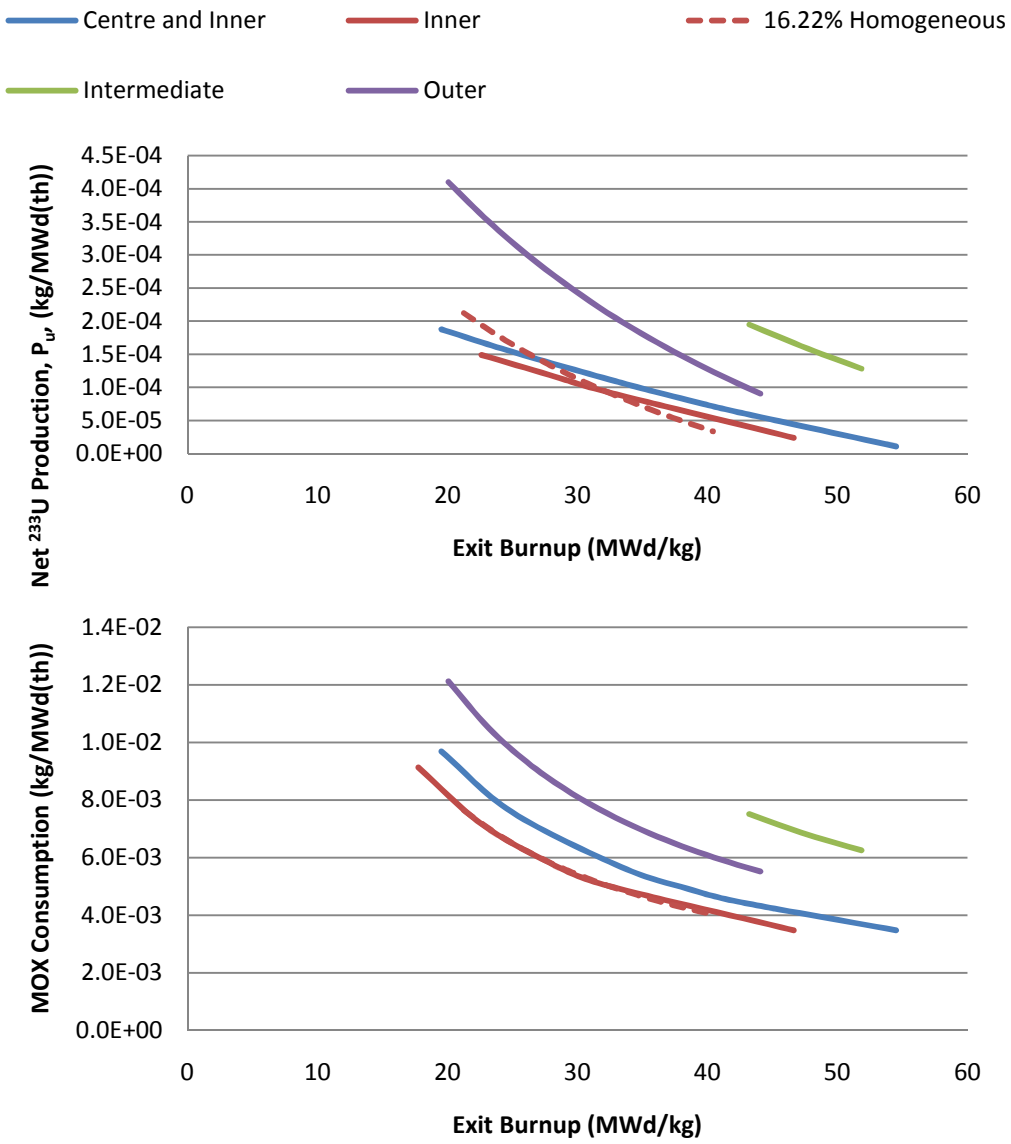

Figure 7.19 – ^{233}U production and MOX consumption of a (Th,^{233}U,MOX)-fuelled CANDU reactor with a heterogeneous lattice

7.2.2 Spent Fuel

The MOX-fuel is less fissile than the pure plutonium, leading to more of it being required to drive the thorium fuel. As a consequence of this, MOX-driven thorium fuel contains more TRUs than plutonium-driven thorium fuel. MOX fuel also contains the

higher isotopes of uranium which weren't present in spent plutonium-driven thorium fuel. The composition of the spent fuel is shown in Figure 7.20.

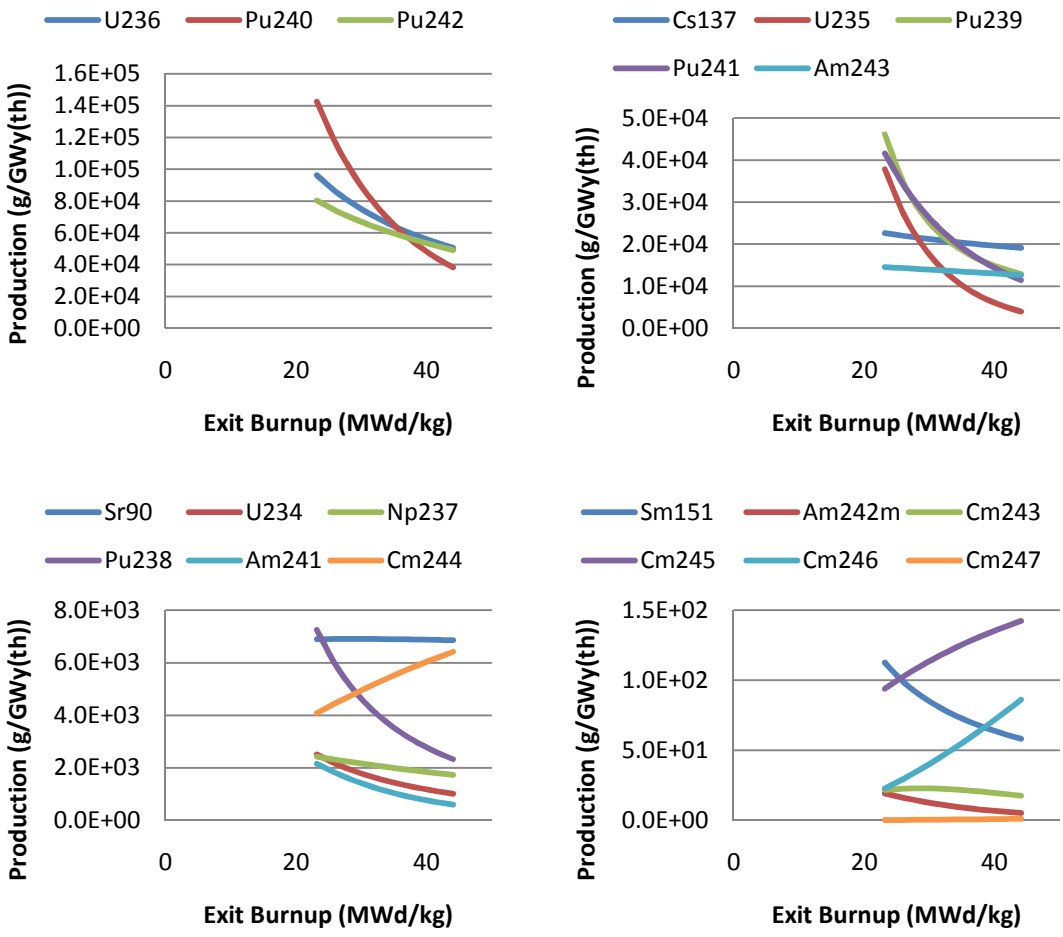

Figure 7.20 – Rate of production of minor actinides and medium lived fission products in a (Th,^{233}U,MOX)-fuelled CANDU reactor with MOX in alternating pins in the outer ring

7.2.3 Controllability

7.2.3.1 Coolant Void Reactivity

The average CVR of the homogenous cases with MOX driver are higher than the equilibrium CVR of a NU-fuelled CANDU reactor, 10 mk. However, when the driver fuel is situated in only the outer ring, there is a significant reduction in CVR. The reverse is true

when the driver fuel is situated in the inner half of the lattice. This is shown in Figure 7.21 and Figure 7.22.

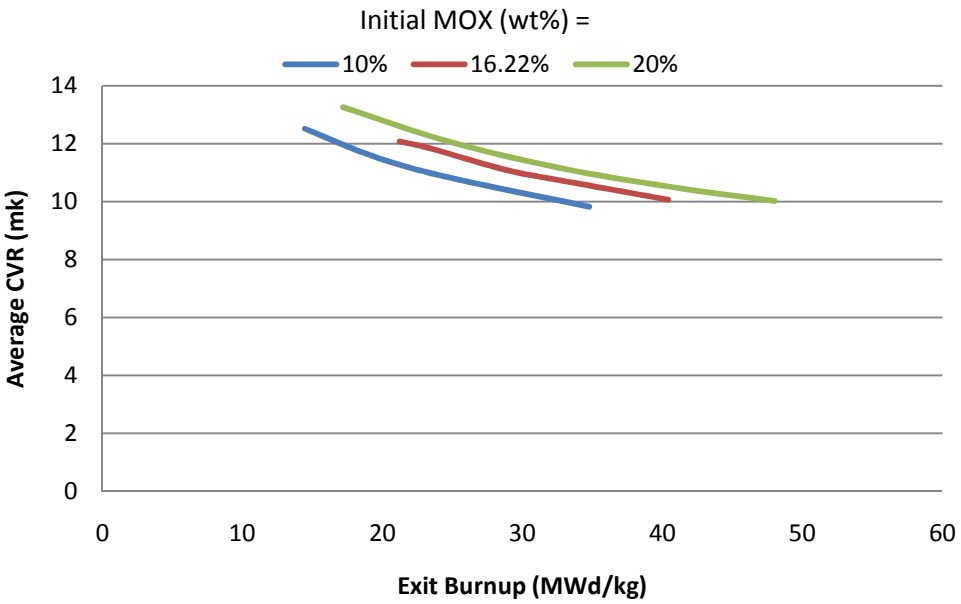

Figure 7.21 – Average CVR of a (Th,^{233}U,MOX)-fuelled CANDU reactor with a homogenous lattice

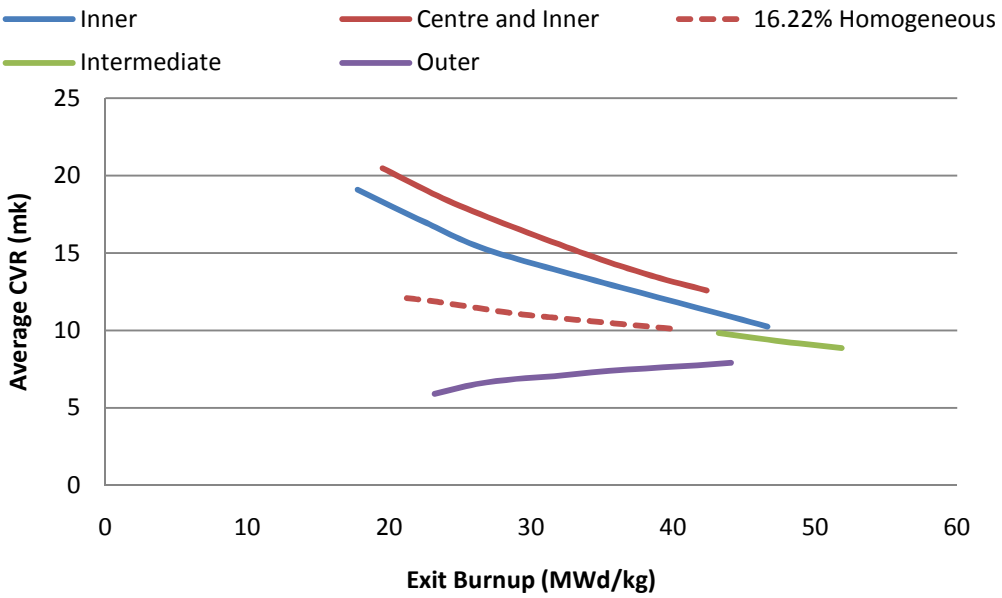

Figure 7.22 – Average CVR of a (Th,^{233}U,MOX)-fuelled CANDU reactor with a heterogeneous lattice

7.2.3.2 Delayed β Fraction

Despite the addition of some ^{235}U, the delayed β fraction of a MOX-driven thorium-fuelled CANDU reactor is still less than that of a NU-fuelled CANDU reactor. Figure 7.23 shows that the concentration of MOX has very little effect on the delayed β fraction.

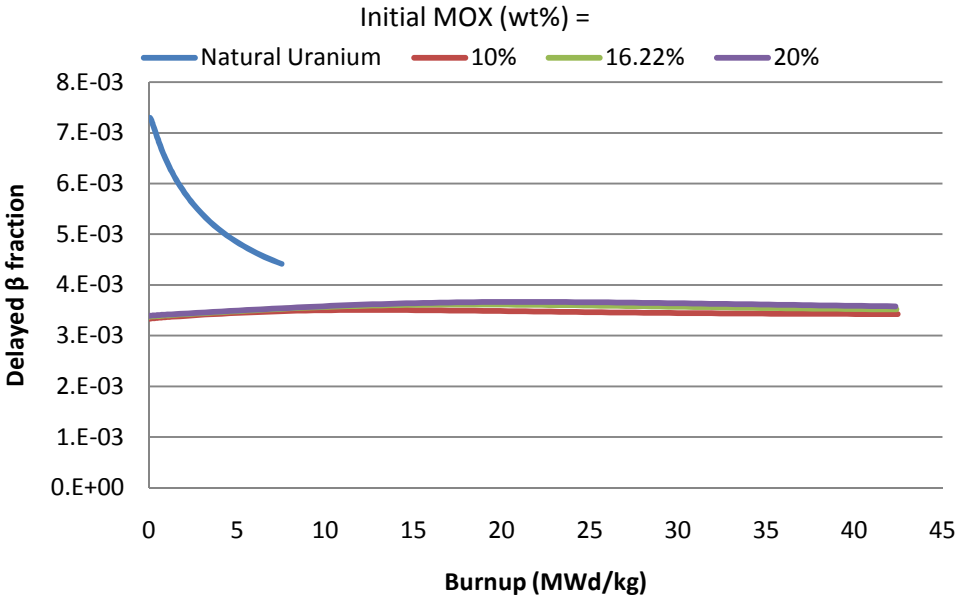

Figure 7.23 – Delayed β fraction of a (Th,^{233}U,MOX)-fuelled CANDU reactor

7.3 Low-Enriched Uranium Driver

In variant 4, the driver fuel is not derived from spent fuel. Instead, natural uranium is enriched and directly used to drive a thorium-fuelled CANDU reactor. For the sake of comparison, the enrichment of the uranium was chosen to be the same as for the LWRs in variants 1-3, 4.11%. Due the presence of uranium, a LEU driver necessitates the same level of heterogeneity as a MOX driver so the last configuration from Table 7.3 (i.e. LEU in alternating pins of the outer ring) is considered. Again, only the full power case (i.e. 32 W/g) is considered.

7.3.1 Fissile Inventories

Figure 7.24 shows the trend that ^{233}U production and driver-fuel consumption rates decrease with increasing exit burnup. When the LEU is loaded in only the outer rings, the ^{233}U production increases dramatically but the LEU consumption rate remains approximately the same as the homogeneous case.

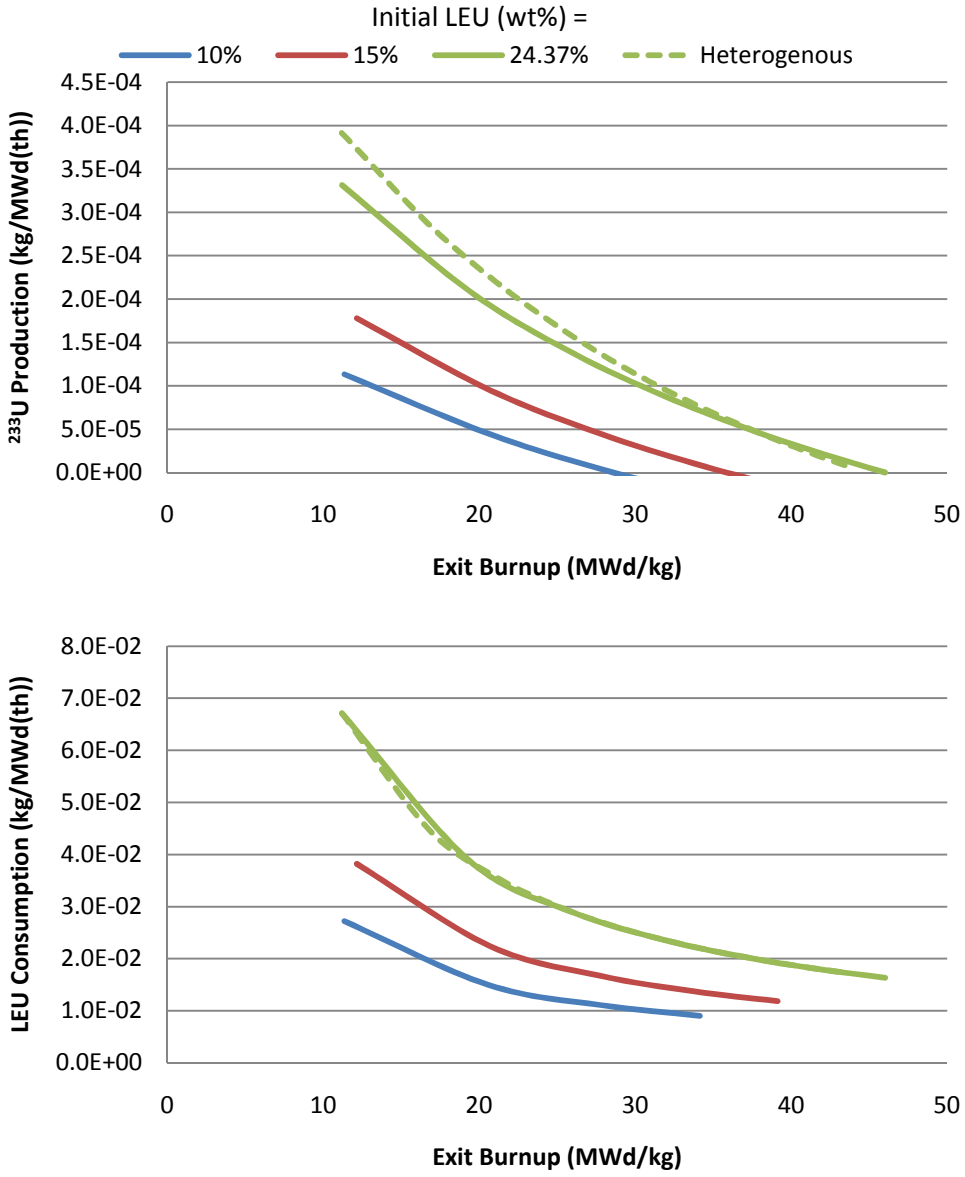

Figure 7.24 – ^{233}U production and LEU consumption of a (Th,^{233}U,LEU)-fuelled CANDU reactor with a heterogeneous lattice

7.3.2 Spent Fuel

Even though plutonium is not loaded in the reactor, Figure 7.25 shows that there are significant plutonium concentrations at discharge. Also of note is that the ^{235}U concentration in the spent fuel sharply decreases with increasing exit burnup indicating that the fissile content of the driver fuel is more completely utilised at higher exit burnups.

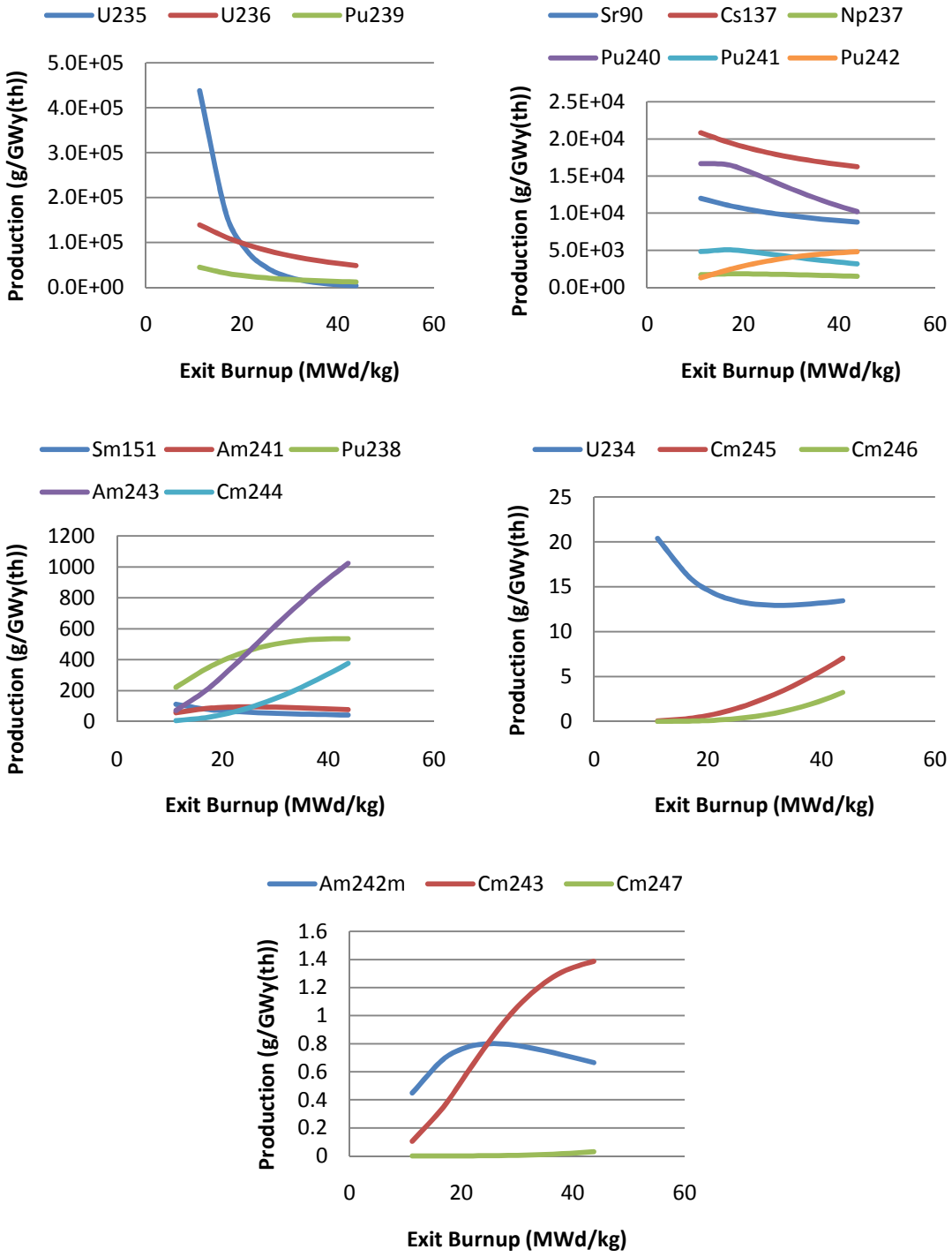

Figure 7.25 – Rate of production of minor actinides and medium lived fission products in a (Th,^{233}U,LEU)-fuelled CANDU reactor with LEU in alternating pins in the outer ring

7.3.3 Controllability

7.3.3.1 Coolant Void Reactivity

The CVR of the homogeneous LEU-driven reactor is shown in Figure 7.26. Only by loading the LEU in the outer ring is it possible to achieve a CVR less than that of a NU-fuelled CANDU reactor as shown by the heterogeneous case in the figure.

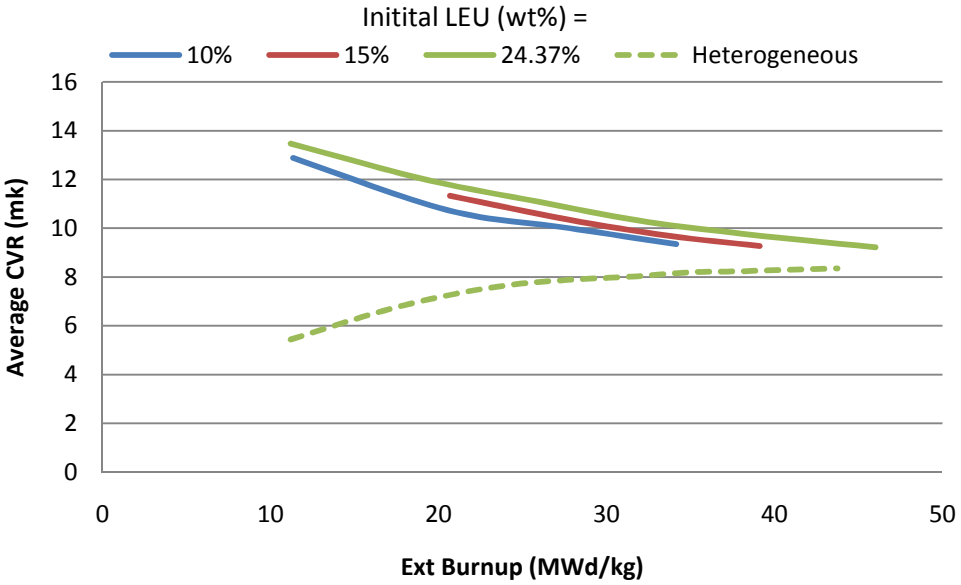

Figure 7.26 – Average CVR of a (Th,^{233}U,LEU)-fuelled CANDU reactor

7.3.3.2 Delayed β Fraction

With a LEU driver, a significantly higher proportion of the fissions are from ^{235}U when compared to the other drivers. This produces greater delayed β fractions that are closer to what would be expected from a NU-fuelled CANDU reactor.

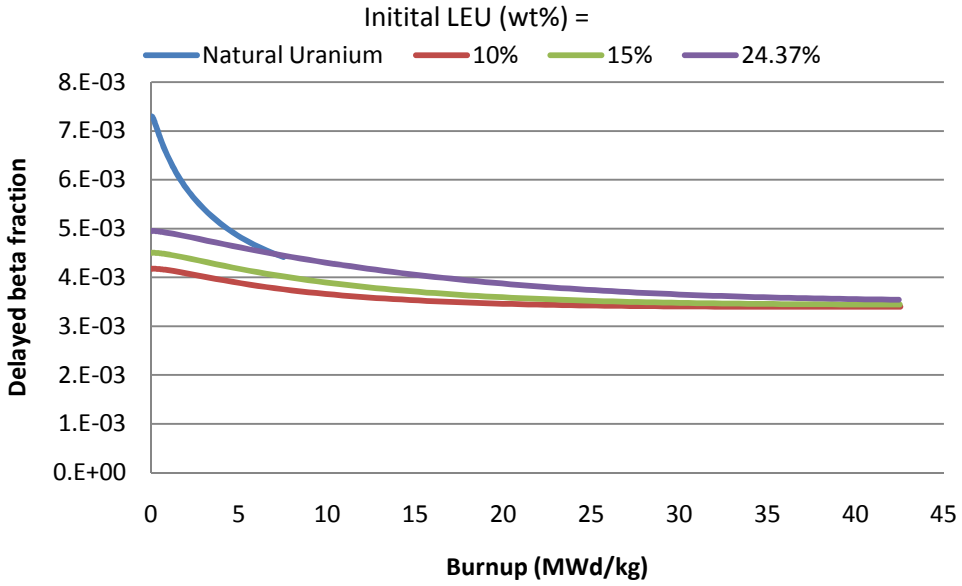

Figure 7.27 – Delayed β fraction of a (Th,^{233}U,LEU)-fuelled CANDU reactor

8 Mass Flows

This chapter presents the resource consumption and reprocessing demand for each variant. The mass flows are shown as function of the exit burnup of the thorium-fuelled CANDU reactors. The formulae used for calculating these quantities are presented in appendix A.

8.1 Variant 1a

As was shown in Figure 6.1, the CR of reactor B approaches 1 at low exit burnups. If reactor B were to achieve a SSET cycle (i.e. have a CR ≥ 1), then no fissile feed would be required and the reactor park would have no energy production from PWRs or reactor A. At higher exit burnups, reactor B consumes more ^{233}U. This requires larger capacity of reactor A and, consequentially, a larger capacity of PWRs. This trend is shown in Figure 8.1. This leads to the counter intuitive trend of a less-sustainable fuel cycle for higher exit burnups that is shown in Figure 8.2. Also shown in Figure 8.2 is the fact that natural uranium consumption is not strongly dependent on the specific concentration or

homogeneity of ^{233}U and plutonium. Rather, it is dependent on the exit burnup achieved from the combination of the fissile components.

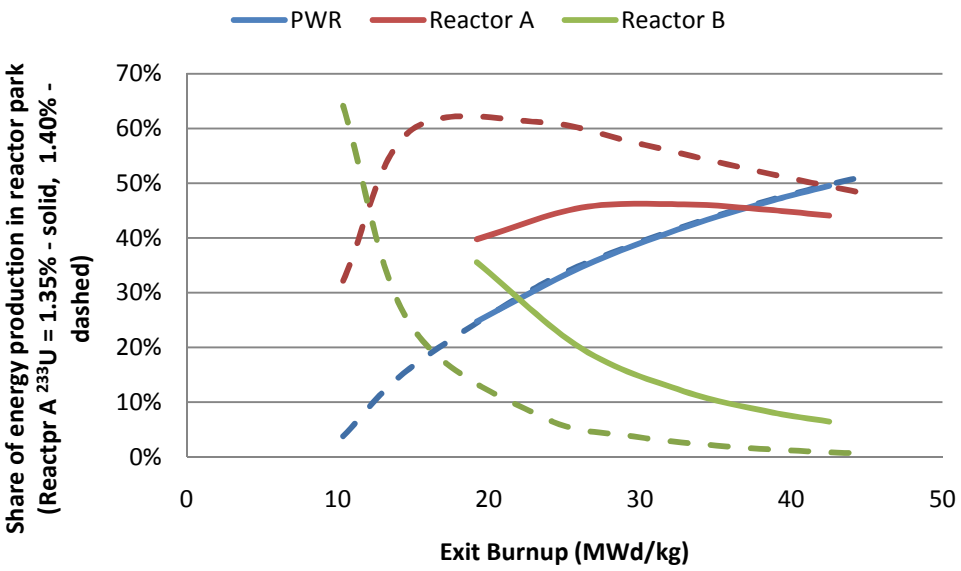

Figure 8.1 – Reactor share for variant 1a

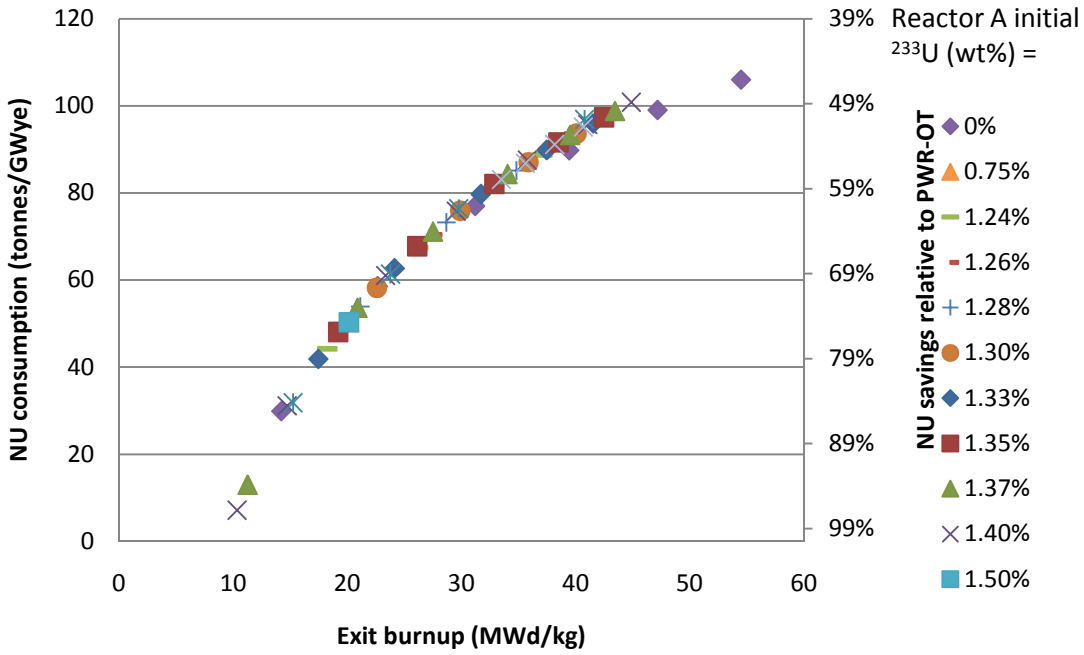

Figure 8.2 – Rate of NU consumption for variant 1a

As shown in the previous figure, at an exit burnup of 20 MWd/kg, the thorium recycling scheme reduces the natural uranium consumption by 75% relative to the PWR once-through fuel cycle and decreases to 53% at 40 MWd/kg. The obvious disadvantage of lower burnup fuel is the increased burden on reprocessing. This is shown in Figure 8.3.

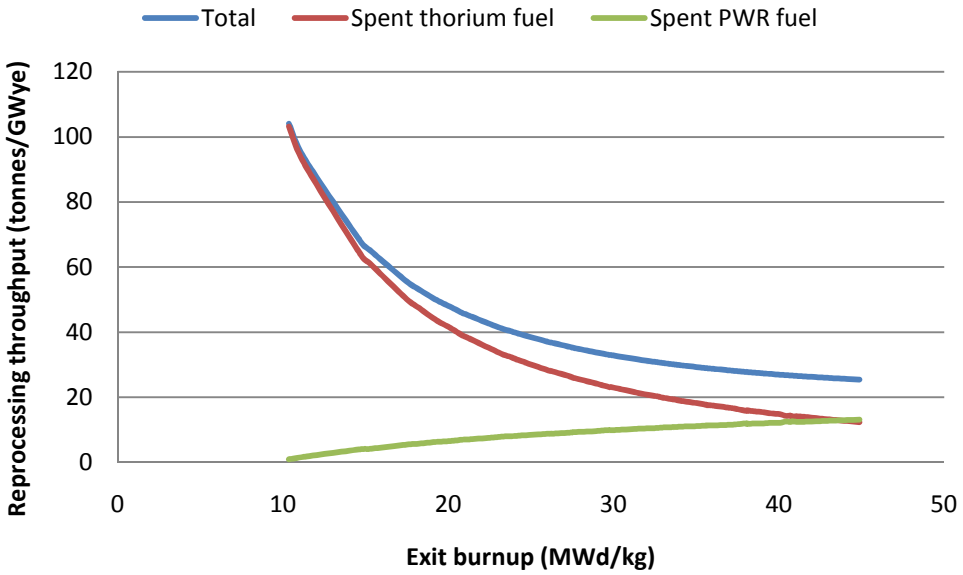

Figure 8.3 – Reprocessing demand for variant 1

Due to the presence of some strong gamma emitters in the spent fuel and the novelty of the technology, it is likely that thorium reprocessing will be several times more expensive than conventional uranium-based fuel reprocessing (e.g., the PUREX process) [35]. For this reason, it can be concluded that the reprocessing cost is a major obstacle for the realization of a SSET fuel cycle.

8.1.1 Sensitivity

Figure 8.4 shows the sensitivity of NU consumption to the various design changes investigated in chapters 6.2 and 0 .

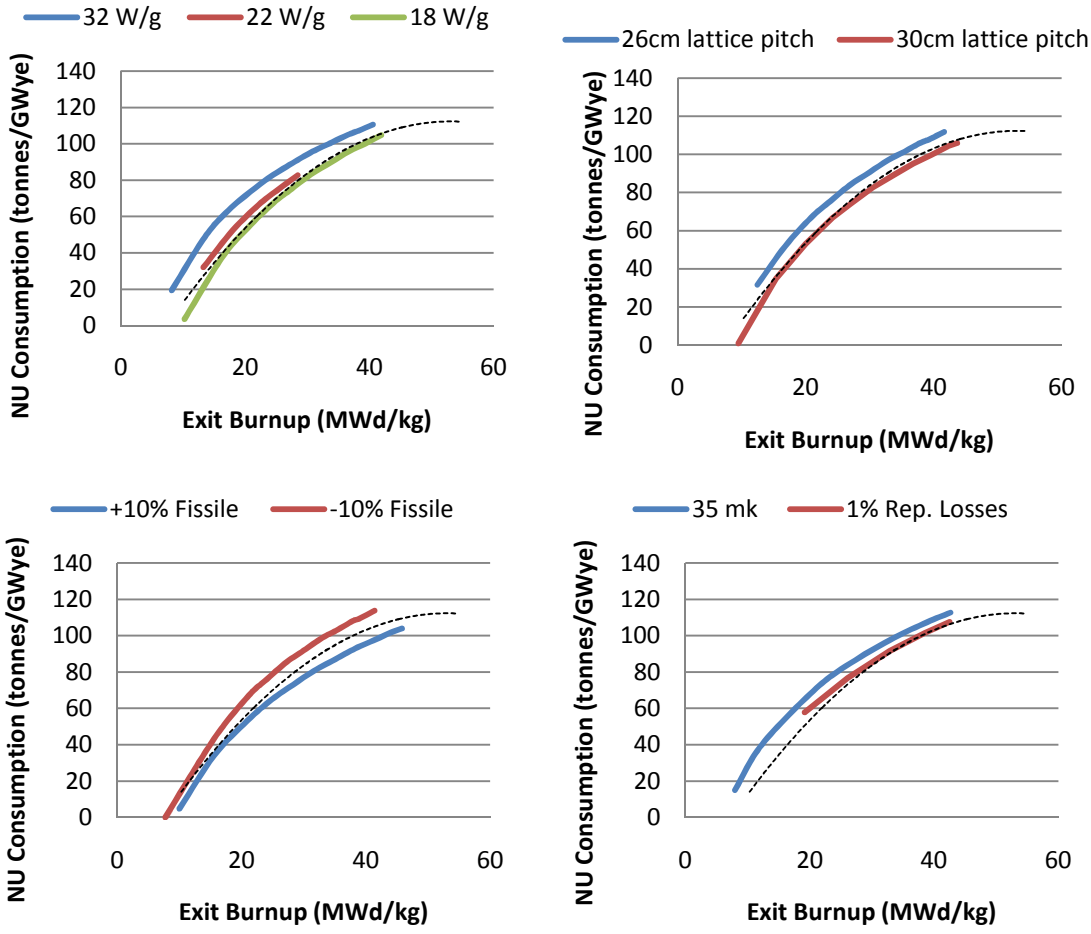

Figure 8.4 – Sensitivity of NU consumption for variant 1a. The black line represents the base case.

Table 8.1 summarizes the sensitivity of NU consumption in variant 1a. The sensitivity analysis shows that at low exit burnups, when the reactor park is predominantly thorium reactors, the NU consumption is very sensitive to small changes in the reactor design.

Parameter changed	Change in NU Consumption at Exit Burnup	
	20 MWd/kg	40 MWd/kg
Increase in parasitic absorption to 35 mk	23.22%	4.89%
Reprocessing losses doubled to 1%	14.78%	4.58%
Reactor power decreased to 18 W/g	-0.11%	-0.90%
Reactor power increased to 22 W/g	14.69%	1.89%
Reactor power increased to 32 W/g	34.89%	5.57%
Lattice pitch decreased to 26 cm	23.21%	6.48%
Lattice pitch increased to 30 cm	-0.49%	-3.95%
Fissile Pu increased by 10%	-5.08%	-5.04%
Fissile Pu decreased by 10%	20.17%	7.42%

Table 8.1 – Sensitivity of NU consumption for variant 1a

This effect can be explained by examining the reactivity curves of thorium and uranium fuels shown in Figure 8.5. Because thorium fuel has better breeding characteristics than uranium fuel, the decrease in reactivity over burnup is more gradual. A shallow reactivity curve will cause a small change in reactivity to result in a large change in exit burnup. This highlights the necessity for a reactor with a good neutron economy and is the reason why CANDU reactors are most often the focus of thorium fuel cycle studies.

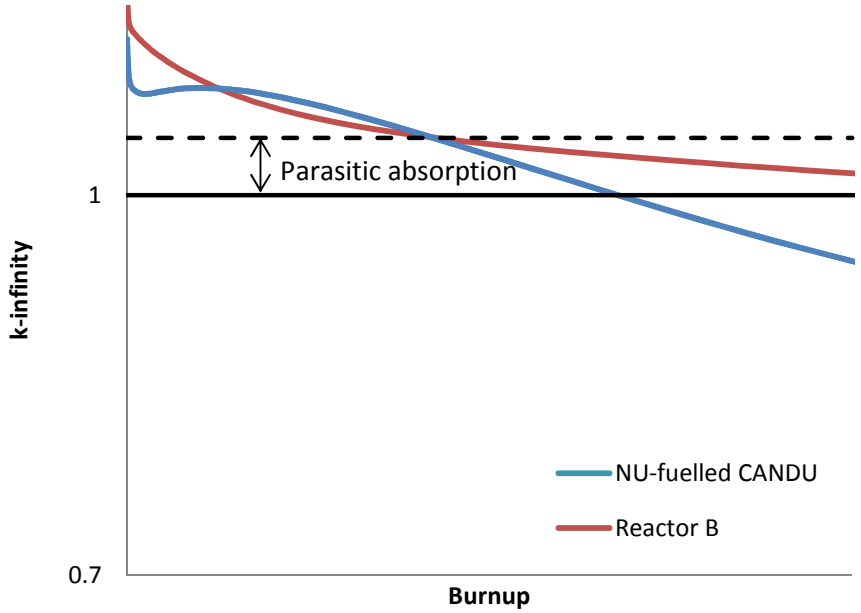

Figure 8.5 – A comparison of k-infinity between a thorium-fuelled reactor and a NU-fuelled reactor

Also of note from the sensitivity study is that, although it results in significantly higher NU consumption, full power CANDU reactors do achieve appreciable NU savings. Because of the economic repercussions of operating a reactor at decreased power, only full power reactors will be examined in later chapters.

8.1.2 $BU_A \neq BU_B$

Figure 8.1 shows that, for greater ^{233}U loading in reactor A, the share of energy production from reactor A increases. For the case where the exit burnup of reactor A is equal to that of reactor B, the reactors have similar fissile consumption rates and changes in ^{233}U loading result in the same NU consumption. However, as shown in chapters 6 and 7, the thorium fuel cycle is optimized at lower exit burnups. Therefore, if the exit burnup of one is less than the other, then changing the relative share of energy production from reactors A and B would change the fuel cycle's NU consumption. As

shown in Figure 8.6 and Figure 8.7, NU consumption increases when the share of the higher exit burnup reactor is increased.

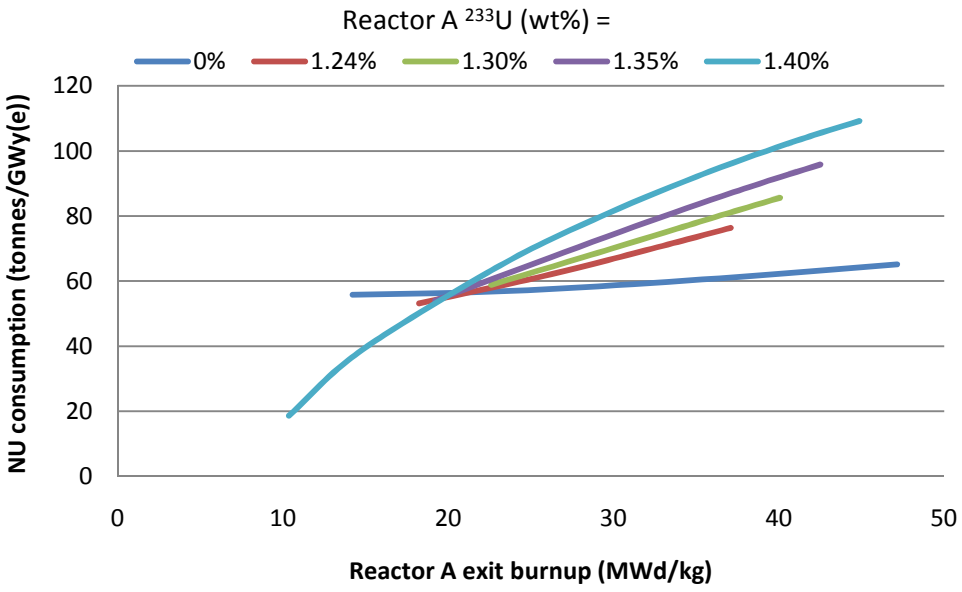

Figure 8.6 – NU consumption of variant 1a for BU_B = 20 MWd/kg

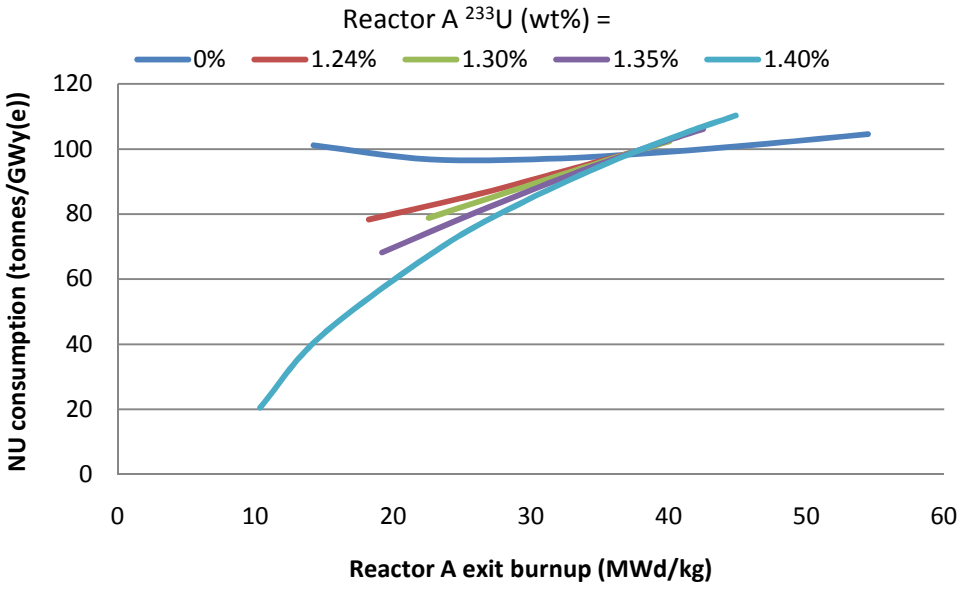

Figure 8.7 – NU consumption of variant 1a for BU_B = 40 MWd/kg

For this study, there is no motivation to choose one thorium reactor over the other. However, if implementation favoured one, then this could be used as a guideline for optimization.

8.2 Variant 1b

The RU-fuelled CANDU reactor was simulated using WIMS. For the uranium composition given in Table 5.2, the reactor achieved an exit burnup of 20.22 MWd/kg. This agrees within 1MWd/kg with the values suggested in a study by Oak Ridge National Laboratory [47]

The amount of available RU, and therefore the amount of energy produced by RU-fuelled CANDU reactors, is proportional to the amount of energy produced by PWRs as is shown in Figure 8.8.

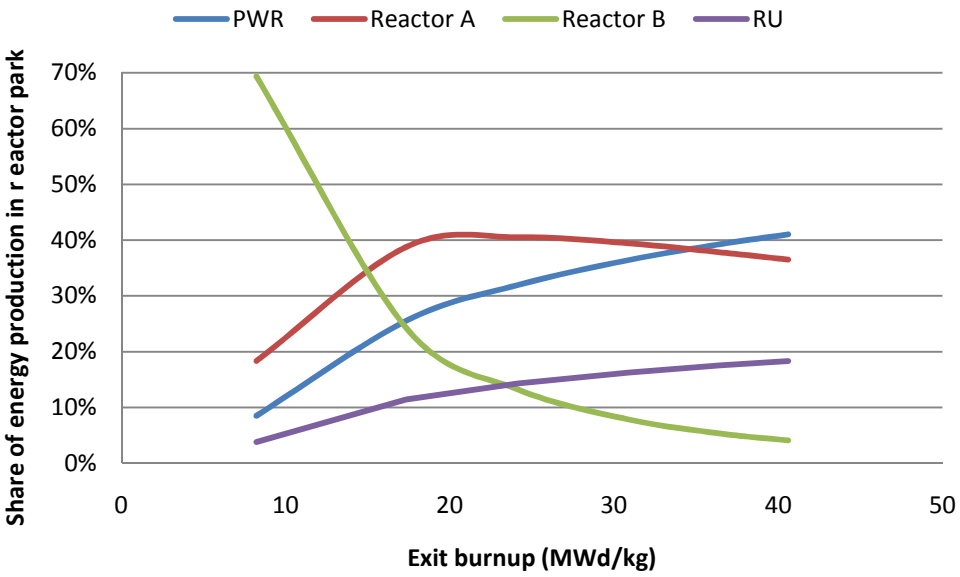

Figure 8.8 – Reactor share for variant 1b

This reduces the share of energy produced by the PWRs and results in decreased uranium consumption. As the share of PWRs is larger, this effect is more pronounced at high exit burnups, as shown in Figure 8.9.

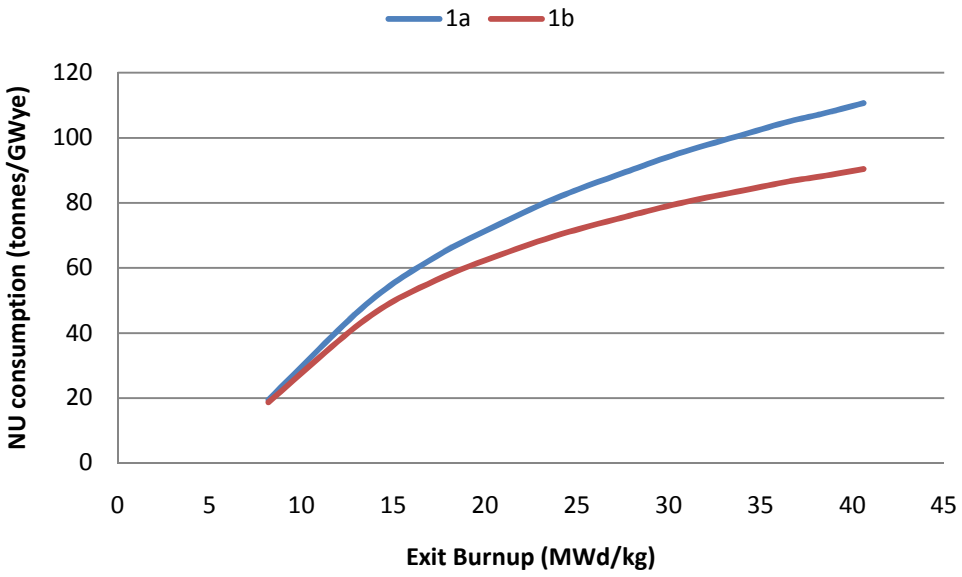

Figure 8.9 – Rate of NU consumption for variant 1b

8.3 Variant 1c

Americium and curium are significant contributors to the heat load of spent nuclear fuel. Therefore, there is interest in recycling these elements before moving the spent fuel to long term storage. AECL has conducted a simulation that examines the possibility of burning americium and curium in a SEU-fuelled CANDU reactor [48]. The americium and curium, together with the lanthanides, were loaded in the centre pin of a 43-element bundle. This served the dual purpose of burning the spent fuel and suppressing the CVR. The lanthanides were included to simplify the reprocessing method and decrease cost. In this study, the americium, curium, and lanthanides from all of the reactors are combined and, after 10 years, loaded in the centre pin of a 37-element RU-fuelled bundle. As the isotopic composition of the mixture changes with the

exit burnup of the CANDU reactors, only two exit burnups were considered – 20 MWd/kg and 40 MWd/kg.

The amount of AmCmLn that can be burned depends on the amount of the RU-fuelled CANDU reactors in the reactor park. At 20 MWd/kg, 13.7% of the AmCmLn is loaded into the CANDU reactor and, at 40 MWd/kg, the amount increases to 22.0%. Table 8.2 summarizes the mass flows of variant 1c.

	Exit Burnup (MWd/kg)	
	20	**40**
AmCmLn reprocessed	13.70%	22.03%
RU-CANDU exit burnup (MWd/kg)	12.90	13.01
NU consumption (tonnes/GWy(e))	63.23	89.90

Table 8.2 – Summary of mass flows for variant 1c

Although some americium is fissioned in the reactor, some transmutes to curium. As shown in Table 8.3, this results in a net destruction of americium but a net production of curium. The consequences of this are discussed in chapter 10.

	^{241}Am	^{242m}Am	^{243}Am	Total Am
Initial (wt%)	0.81	3.03E-03	0.95	1.76
Change in concentration	-63.23%	6.27%	-18.58%	-40.69%

	^{243}Cm	^{244}Cm	^{245}Cm	^{246}Cm	^{247}Cm	Total Cm
Initial (wt%)	2.08E-03	0.29	1.21E-02	1.76E-03	1.72E-05	0.30
Change in concentration	102.52%	70.45%	-21.10%	175.65%	218.31%	67.66%

Table 8.3 – Destruction and production of Am and Cm in a RU-fuelled CANDU reactor for variant 1c with Reactor A and B exit burnup = 20MWd/kg

8.4 Variant 2a

Figure 8.10 shows the share of energy production in the reactor park for the case where the MOX fuel is in every second pin of the outer ring of the bundle. As can be seen, reactor A has a smaller share in comparison to variant 1.

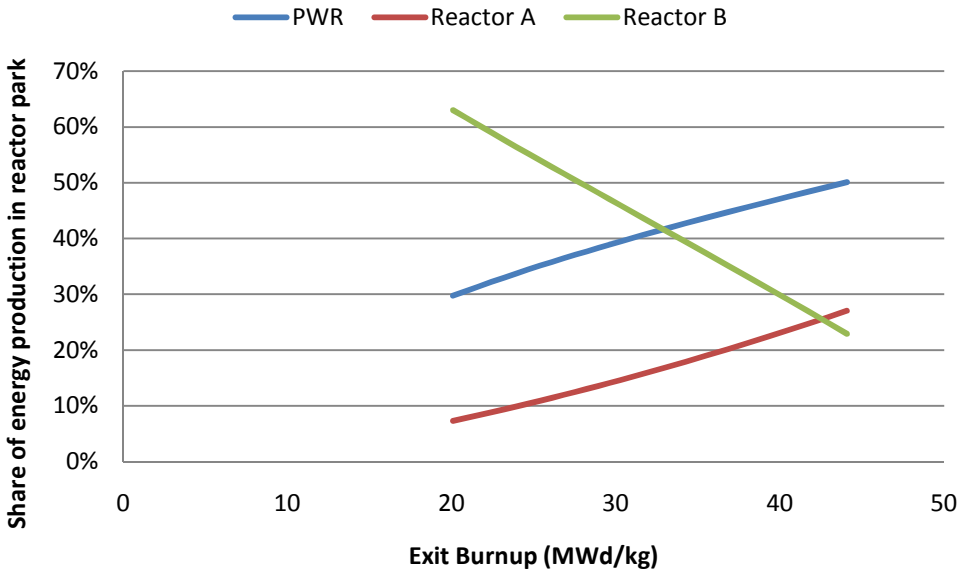

Figure 8.10– Reactor share for variant 2a

MOX fuel is less fissile than plutonium fuel so it has an order of magnitude greater concentration in reactor A. This leads to the NU consumption having a stronger dependence on the driver fuel concentration and location as shown in Figure 8.11.

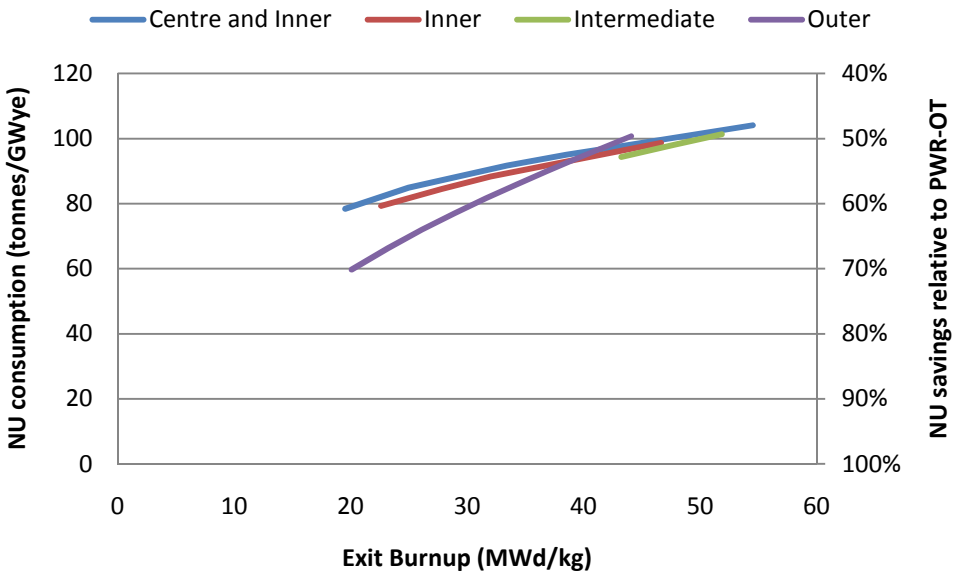

Figure 8.11 – Rate of NU consumption for variant 2a

The reprocessing throughput for variant 2 is shown in Figure 8.12. As can be seen, it exhibits similar trends as for variant 1.

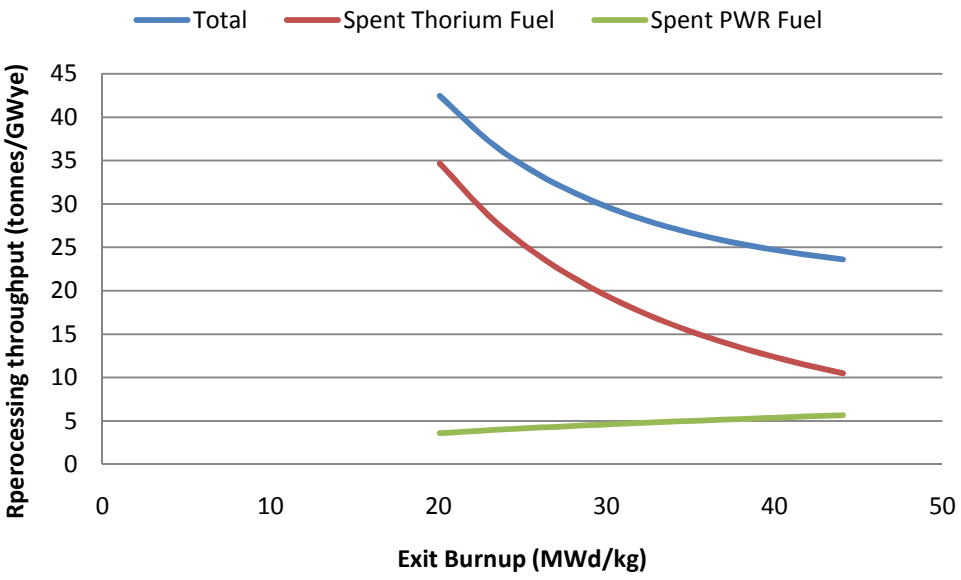

Figure 8.12 – Reprocessing demand for variant 2

8.5 Variant 2b

Like in variant 1, the introduction of a RU-fuelled reactor decreases the NU consumption. However, since variant 2a already uses some of the uranium from the spent PWR fuel, the effect is not as pronounced. This is shown in Figure 8.13 and Figure 8.14.

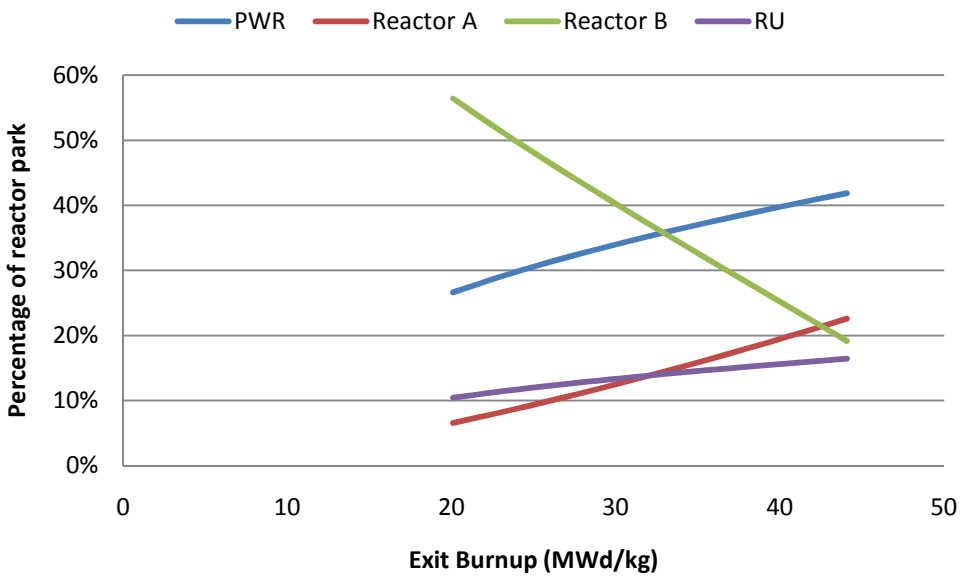

Figure 8.13 – Reactor share for variant 2b

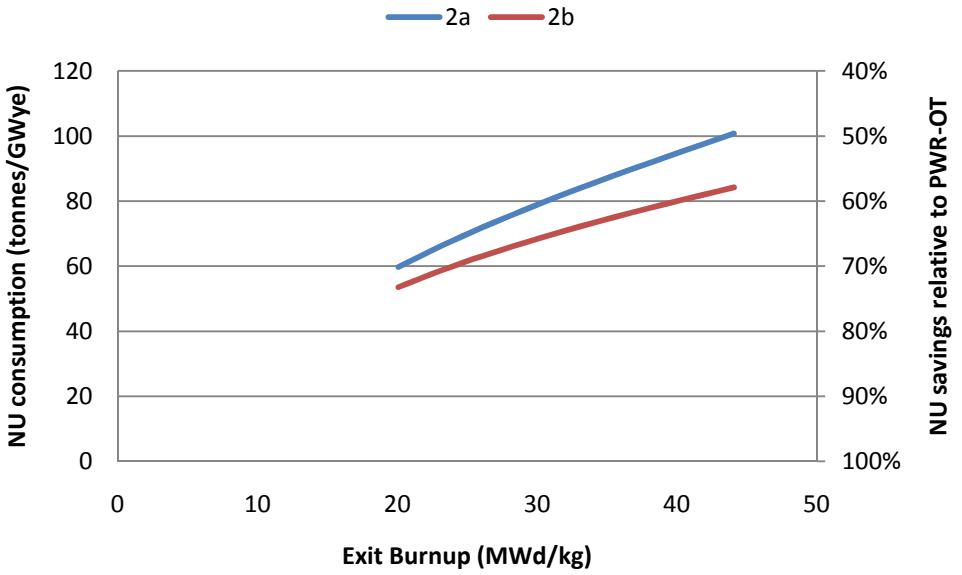

Figure 8.14 – Rate of NU consumption for variant 2b

8.6 Variant 2c

As there is less RU available in variant 2c than in variant 1c, the amount of americium and curium that can be reprocessed is even more limited. This is shown in Table 8.4

	Exit Burnup (MWd/kg)	
	20	**40**
AmCmLn reprocessed	7.04%	10.77%
RU-CANDU exit burnup (MWd/kg)	12.01	12.78
NU consumption (tonnes/GWy(e))	59.65	94.69

Table 8.4 – Summary of mass flows for variant 2c

8.7 Variant 3

Figure 8.15 shows that, in variant 3, the majority of the energy is produced by reactor A. The rate of NU consumption and reprocessing demand is shown in Figure 8.16.

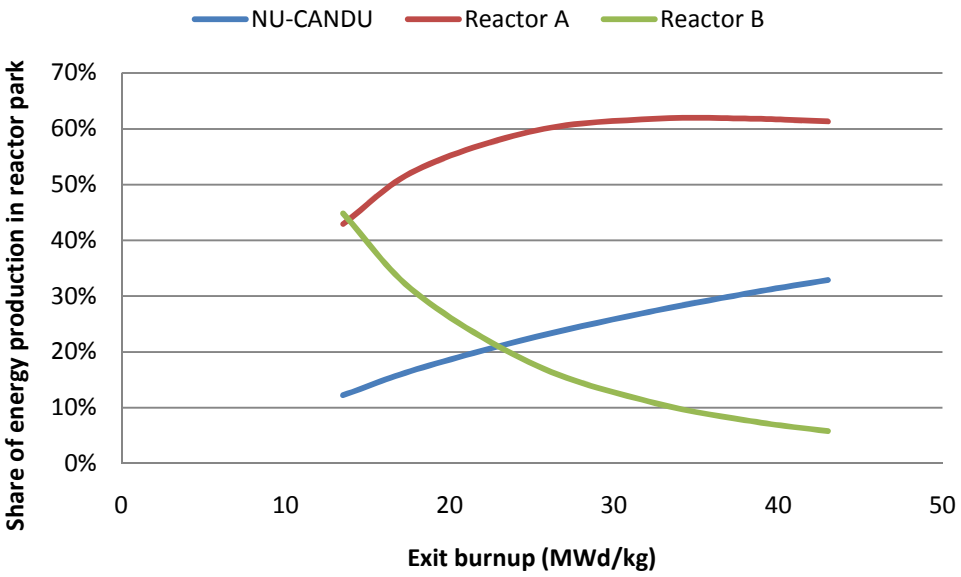

Figure 8.15 – Reactor share for variant 3

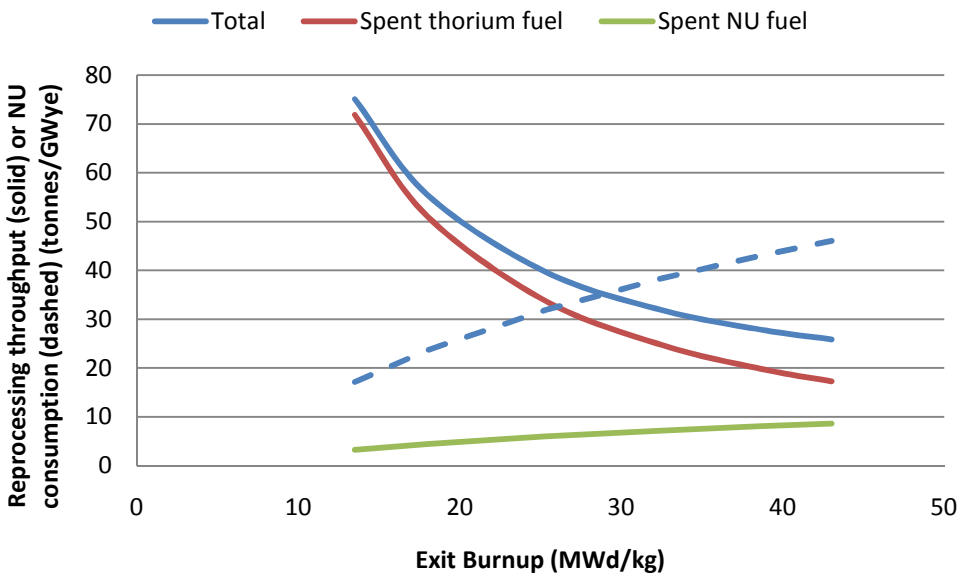

Figure 8.16 – Rate of NU consumption and reprocessing demand for variant 3

8.8 Variant 4

In variant 4, reactor A is a very efficient breeder. This, together with the absence of a driver reactor, leads to a large proportion of the energy in the reactor being produced by reactor B as shown in Figure 8.17.

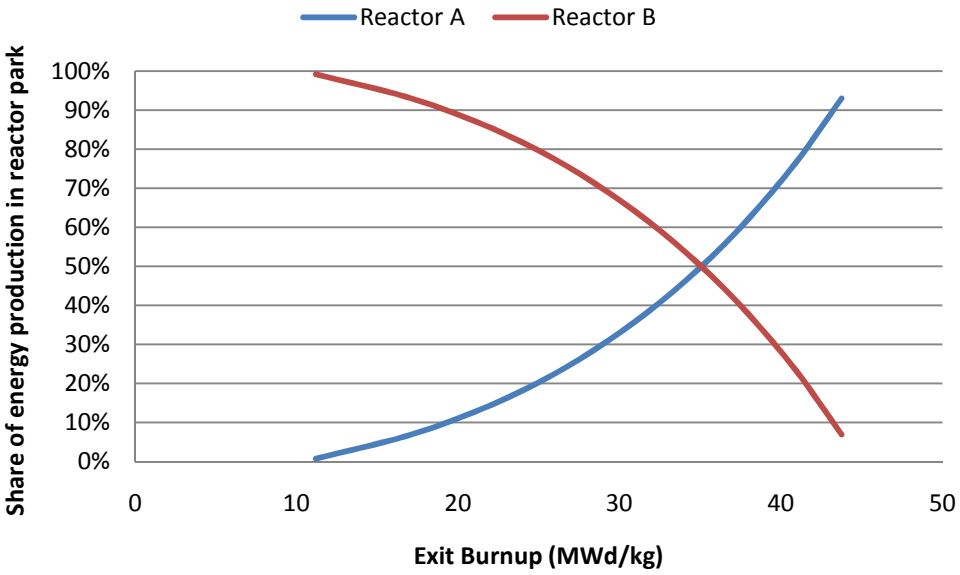

Figure 8.17 – Reactor share for variant 4

Figure 8.18 shows that the NU consumption in variant 4 exhibits some dependence on driver fuel concentration but only a weak dependence on heterogeneity.

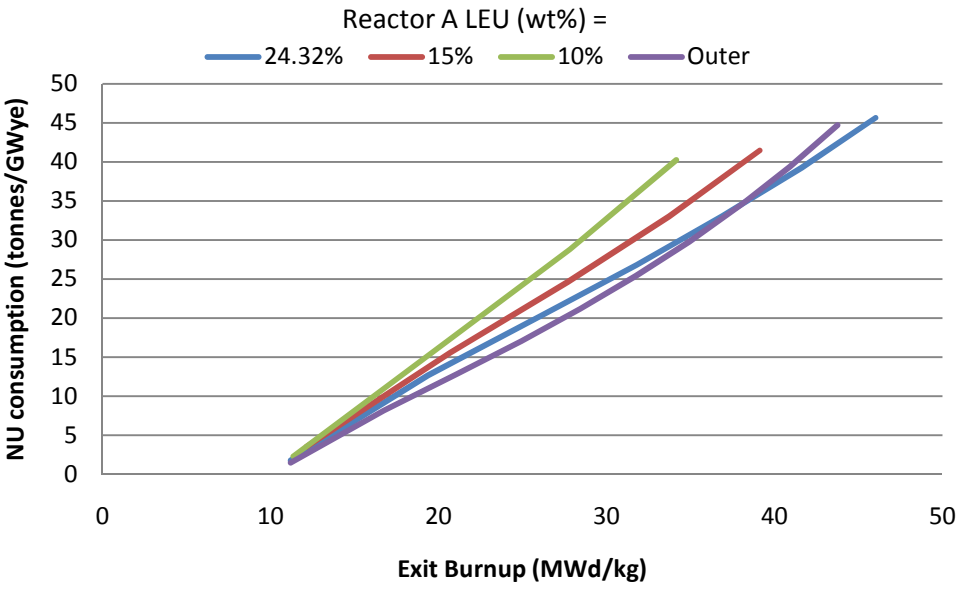

Figure 8.18 – Rate of NU consumption for variant 4

9 Global Scenario

In the previous chapter, the mass flows in a constant-capacity reactor park were examined. This ignored the limitations on the rate of which a new fuel cycle can be introduced to a pre-existing global reactor park. As there is a delay between the time a reactor is introduced and the time it produces spent fuel which can be reprocessed, the introduction of fissile-consuming reactor will lag behind the introduction of fissile-producing reactors. In a growing reactor park, this translates into a larger share of PWRs and consequentially higher uranium consumption.

For this simulation, variants 1a and 2a with were considered. The CANDU reactors were modelled with 32 W/g power density and 0% initial ^{233}U in reactor A. The fuel cycle and reactor characteristics are presented in chapters 5.3, 6, and 7. It was assumed that the thorium reactors were first introduced in 2010. To optimize the fuel cycle, the entire reactor to park was set as PWRs. Then, reactor A capacity was incrementally added until the available fissile plutonium reached 0. Then, reactor B was introduced until there was no available ^{233}U. This crude guess and check optimization does not represent the best case scenario but has been used other studies [1]. In the best case scenario, the fissile inventories would be held at 0 by introducing more capacity immediately as the resources are available. As shown in Figure 9.1, the guess and check method produces large fluctuations in the fissile inventories.

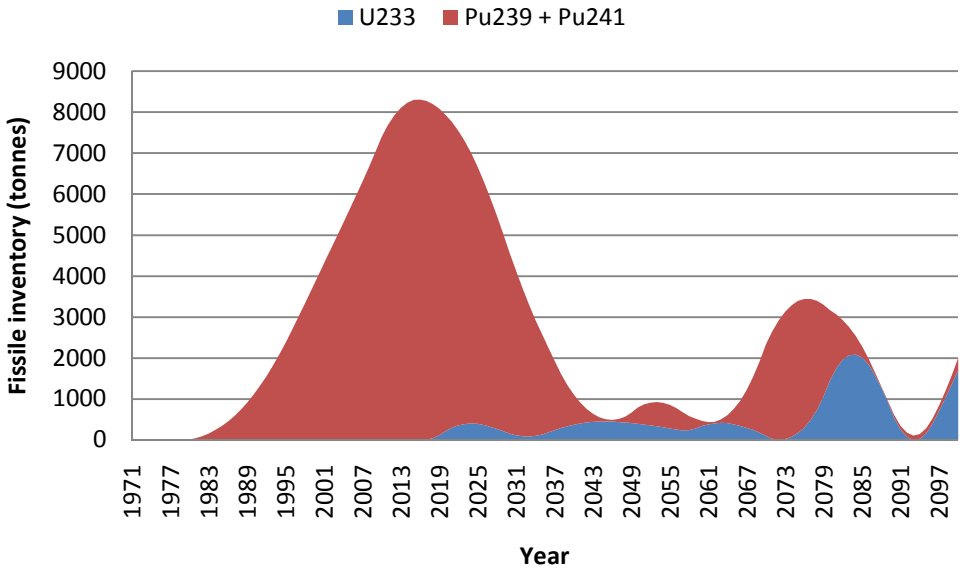

Figure 9.1 – Fissile inventories for global scenario simulations of variant 1a

Figure 9.2 and Figure 9.3 show the reactor share for both variants. As can be seen, even by 2100, a large majority of the energy is still produced by PWRs. This suggests that the proposed fuel cycles may be less efficient than what was presented in chapter 8.

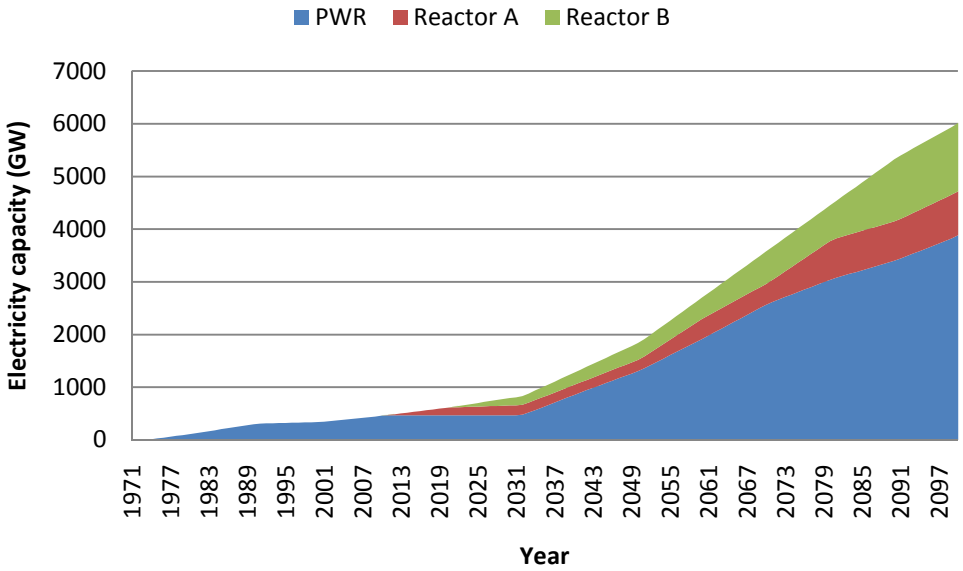

Figure 9.2 – Reactor share for global scenario simulation of variant 1a

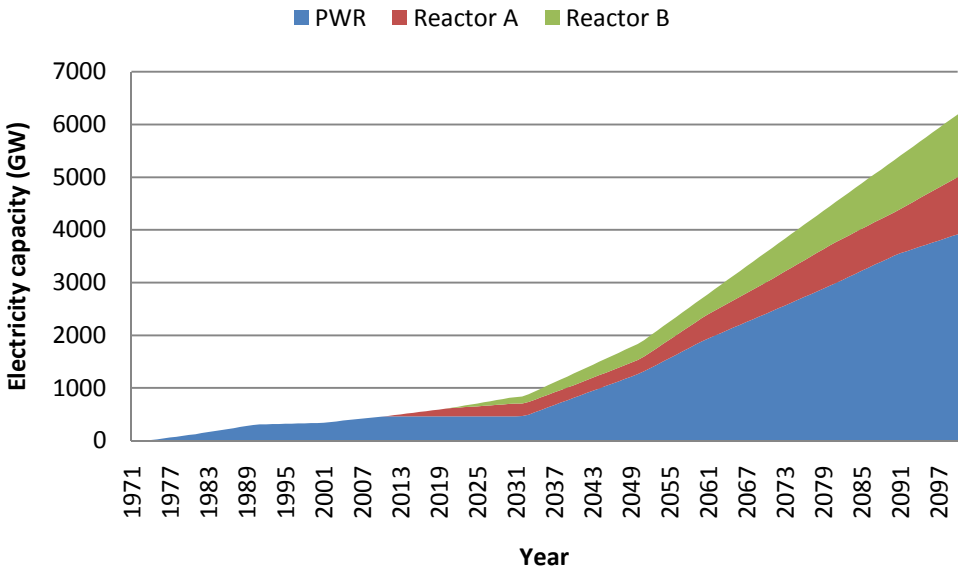

Figure 9.3 – Reactor share for global scenario simulation of variant 2a

The resultant uranium savings, shown in Figure 9.4 and

	Savings Relative to PWR-OT	
	2050	2100
Variant 1a	14.24%	21.79%
Variant 2a	14.39%	21.11%

Table 9.1, agree with savings predicted in the GAINS report [1]. Although 15%-20% is not an insignificant amount, it does not represent a widespread shift from uranium fuels

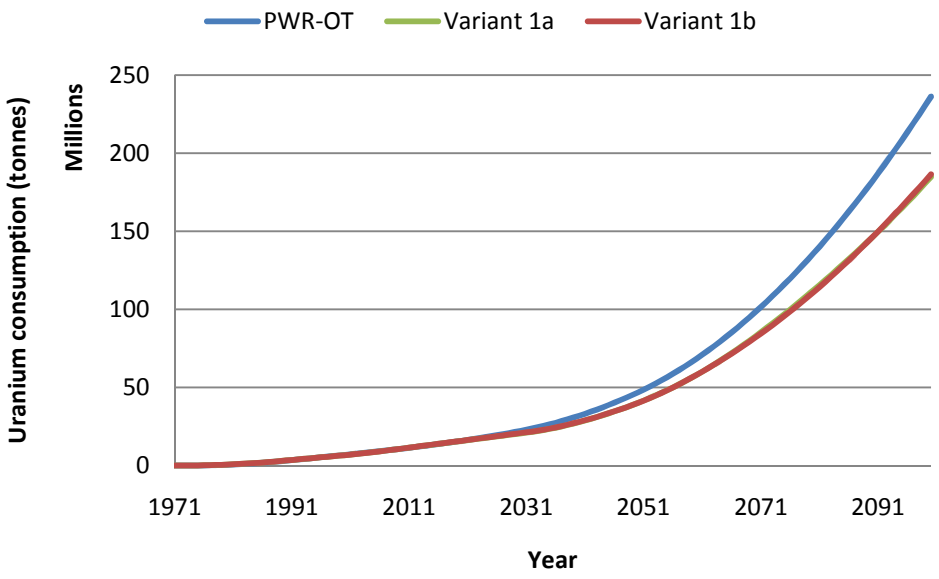

Figure 9.4 – Uranium consumption for global scenario simulation

	Savings Relative to PWR-OT	
	2050	2100
Variant 1a	14.24%	21.79%
Variant 2a	14.39%	21.11%

Table 9.1 – Summary of uranium consumption for global scenario simulation

10 Spent Fuel Characteristics

This chapter examines the spent fuel characteristics of each variant. To do this, the spent fuel from each reactor was discharged at the same time and combined in proportion to each reactor's share of the reactor park. The amount of spent fuel in each variant was normalized for same energy produced and it was assumed for every variant that reactors A and B achieved an exit burnup of 40 MWd/kg. The fissile concentrations needed to achieve this exit burnup are outlined in Table 10.1. The driver fuel was graded for variants 2 and 4 as it contains uranium and, therefore, had to be kept separate from the thorium and ^{233}U. Because it results in a favourable CVR, this was done by loading the driver fuel in every 2nd outer pin, as previously shown in Figure 7.17.

	Variant	^{233}U (wt%)	Driver (wt%)	Notes
Reactor A	1	1.40	1.17	
	2	0.55	24.32	Graded driver
	3	1.40	1.06	
	4	1.27	24.32	Graded driver
Reactor B	-	1.85	-	

Table 10.1 – Initial composition of fuels in reactors A and B

It is likely that the ultimate disposal of high-level waste will be in a deep geological repository. However, several different geological formations are currently being considered. In Canada and elsewhere, hard rock formations such as granite are being examined. Argillaceous and salt formations are considered in many European countries and volcanic formations such as Yucca mountain are considered in the United States [28]. The challenges facing the disposal of a certain spent fuel will vary between each repository type. However, some attributes can be used to provide broad characterization of the spent fuel over different repository types. These spent fuel characteristics include:

- thermal power
- gamma power
- radioactivity
- inhalation and ingestion hazards

The thermal power of the spent fuel gives a good indication of the volume required for the repository and, therefore, is often the primary metric when evaluating spent fuels.

Gamma radiation is difficult to shield so the gamma power gives an indication of the handling hazard of the spent fuel. This presents an added health hazard and cost for

disposal. However, increased gamma power can also be viewed as an inherent proliferation barrier and, therefore, a positive characteristic.

Radioactivity, and inhalation and ingestion hazards are a measure of this risk to humans if the spent fuel were to be released from the repository. Long term disposal is designed to avoid exposing the spent fuel so these metrics are less relevant – at least in the time frame that a disposal can be considered reliable. Furthermore, the amount of spent fuel that is released to the public in the very long term is dependent on the mobility of the elements and the type of repository. If this were taken into account, the relative hazards of the spent fuel from each variant could be very different than what is presented in this chapter. However, as the general public is often concerned with these metrics there is some merit in their evaluation.

10.1 Variant 1

Figure 10.1 shows that, after approximately 50 years, the thermal power of the spent fuel from variant 1a is less than that of the spent fuel from the PWR-OT cycle and is reduced by as much as 80% in the long term. The dramatic decrease in thermal power can be attributed to the lower TRU production of thorium fuel and the increased fuel utilisation of the fuel cycle.

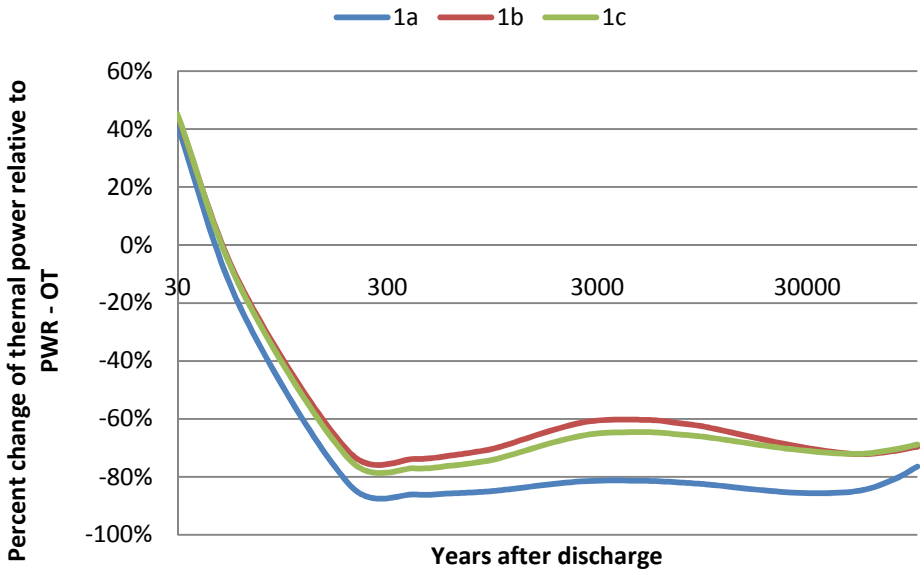

Figure 10.1 – Thermal power of spent fuel in variant 1 relative to PWR-OT cycle

Despite producing a small mass of spent fuel, it can be seen that the spent fuel from variants 1b and 1c have a higher thermal power than variant 1a. This can be attributed to additional plutonium produced in the RU-fuelled CANDU reactor which, as shown in Figure 10.2, is a significant contributor to the long term heat load. Also shown in Figure 10.2 is that the slightly lower thermal power in variant 1c is due to the destruction of ^{241}Am.

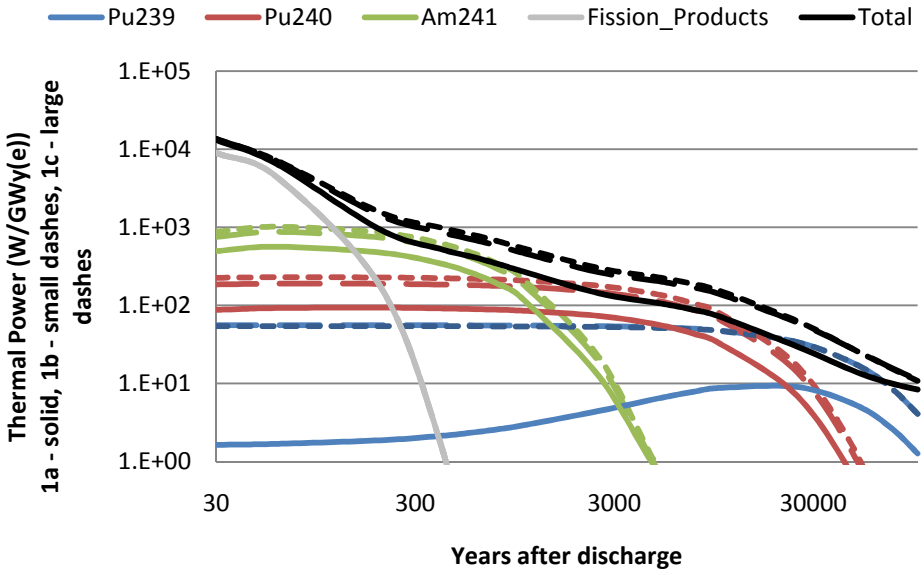

Figure 10.2 – Thermal power of major contributing isotopes in spent fuel of variant 1

A well-known property of the thorium fuel cycle is increased gamma power in the spent fuel due to the decay products of ^{232}U. Figure 10.3 shows that the gamma power of the spent fuel in the thorium fuel cycle is several orders of magnitude greater than that of the PWR-OT cycle. However, this effect is only seen in the short term as, by approximately 400 years after discharge, the fission products have almost completely decayed. This is shown in and Figure 10.4.

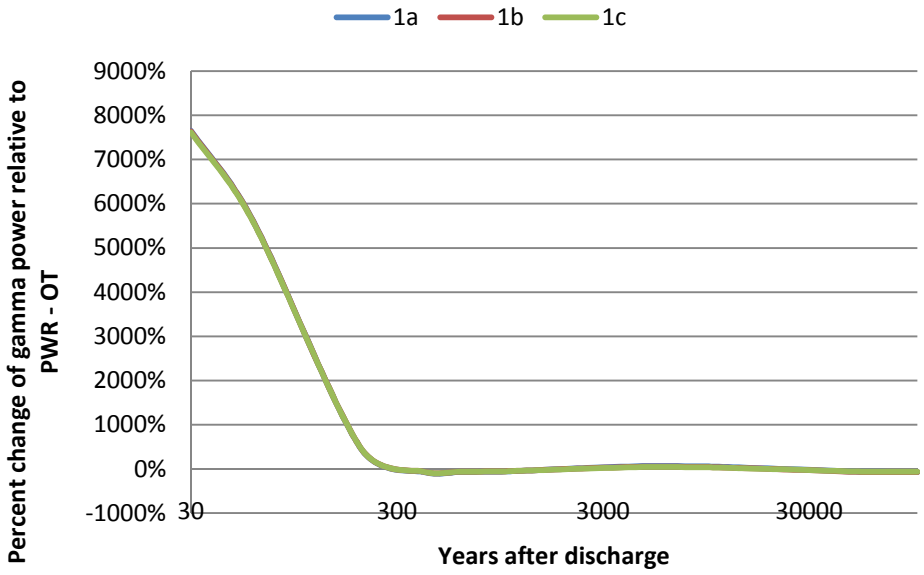

Figure 10.3 – Gamma power of spent fuel in variant 1 relative to PWR-OT cycle

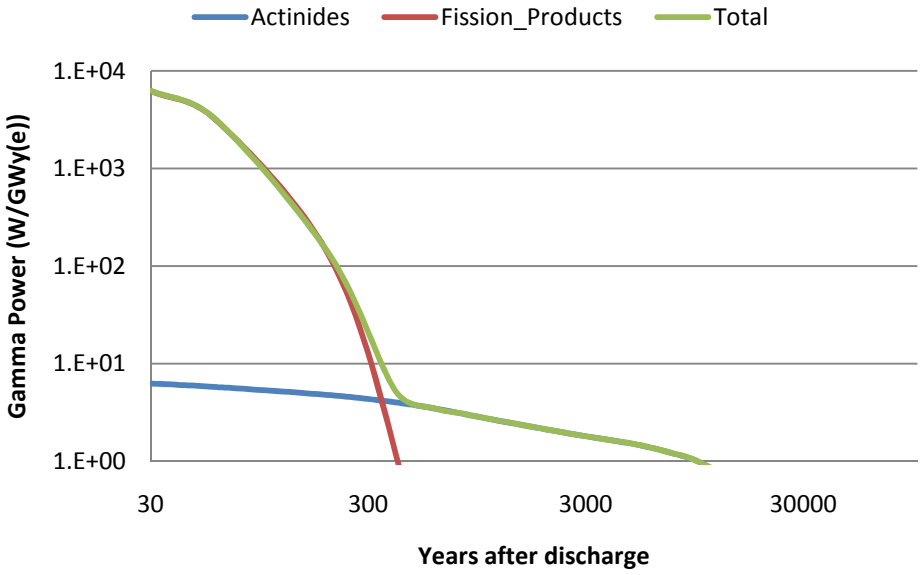

Figure 10.4 – Gamma power of spent fuel in variant 1a

After approximately 100 years, the radioactivity of variant 1 is less than that of the PWR-OT cycle and in the long term the radioactivity is several times less. Again due to the increased plutonium production, variants 1b and 1c are more radioactive in the

long term than variant 1a. This is shown in Figure 10.5. The inhalation and ingestion hazards follow a similar trend and are shown in Figure 10.6.

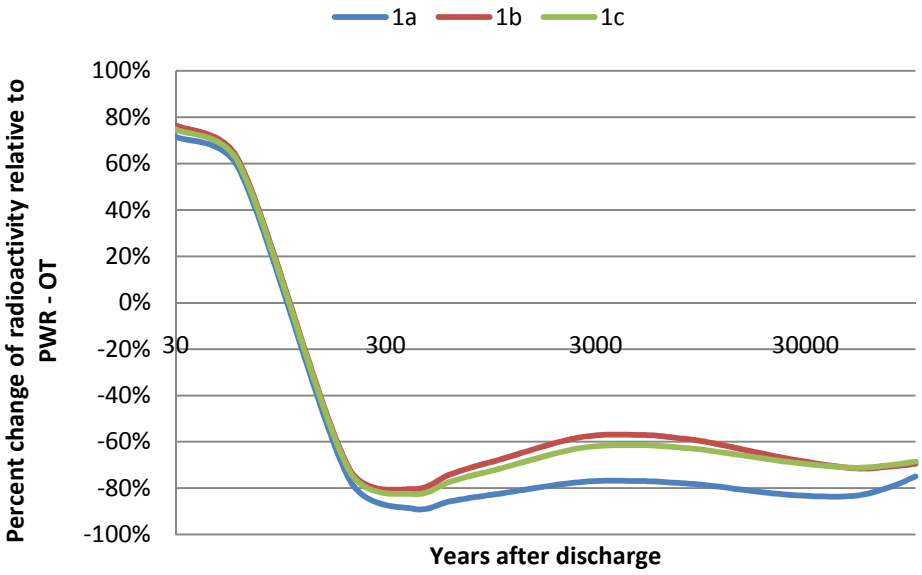

Figure 10.5 – Radioactivity of spent fuel in variant 1 relative to PWR-OT cycle

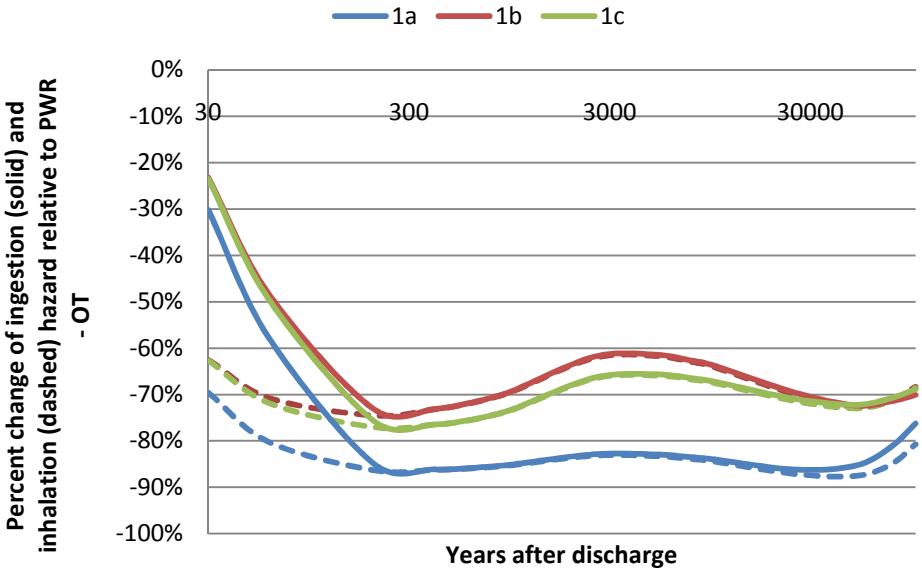

Figure 10.6 – Inhalation and ingestion hazard of spent fuel in variant 1 relative to PWR-OT cycle

10.2 Variant 2

In variant 2, uranium is loaded into reactor A leading to an increased production of TRUs. However, as shown in Figure 10.7, this still generates spent fuel with a lower longer term thermal power than spent PWR-OT fuel.

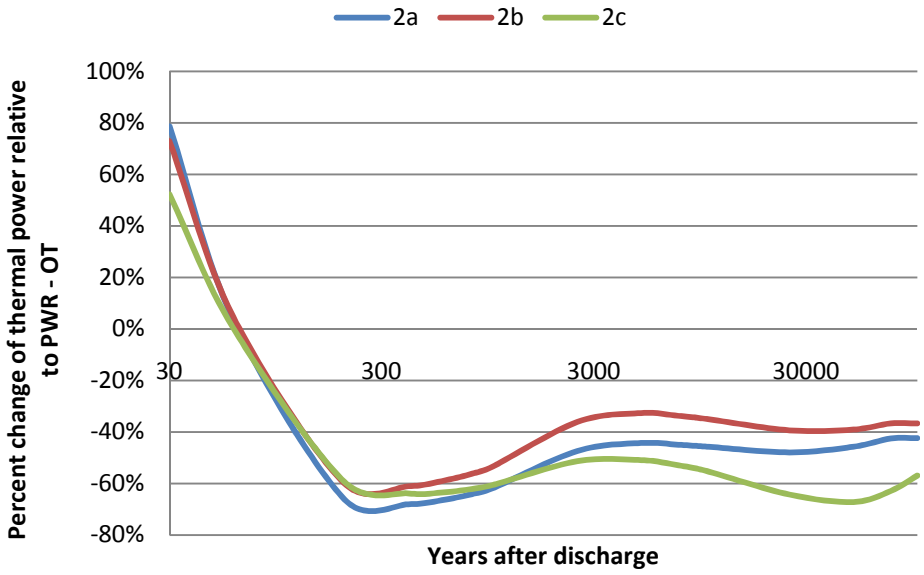

Figure 10.7 – Thermal power of spent fuel in variant 2 relative to PWR-OT cycle

Figure 10.8 shows that the efficient destruction of americium reduces the thermal power of the spent fuel in variant 2c.

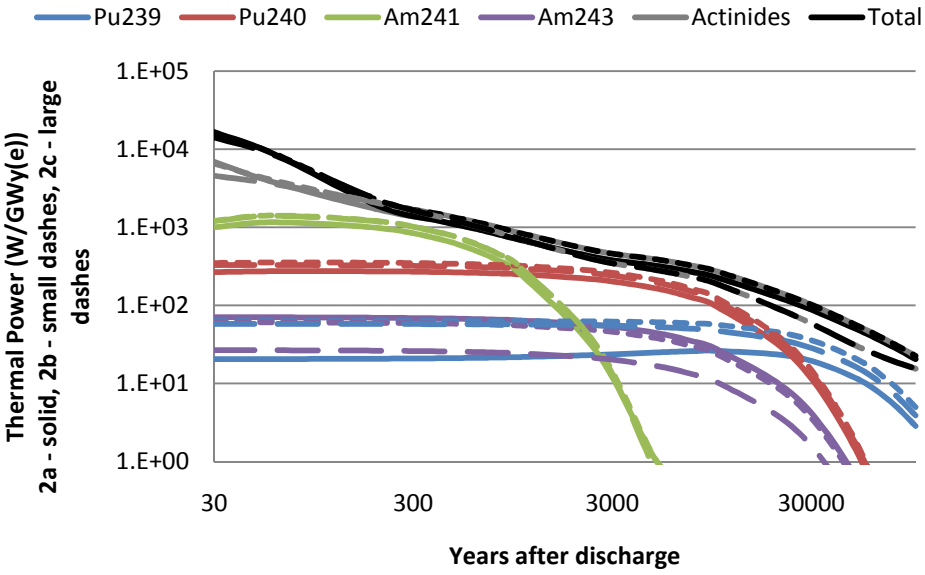

Figure 10.8 – Thermal power of major contributing isotopes in spent fuel of variant 2

Similarly, Figure 10.9 and Figure 10.10 show that variant 2c is effective at reducing the danger of the spent fuel in the long term. However, in all three variants, the spent fuel characteristics are favourable in comparison to the PWR-OT cycle.

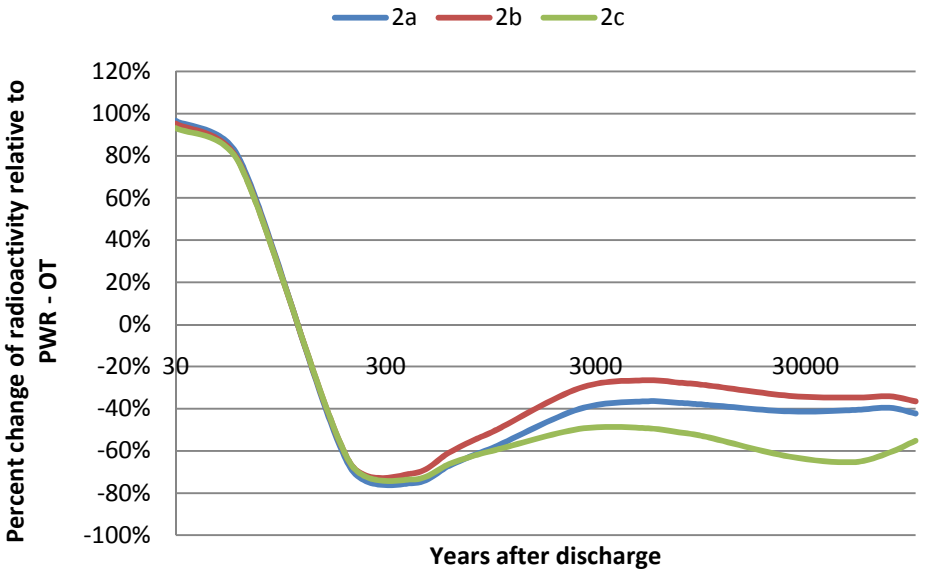

Figure 10.9 – Radioactivity of spent fuel in variant 2 relative to PWR-OT cycle

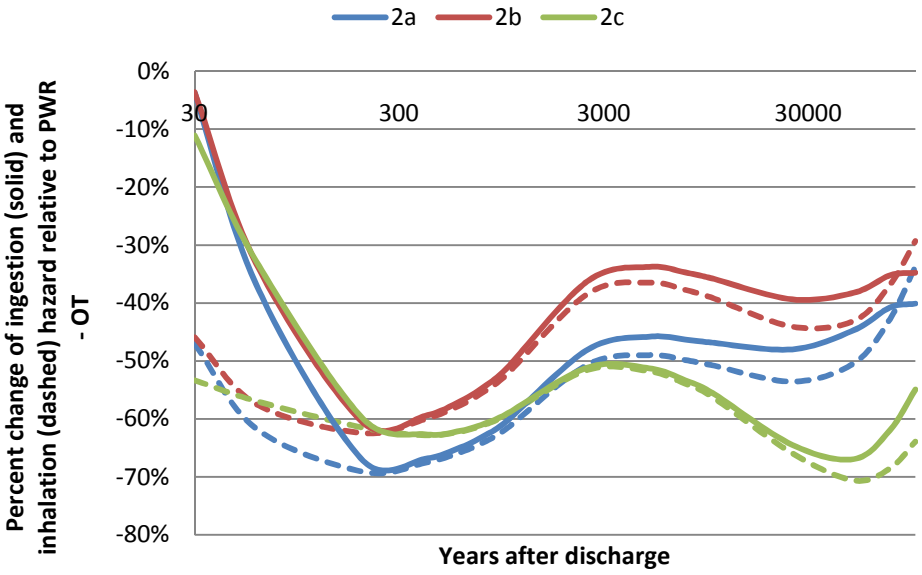

Figure 10.10 – Inhalation and ingestion hazard of spent fuel in variant 2 relative to PWR-OT cycle

10.3 Variants 1-4

It is evident from Figure 10.11 that, due to the increased plutonium production in reactor A, the spent fuel in variant 2 has a significantly higher thermal power than the other variants. In variant 4, plutonium production in reactor A is also high but, because there is no driver reactor, the plutonium production of the entire fuel cycle is significantly lower than in variant 2.

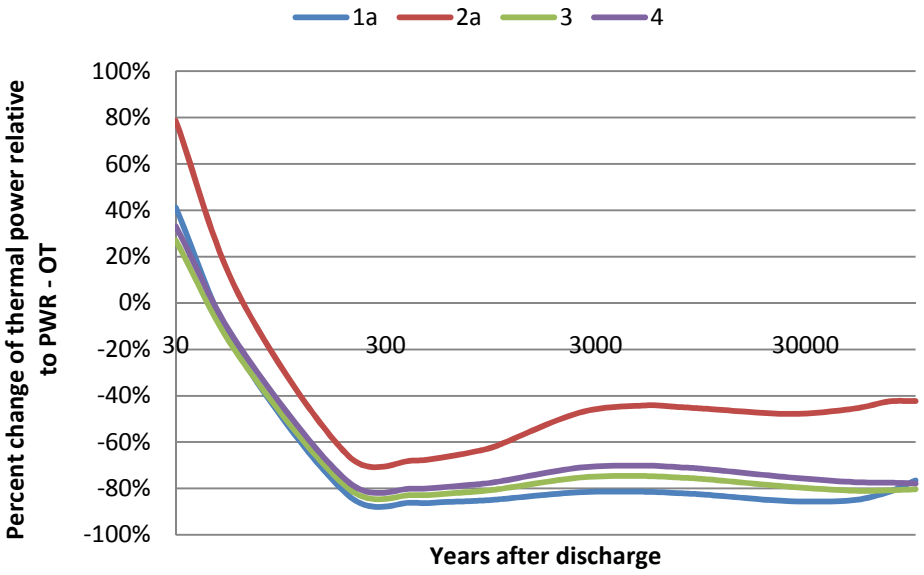

Figure 10.11 – Thermal power of spent fuel in thorium fuel cycle relative to PWR-OT cycle

As expected, the gamma power of spent fuel from all of the variants is significantly higher than for the PWR-OT cycle. This is shown in Figure 10.12.

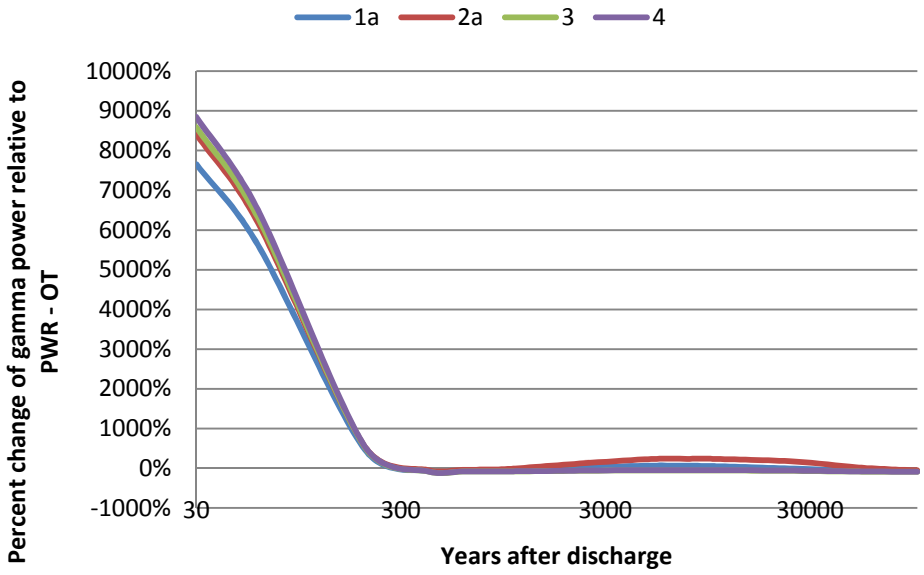

Figure 10.12 – Gamma power of spent fuel in thorium fuel cycle relative to PWR-OT cycle

The increased plutonium production in variant 2 also results in higher radioactivity, and inhalation and ingestions hazards than in the other variants. This is shown in Figure 10.13 and Figure 10.14.

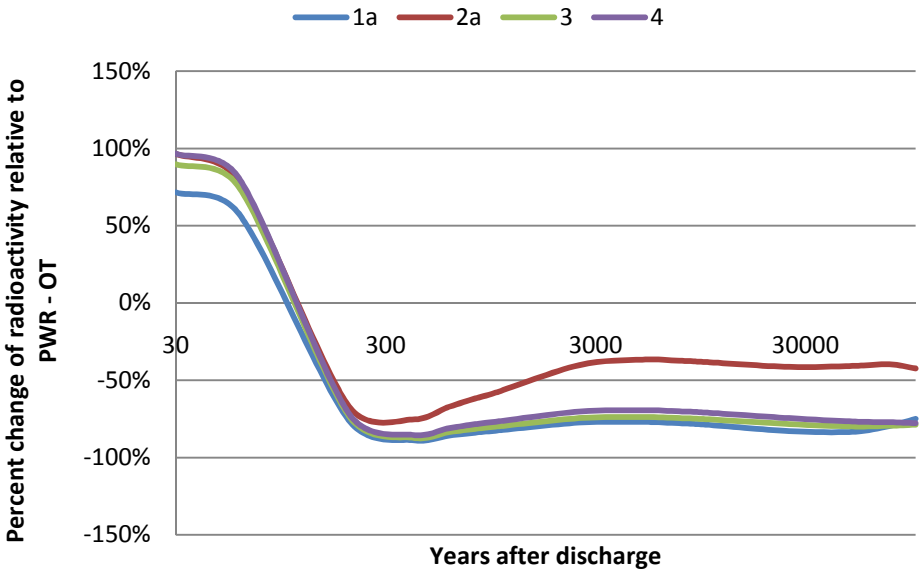

Figure 10.13 – Radioactivity of spent fuel in thorium fuel cycle relative to PWR-OT cycle

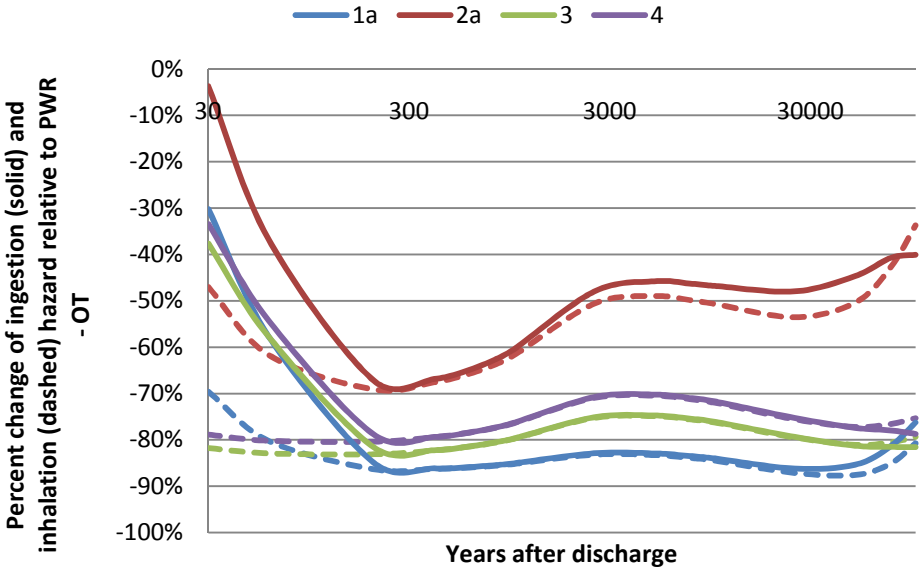

Figure 10.14 – Inhalation and ingestion hazard of spent fuel in thorium fuel cycle relative to PWR-OT cycle

11 Conclusion

In this chapter, the benefits and drawbacks of each variant will be examined. Conclusions as to the merits of one variant over the other will be drawn when possible. However, the decision to implement one variant over the other would, of course, depend on which characteristics are most important to the decision maker.

In order to simplify the comparison, several restrictions had to be made as to which characteristics were considered. For comparing the uranium consumption and reprocessing demands, only 20 MWd/kg and 40 MWd/kg CANDU exit burnups were considered as representative low and high exit burnups. To compare the spent fuel characteristics, only the 40 MWd/kg exit burnup case was considered. Also, it was necessary to choose a specific amount of time after discharge at which to evaluate the spent fuel characteristics.

The heat load was evaluated at 60 and 200 years after discharge. It is likely that spent fuel will be cooled above ground for many decades before it is moved to the geological repository. A longer waiting time before disposal results in a lower heat load of the spent fuel and, consequently, a smaller repository size. However, extended above ground storage is a safety hazard. Therefore, 60 years after discharge was chosen as an appropriate compromise to represent the time at which the spent fuel enters the repository. After approximate 200 year most of the fission products have decayed. Therefore, it is a good measure of the heat contribution from the actinides. For these reasons, these two years are used to benchmark the heat load of each variant. The gamma power is also evaluated at 60 years as gamma radiation poses a logistical obstacle to moving and handling the spent fuel. The health hazards of spent fuel are only relevant when the integrity of the repository comes into question. Therefore, 1000 years after discharge was chosen as the time at which they were calculated. This agrees with the time frame suggested in a report by the OECD [28].

Adding a RU-fuelled CANDU reactor to the fuel cycle has both advantages and disadvantages. Looking at Figure 11.1, it can be seen that variant 1a has higher NU consumption and reprocessing demands than variants 1b and 1c. However, the thermal power and health hazard metrics are all lower. Including MA burning in the RU-fuelled CANDU reactor has a positive effect as variant 1c scores similar or better on all metrics in comparison to variant 1b. The gamma power of all three variants is roughly the same.

A similar trend is seen in variant 2. In Figure 11.2, variants 2b and 2c show lower NU consumption and reprocessing demands than variant 2a. However, variant 2b has higher thermal power and health hazards than 2a. The thermal power at 60 years after discharge as well as the health hazards show a marked improvement in variant 2c compared to variant 2b. Again, gamma power of all the three variants is similar.

Figure 11.3 compares variants 1c, 2c, 3, and 4. In the figure it can be seen that variant 4 consumes the least uranium, followed by variant 3, then variant 2, and, lastly, variant 1. This suggests that the most efficient way to utilise the thorium fuel cycle is to directly fabricate a driver fuel rather than to generate the driver fuel from the spent fuel of another reactor. In variant 3, there are no PWRs so its lower uranium consumption in comparison to variants 1 and 2 further emphasizes the efficiency of CANDU reactors. As shown in chapter 9, the ability to introduce thorium fuel to a growing reactor park is hampered by the availability of fissile resources. This leads to far less optimistic scenarios as has been predicted in the steady-state case. However, as variant 4 is not dependent on other reactors for the fissile material, it will not face the same problems and will have an even larger gap over the other variants in terms of uranium consumption. Furthermore, the benefits of variant 4 are seen in both the front-end and back-end of the fuel cycle. On top of the superior uranium consumption, it also has both lower thermal power and health hazards than variants 1 or 2. The drawback of variant 4

is that it has the highest gamma power of the variants and requires significantly more spent thorium fuel reprocessing.

Variant 1 has only slightly higher uranium consumption than variant 2 but is superior to it by every other metrics suggesting that it may be the preferred variant. However, this evaluation ignored the proliferation resistance of each variant. In variant 1, there is a stream of pure plutonium whereas variant 2 does not. This alone may be incentive to choose one variant over the other.

This thesis has provided a broad scoping of different means for utilising thorium fuel cycles in CANDU reactors. However, there are many places where more detailed inspection is necessary. The author humbly submits three areas that may be the most pressing and relevant. Firstly, optimization of the CANDU-reactor in a full core model for the effective and safe use of thorium fuel is essential. Only rudimentary design changes were considered in this thesis and much more intensive optimisation is possible. The purpose of this would be to allow ^{233}U to be more efficiently bred and the reactor to be operated safely within the regulatory limits. Secondly, the approach to equilibrium case should be considered in combination with a similar study to this in order to provide a more complete prediction of the ability to introduce thorium fuel cycles as quickly as possible. The more time that passes before thorium fuel cycles are introduced, the closer the nuclear industry comes to facing major uranium shortages. Lastly, this thesis did not discuss the economic repercussion of each variant. A detailed examination of the costs may better yet show the advantageous of one variant over the others.

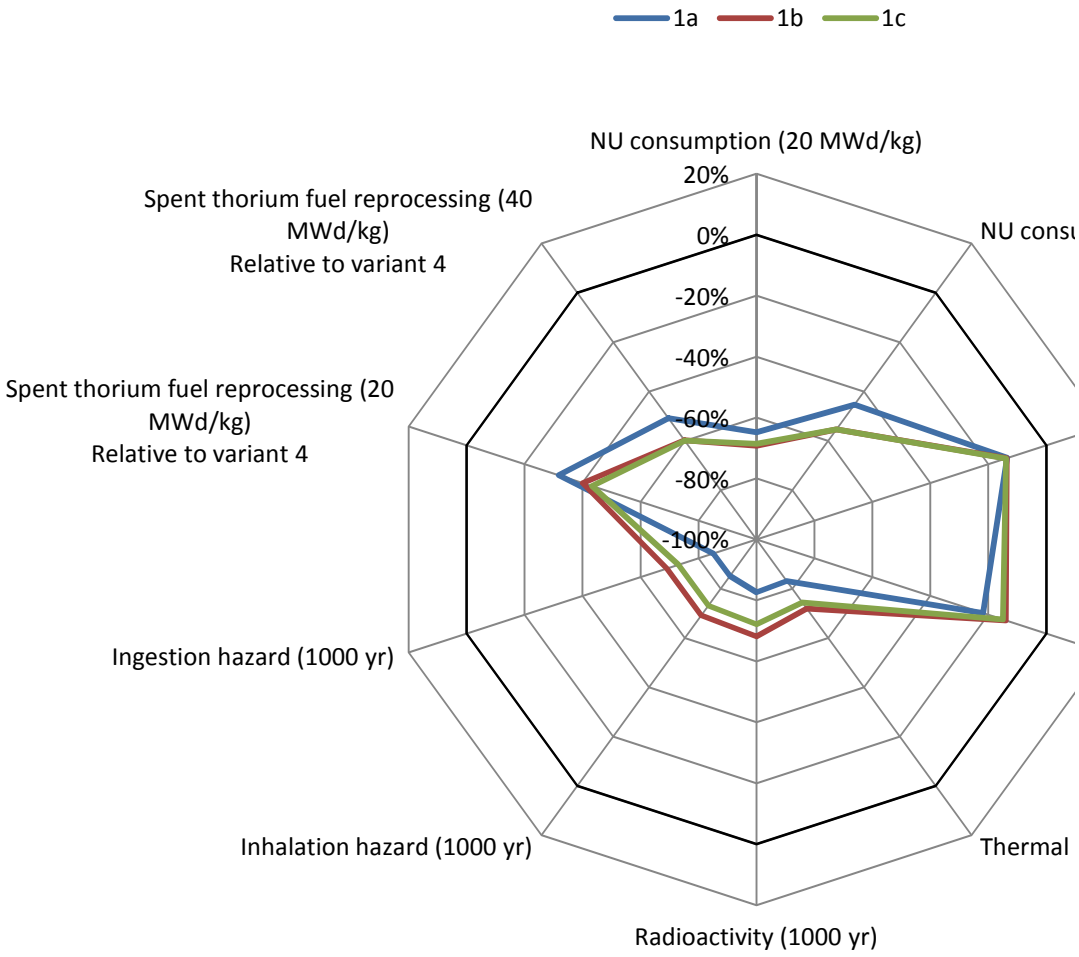

Figure 11.1 – Summary of results of variant 1

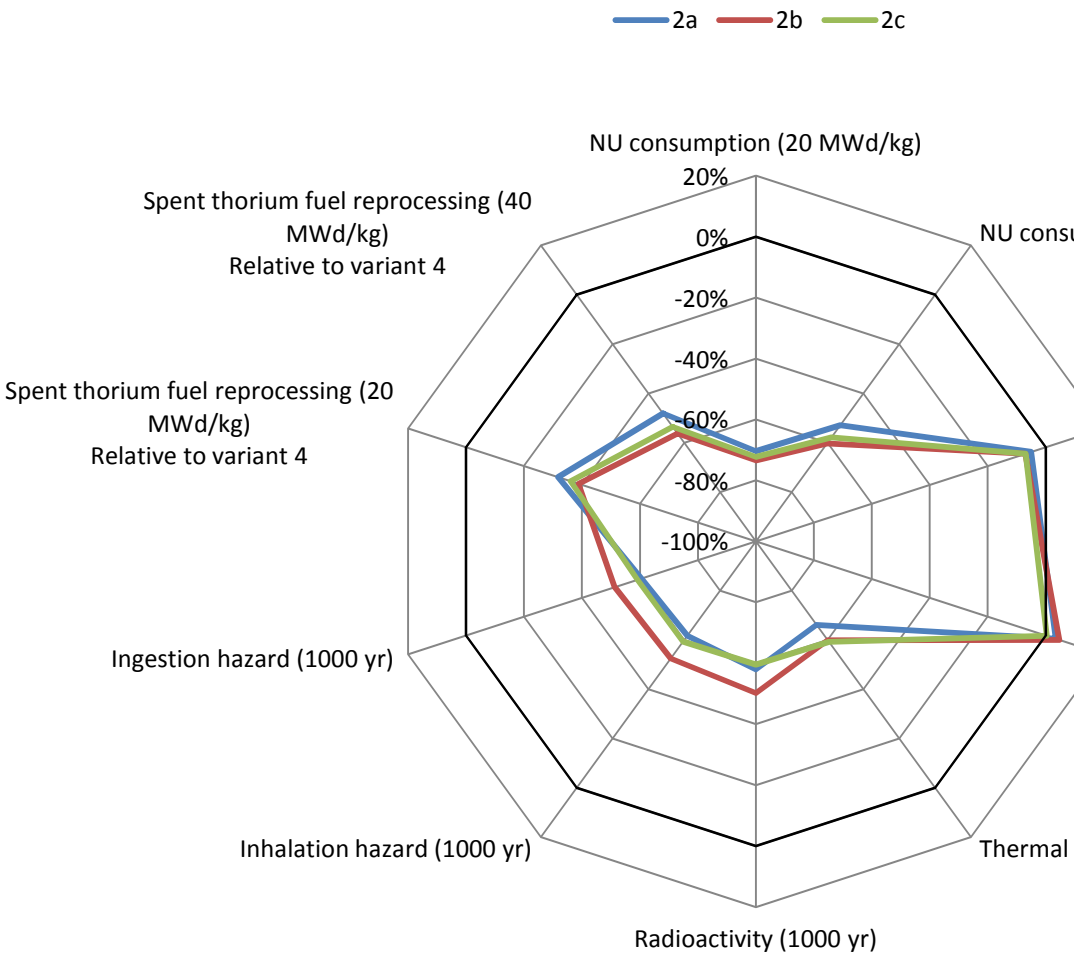

Figure 11.2 – Summary of results of variant 2

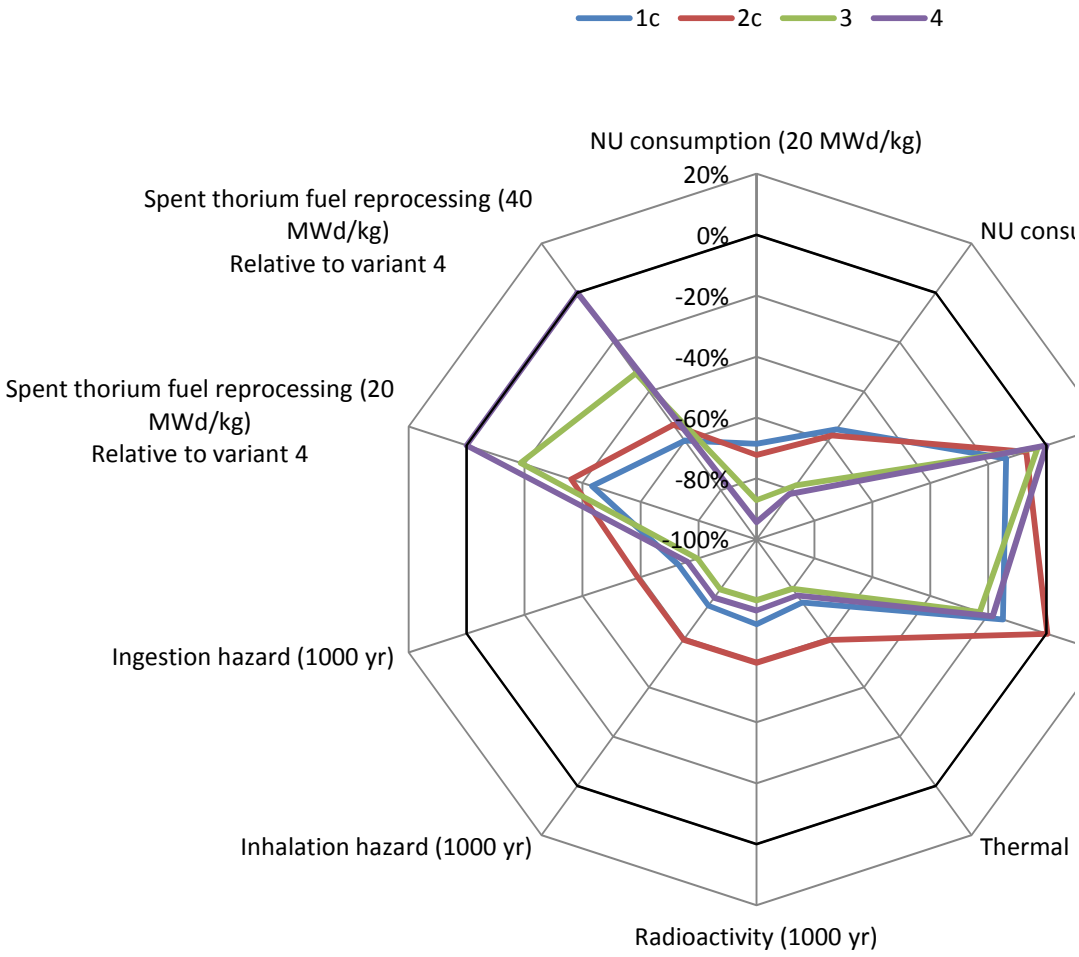

Figure 11.3 – Summary of results of variants 1 through 4

A Mass Flow Calculations

The amount energy production from a certain reactor that is required for there to be equilibrium fissile production and consumption with another reactor is termed the support ratio. Assuming the same specific power and thermal efficiency, the support ratio of reactor B to A is given by $SR_{B:A}$.

$$SR_{B:A} = \left|\frac{U_A}{U_B}\right| \tag{A.1}$$

U_i is given by equation (6.3). In the case where the exit burnups of both reactors are the same, a curve was fit to Figure 6.2. From the curve, U_B was calculated as a function of burnup.

In variants 1, 2, and 3, the fissile driver is separated from the spent fuel of a uranium-fuelled reactor. The support ratio of the driver reactors to reactor A is given by $SR_{Driver:A}$

$$SR_{Driver:A} = \left|\frac{C_i}{P_i}\right| \tag{A.2}$$

where C_i is the consumption rate of driver fuel i consumption in reactor A and is given by equation (7.1) and P_i is the rate of driver fuel production. For variants 1 and 3, the driver fuel is plutonium and its production is given by equation (A.3).

$$P_{Pu} = \frac{M_{Pu}}{BU_{Driver}} \tag{A.3}$$

where M_{Pu} is the mass fraction of plutonium in the spent fuel. In variant 2, the driver fuel is MOX. As the plutonium concentration in the MOX fuel is enriched to 9%, the rate of MOX production is given by equation (A.4).

$$P_{MOX} = P_{Pu} \times \frac{1}{9\%} = 2.98 \times 10^{-3}\ \mathrm{kg/MWd}_{Driver} \tag{A.4}$$

In variants b and c, a CANDU reactor is fuelled by the uranium separated from spent PWR fuel. The rate of RU production is given by P_{RU}

Variants 1b,c $$P_{RU} = P_{Pu} \times \frac{M_U}{M_{Pu}} \tag{7.5}$$

Variants 2b,c $$P_{RU} = P_{Pu} \times \frac{M_U}{M_{Pu}} \times 91\% \tag{7.6}$$

The ratio of energy produced by the RU to energy produced reactor A is then given by $SR_{RU:A}$

$$SR_{RU:A} = P_{RU} \times SR_{Driver:A} \times BU_{RU} \tag{A.5}$$

Equation (A.6) gives the ratio of energy production in each reactor to the energy production in the entire fuel cycle.

$$SR_{i:Total} = \frac{SR_{i:A}}{\sum SR_{i:A}} \tag{A.6}$$

where $SR_{A:A}=1$

The amount of NU consumption is proportional to the amount energy production from the driver reactors in variants 1, 2, and 3 and the amount of energy production from reactor A in variant 4. This is given by C_{NU}.

Variants 1,2,3 $$C_{NU} = \frac{SR_{Driver:Total}}{BU_{Driver}\, e_{Driver}} \left(\frac{x_p - x_t}{x_f - x_t} \right) \tag{A.7}$$

Variant 4 $$C_{NU} = \frac{SR_{A:Total}}{BU_A\, e_A} \left(\frac{x_p - x_t}{x_f - x_t} \right) \tag{A.8}$$

where C_{NU} is the natural uranium consumption of the fuel cycle in kg/MWd(e), e_i is the thermal efficiency of reactor i, x_f is the enrichment of the uranium feed (i.e. 0.71%), x_t is the enrichment of the tails, and x_p is the enrichment of the product.

The amount of reprocessing in kg/MWd(e) of spent uranium fuel is given by R_U and of spent thorium fuel is given by R_{th}.

$$R_U = \frac{SR_{Driver:Total}}{BU_{Driver}\, e_{Driver}} \tag{A.9}$$

$$R_{Th} = \frac{SR_{A:Total}}{BU_A\, e_A} + \frac{SR_{B:Total}}{BU_B\, e_B} \tag{A.10}$$

B Sample Input Files

B.1. WIMS-AECL

```
Cell Cluster
Sequence Pij

lines  0.       5.19000  100  7
lines  5.168900  9.40     53  1

symmetry -12 0d 30d

*
Annulus #   1.317184 Coolant
Annulus #   1.959137 Coolant
Annulus #   2.601089 Coolant
Annulus #   3.243042 Coolant
Annulus #   3.884995 Coolant
Annulus #   4.526947 Coolant
Annulus #   5.190000 Coolant
Annulus #   5.411550 PT
Annulus #   5.633100 PT
Annulus #   6.447800 Gap
Annulus #   6.587500 CT
Annulus #   7.187500 Moder
Annulus #   7.787500 Moder
Annulus #  8.60 Moder
Annulus #  9.21913 moder
Annulus #  9.40 Moder
```

```
nPijAn #

Annulus # 10.15541 moder      * lp 18.0 cm
Annulus # 10.71960 moder      * lp 19.0 cm
Annulus # 11.28379 moder      * lp 20.0 cm
Annulus # 11.84798 moder      * lp 21.0 cm
Annulus # 12.41217 moder      * lp 22.0 cm
Annulus # 12.97636 moder      * lp 23.0 cm
Annulus # 13.54055 moder      * lp 24.0 cm
Annulus # 14.10    moder
Annulus # 14.65    moder
Annulus # 15.2     moder
Annulus # 15.7     moder
Annulus # 16.121717 Moder *  lp 14.287500 cm

Array # 1   1 0  0
Rodsub # #    .431544 Fuel_1
Rodsub # #    .610295 Fuel_1
Rodsub # #    .652183 clad

Array # 1   6   1.488000    .000000
Rodsub # #    .431544 Fuel_2 90d Fuel_2 270d
Rodsub # #    .610295 Fuel_2 90d Fuel_2 270d
Rodsub # #    .652183 clad

Array # 1  12   2.874500    .261799
Rodsub # #    .431544 Fuel_3 90d Fuel_3 270d
Rodsub # #    .610295 Fuel_3 90d Fuel_3 270d
Rodsub # #    .652183 clad

Array # 1  18   4.323000    .000000
Rodsub # #    .431544 Fuel_4 90d Fuel_4 270d
Rodsub # #    .610295 Fuel_4 90d Fuel_4 270d
Rodsub # #    .652183 clad
*

newres  4  0.1  -14  0.d  25.7142857d
Tolerance 1e-6

FewGroups  1  2  3  4  5  6  7  8  9 $
     10 11 12 13 14 15 16 17 18 19 $
```

```
      20 21 22 23 24 25 26 27 28 29 $
      30 31 32 33 34 35 36 37 38 39 $
      40 41 42 43 44 45 46 47 48 49 $
      50 51 52 53 54 55 56 57 58 59 $
      60 61 62 63 64 65 66 67 68 69 $
      70 71 72 73 74 75 76 77 78 79 $
      80 81 82 83 84 85 86 87 88 89 *  89 group
Suppress 1 1 1 1   1 1 1 1   1 1 1 1   0 1 0 0

Buckling 1e-4 1e-4 1e-5 1e-5
Water Coolant   .8074   561.285 Cool DD2O=98.764
Water moder  1.08875  336.16 Moder DD2O=99.95
noburn moder

*
Material PT  6.5018  573.16 Moder $
  Nb93=2.65 $
  Fe54=0.007339 Fe56=0.119472 Fe57=0.002808 Fe58=0.000380 $
  Cr50=0.000417 Cr52=0.008370 Cr53=0.000967 Cr54=0.000245 $
  Ni58=0.004368 Ni60=0.001740 Ni61=0.000077 Ni62=0.000249 Ni64=0.000066 $
  Mn55=0.005 $
  Zr90=49.172123 Zr91=10.842638 Zr92=16.755391 Zr94=17.349846 Zr96=2.854732 $
  C=0.008 O16=0.135 B10=0.0000294
Material Gap .00128 459.66 Moder C=27.11 O16=72.89  *CO2 1.98 kg/m3 at 298 C
Material CT  6.4635  346.16 Moder $
  Fe54=0.011856 Fe56=0.192993 Fe57=0.004537 Fe58=0.000614 $
  Ni58=0.004704 Ni60=0.001874 Ni61=0.000083 Ni62=0.000268 Ni64=0.000071 $
  Cr50=0.004174 Cr52=0.083699 Cr53=0.009674 Cr54=0.002453 $
  Zr90=49.663374 Zr91=10.950961 Zr92=16.922785 Zr94=17.523178 Zr96=2.883252 $
  C=0.04 O16=0.125 Nb93=0.01 Mn55=0.005 B10=.0000698
*

*
Material PuO2  9.70 859.99 fuel O16=13.389  $
       PU238=2.5 Pu239=54.2 Pu240=23.8 Pu241=12.6 Pu242=6.8

Material ThO2  9.70   859.99 Fuel Th232=100.0 O16=13.79
Material UO2  9.70  859.99 Fuel U233=100.0 O16=13.79

Mixture ThPu_1  ThO2=0.9745 UO2=0.0135 PuO2=0.012   859.99 fuel
```

```
*
Material Fuel_1  ThPu_1
Material Fuel_2  ThPu_1
Material Fuel_3  ThPu_1
Material Fuel_4  ThPu_1
*
*
Material Clad  6.4635  573.16 Clad $
  Fe54=0.011856 Fe56=0.192993 Fe57=0.004537 Fe58=0.000614 $
  Ni58=0.004704 Ni60=0.001874 Ni61=0.000083 Ni62=0.000268 Ni64=0.000071 $
  Cr50=0.004174 Cr52=0.083699 Cr53=0.009674 Cr54=0.002453 $
  Zr90=49.663374 Zr91=10.950961 Zr92=16.922785 Zr94=17.523178 Zr96=2.883252 $
  C=0.04 O16=0.125 Nb93=0.01 Mn55=0.005 b10=.0000698
density clad=1.132060
*
*   write 1
Power   1   8  0.1 1 0.0001
begin
leakage -6
CELLAV
buckling 1e-4 1e-4
benoist 1
beeone 1
Reaction all=0
Print 1 1 1 0 0 1
material 0
BEGIN
POWER   1 22 0.2 1
BEGIN
BEGIN
POWER   1 32 0.4 1
BEGIN
BEGIN
POWER   1 32 0.5 1

…Repeated…

POWER   1 32 0.5 1
BEGIN
BEGIN
STOP
```

B.2. ORIGEN

```
=origen
-1$$ 400000 e
0$$ a11 71 e t
Simple power history
3$$ 28 4 0  a4 -82  a16 2 a33 0 e
4** 0.886228 25.0 1.0 e t
35$$ 0 t
56$$ 5 5 1 a5 1 a6 1  a10  0  a13 22  a14 1  1 a17 2 e
57** 0 e t
SF
73$$ 922340 922350 922360 922380 912310 932370
 942380 942390 942400 942410 942420 952410 952421 952430
 962430 962440 962450 962460 962470 38900 551370 621510 e
74** 1.12E+03 1.59E+04 4.79E+04     6.91E+06 1.10E+03
 5.56E+03 1.48E+03 2.11E+042.01E+04 8.01E+03 1.23E+04
 6.40E+02 1.08E+01 3.29E+037.95E+00 1.07E+03 4.25E+01
 7.32E+00 7.45E-02 2.13E+04 4.39E+042.92E+02 e
75$$ 2 2 2 2 2 2 2 2 2 2 2 2 2 2 2 2 2 2 3 3 3 e
59** 1e7 1e7 1e7 1e7 1e7 e
60** 1   3   6   10  30  e
61** f 1e-42
65$$ a1 15r1 a22 15r1 a43 15r1 e
 6t
56$$ 0 15 a5 4 a6 1 a10 5 a13 0 a14 5 1 a17 0 e
57** 0 e t
SF decaying for 100000 years
60** 30 60 200 400 600 800 1000 2500 5000 7500
 10000 25000 50000 75000 100000
61** f 1e-42
65$$ a25 1 a46 1 e
 6t
' write decay inventories
56$$ 0 -10 a10  1  e t
56$$ f0 t
end
```

Bibliography

1. G.W.R. Edwards, *Illustrative Cases Using the GAINS Framework*, 2011, Atomic Energy of Canada Ltd.: Chalk River, Ontario, Canada 153-123700-TE-003.

2. *Analysis of Uranium Supply to 2050*, 2001, International Atomic Energy Agency: Vienna, Austria

3. *Classification of Uranium Reserves/Resources*, 1998, International Atomic Energy Agency: Vienna, Austria IAEA-TECDOC-1035.

4. P. Rodriguez and C.V. Sundaram, *Nuclear and Materials Aspects of the Thorium Fuel Cycle.* Journal of Nuclear Materials, 1981. **100**: p. 227-249.

5. J. R. Lamarsh and A. J. Baratta, *Introduction to Nuclear Engineering*. 3rd ed2001: Prentice Hall.

6. P. Boczar, P.S.W. Chan, G.R. Dyck, R.J. Ellis, R.T. Jones, J.D. Sullivan, and P. Taylor, *Thorium Fuel Cycle Studies for CANDU Reactors*, 1998, Atomic Energy of Canada Ltd.: Chalk River, Ontario, Canada

7. *China's Nuclear Fuel Cycle*. 2011 [cited 2011 April]; Available from: http://www.world-nuclear.org/info/inf63b_china_nuclearfuelcycle.html.

8. *Shippingport Atomic Power Reactor: National Historic Mechancial Engineering Landmark*. in *Presentation Ceremony*. 1980. United States: National Historic Mechanical Engineering Landmark Program.

9. T. Candelieri. *Operative Experience in First Campaign for Reprocessing of Uranium-Thorium Elk-River Fuel Elements*. in *Technical committee meeting on utilization of thorium-based nuclear fuel: current status and perspectives*. 1985. Vienna, Austria: International Atomic Energy Agency.

10. W. Wachholz, *The Present State of HTR Concept Based on Experience Gained from AVR and THTR*, 1987, Hochtemperatur-Reaktorbau GmbH: Mannheim, Federal Republic of Germany

11. *Nuclear Power in India*. 2011 [cited 2011 April]; Available from: http://www.world-nuclear.org/info/inf53.html.

12. J. Veeder and R. Didsbury, *A Catalogue of Advanced Fuel Cycles in CANDU-PHW Reactors*, 1985, Atomic Energy of Canada Ltd.: Chalk River, Ontario, Canada AECL-8641.

13. S. Banerjee and F.W. Barclay, *Characteristics of Plutonium-Topped Thorium Cycles in Heavy-Water-Moderated Pressure Tube Reactors.* Nuclear Technology, 1979. **43**: p. 55-62.

14. B.R. Bergelson, A.S. Gerasimov, and G.V. Tikhomirov, *Optimization of the Self-Sufficient Thorium Fuel Cycle for CANDU Power Reactors.* Nuclear Technology & Radiation Protection, 2008.

15. A. Furuhashi, T. Shirakawa, and E. Takeda, *Hold-Own Breeding in Thorium-Loaded CANDU Type Lattices.* Bulletin of Tokyo Institute of Technology, 1968. **83**: p. 23-39.

16. *Potential of Thorium Based Fuel Cycles to Constrain Plutonium and Reduce Long Lived Waste Toxicity*, 2003, International Atomic Energy Agency: Vienna, Austria IAEA-TECDOC-1349.

17. B.R. Bergelson, A.S. Gerasimov, and G.V. Tikhomirov, *The Mode of Operation of CANDU Power Reactor in Thorium Self-Sufficienct Fuel Cycle.* Nuclear Technology & Radiation Protection, 2008.

18. B.R. Bergelson, A.S. Gerasimov, and G.V. Tikhomirov, *Density Effect of Reactivity in a Heavy-Water Power Reactor Operating in the 233U Self-Fuelling Regime.* Atomic Energy, 2008. **105**: p. 316-323.

19. B.R. Bergelson, A.S. Gerasimov, and G.V. Tikhomirov, *Some Questions on Nuclear Safety of Heavy-Water Power Reactor Operating in Self-Sufficient Thorium Cycle.* Nuclear Technology & Radiation Protection, 2008.

20. S. Banerjee, S.R. Hatcher, A.D. Lane, H. Tamm, and J.I. Veeder, *Some Aspects of the Thorium Fuel Cycle in Heavy-Water-Moderated Pressute Tube Reactors.* Nuclear Technology, 1977. **34**.

21. C.J. Jeong, C.J. Park, and W. Il Ko, *Dynamic Analysis of a Thorium Fuel Cycle in CANDU Reactors.* Annals of Nuclear Energy, 2008. **35**: p. 1842-1848.

22. W.B. Lewis, *How Much of the Rocks and Ocean For Power? Exploiting the Uranium-Thorium Fission Cycle*, 1964, Atomic Energy of Canada Ltd.: Chalk River, Ontario, Canada AECL-1916.

23. W.B. Lewis, *Some Economic Aspects of Nuclear Fuel Cycles*, in *United Nations Conference on the Peaceful Uses of Atomic Energy*1955: Geneva, Switzerland.

24. J.S. Foster and E. Critoph, *The Status of the Canadian Nuclear Power Program and Possible Future Strategies.* Annals of Nuclear Energy, 1975. **2**: p. 689-703.

25. *Thorium Fuel Utilization: Options and Trends*, 2002, International Atomic Energy Agency: Vienna, Austria IAEA-TECDOC-1319.

26. B. Hyland, G.R. Dyck, G.W.R. Edwards, and M. Magill. *Homogenous Thorium Fuel Cycles in CANDU Reactors*. in *Global 2009*. 2009. Paris, France.

27. P.G. Boczar, G.R. Dyck, P.S.W. Chan, and D.B. Buss, *Recent Advances in Thorium Fuel Cycles for CANDU Reactors*, in *Thorium Fuel Utlization: Options and Trends* 2002, International Atomic Energy Agency: Vienna, Austria IAEA-TECDOC-1319.

28. *Advanced Nuclear Fuel Cycles and Radioactive Waste Management*, 2006, OECD, Nuclear Energy Agency NEA No. 5990.

29. B. Hyland, *Recent Advances in Thorium Fuel Cycles with Recycle of U-233 at Atomic Energy of Canada*, 2010, Atomic Energy of Canada Ltd.: Chalk River, Ontario, Canada 153-123740-410-004.

30. V. Jagannathan, Usha Pal, R. Karthikeyan, S. Ganesan, R. P. Jain, and S. U. Kamat, *ATBR – A Thorium Breeder Reactor Concept for Early Induction of Thorium in an Enriched Uranium Reactor.* Nuclear Technology, 2001. **133**.

31. R.K. Sinha and A. Kakodkar, *Design and Development of the AHWR – the Indian Thorium Fuelled Innovative Nuclear Reactor.* Nuclear Engineering and Design, 2006. **236**: p. 683-700.

32. J. Yu, K. Wang, S. You, B. Jia, S. Shen, G. Shi, R. Sollychin, and Y. Ruan, *Thorium Fuel Cycle of a Thorium-based Advanced Nuclear Energy System.* Progress in Nuclear Energy, 2004. **45**: p. 71-94.

33. A. R. Dastur, D.A. Meneley, and D.B. Buss, *Thorium Fuel Cycle Options in CANDU Reactors*, in *Global 95*1995: Versailles, France.

34. W.B. Lewis, *Nuclear Energy: the Source of the Future.* Naturwissenschaften, 1973. **60**: p. 501-506.

35. H. Choi and C.J. Park, *A Physics Study on Thorium Fuel Recycling in a CANDU Reactor Using Dry Process Technology.* Nuclear Technology, 2006. **153**: p. 132-145.

36. M. Milgram, *The Conceptual Basis of a Thorium Fuel Cycle in the Breeding Regime*, 1973, Atomic Energy of Canada Ltd.: Chalk River, Ontario, Canada

37. A. Galperin, A. Radkowsky, and M. Todosow, *A Competitive Thorium Fuel Cycle for Pressurized Water Reactors of Current Technology*, 1998, Ben-Gurion University of the Negev: Beer-Sheva, Israel

38. P. Guillemin, A. Nuttin, A. Bidaud, J. Brizi, N. Capellan, S. David, O. Meplan, and J. Wilson, *Feasible Ways to Achieve High Conversion in Thorium-Fuelled CANDU and PWR Reactors*, in *Global 2009*2009: Paris, France.

39. T. Wang and J. Li, *Research on U-Th Self-Sustaining Cycle in CANDU Reactors.* Chinese Journal of Nuclear Sciences, 2010. **30**: p. 144-149.

40. H.W. Bonin, *Assessment of Thorium Fuels in a CANDU Nuclear Reactor by and Optimal Fuel Management Structure*, in *International Conference on Simulation of Nuclear Reactor Technology*1984: Cambridge, England.

41. *CANDU6 Reactor Assembly*. [cited 2012 April 12]; Available from: http://canteach.candu.org/imagelib/00000-General/CANDU6_Reactor_Assembly.pdf.

42. G. Jonkmans, *WIMS-AECL Version 3.1 User's Manual*, 2006, Atomic Energy of Canada Ltd.: Mississauga, Ontario, Canada

43. *PIE: Takahama-3*. [cited 2010]; Available from: http://www.oecd-nea.org/sfcompo/Ver.2/Eng/Takahama-3/index.html.

44. E.A. Andrianova, V.D. Davidenko, and V.F. Tsibulskiy, *Dynamic of Energy System of Atomic Energy (DESAE 2.2) code: User Manual*, Russian Research Centre Kurchatov Institute: Moscow, Russia

45. *Nuclear Energy Developement in the 21st Century: Global Scenarios and Regional Trends*, in *IAEA Nuclear Energy Series* 2010, International Atomic Energy Agency: Vienna, Austria NP-T-1.8.

46. R.J. Ellis, *Reactor Physics Assessment of the Inclusion of Unseparated Neptunium in MOX Reactor Fuel*, in *Advances in Nuclear Fuel Management IV*2009, American Nuclear Society: Hilton Head Island, South Carolina, USA.

47. R. J. Ellis, *Prospect of Using Reprocessed Uranium in CANDU Reactors, in the US GNEP Program*, 2008, Oak Ridge National Laboratory: Oak Ridge, Tennessee, USA

48. B. Hyland, *Destruction of Americum, Curium and Lanthanides in the Centre Pin of a Standard CANFLEX Fuel Bundle in a CANDU 6 Reactor*, 2011, Atomic Energy of Canada Ltd.: Chalk River, Ontario, Canada 153-123700-440-007.